

1 **Two-way coupled meteorology and air quality models in Asia: a systematic review**
2 **and meta-analysis of impacts of aerosol feedbacks on meteorology and air quality**

3 Chao Gao¹, Aijun Xiu^{1,*}, Xuelei Zhang^{1,*}, Qingqing Tong¹, Hongmei Zhao¹, Shichun Zhang¹,
4 Guangyi Yang^{1,2}, and Mengduo Zhang^{1,2}

5
6 ¹Key Laboratory of Wetland Ecology and Environment, Northeast Institute of Geography and Agroecology, Chinese
7 Academy of Sciences, Changchun, 130102, China

8 ²University of Chinese Academy of Sciences, Beijing, 100049, China

9 Correspondence to: A.J. Xiu (xiuajun@iga.ac.cn) & X.L. Zhang (zhangxuelei@iga.ac.cn)

10
11 **Abstract**

12 Atmospheric aerosols can exert influence on meteorology and air quality through aerosol-
13 radiation interactions (ARI) and aerosol-cloud interactions (ACI) and this two-way feedback has
14 been studied by applying two-way coupled meteorology and air quality models. As one of regions
15 with high aerosol loading in the world, Asia has attracted many researchers to investigate the aerosol
16 effects with several two-way coupled models (WRF-Chem, WRF-CMAQ, GRAPES-CUACE,
17 WRF-NAQPMS and GATOR-GCMOM) over the last decade. This paper attempts to offer
18 bibliographic analysis regarding the current status of applications of two-way coupled models in
19 Asia, related research focuses, model performances and the effects of ARI or/and ACI on
20 meteorology and air quality. There are total 160 peer-reviewed articles published between 2010 and
21 2019 in Asia meeting the inclusion criteria, with more than 79 % of papers involving the WRF-
22 Chem model. The number of relevant publications has an upward trend annually and East Asia,
23 India, China, as well as the North China Plain are the most studied areas. The effects of ARI and
24 both ARI and ACI induced by natural aerosols (particularly mineral dust) and anthropogenic
25 aerosols (bulk aerosols, different chemical compositions and aerosols from different sources) are
26 widely investigated in Asia. Through the meta-analysis of surface meteorological and air quality
27 variables simulated by two-way coupled models, the model performance affected by aerosol
28 feedbacks depends on different variables, simulation time lengths, selection of two-way coupled
29 models, and study areas. Future research perspectives with respect to the development, improvement,
30 application, and evaluation of two-way coupled meteorology and air quality models are proposed.

31
32 **1 Introduction**

33 Atmospheric pollutants can affect local weather and global climate via many mechanisms as
34 extensively summarized in the Intergovernmental Panel on Climate Change (IPCC) reports (IPCC,
35 2007, 2014, 2021), and also exhibit impacts on human health and ecosystems (Lelieveld et al., 2015;
36 Wu and Zhang, 2018). Atmospheric pollutants can modify the radiation energy balance, thus
37 influence meteorological conditions (Gray et al., 2010; Yiğit et al., 2016). Compared to other climate
38 agents, the short-lived and localized aerosols could induce changes in meteorology and climate
39 through aerosol-radiation interactions (ARI, Satheesh and Moorthy, 2005; Tremback et al., 1986)
40 and aerosol-cloud interactions (ACI, Lohmann and Feichter, 2005; Martin and Leight, 1949) or both
41 (Haywood and Boucher, 2000; Sud and Walker, 1990). ARI (previously known as direct effect and
42 semi-direct effect) are based on scattering and absorbing solar radiation by aerosols as well as cloud
43 dissipation by heating (Ackerman et al., 2000; Koch and Genio, 2010; McCormick and Ludwig,
44 1967; Wilcox, 2012), and ACI (known as indirect effect) are concerned with aerosols altering albedo
45 and lifetime of clouds (Albrecht, 1989; Lohmann and Feichter, 2005; Twomey, 1977). As our
46 knowledge base of aerosol-radiation-cloud interactions that involve extremely complex physical
47 and chemical processes has been expanding, accurately assessing the effects of these interactions
48 still remains a big challenge (Chung, 2012; Fan et al., 2016; Kuniyal and Guleria, 2019; Rosenfeld
49 et al., 2019, 2008).

50 The interactions between air pollutants and meteorology can be investigated by observational
51 analyses and/or air quality models. So far, many observational studies using measurement data from
52 a variety of sources have been conducted to analyze these interactions (Bellouin et al., 2008; Groß
53 et al., 2013; Rosenfeld et al., 2019; Wendisch et al., 2002). Yu et al. (2006) reviewed research work
54 that adopted satellite and ground-based measurements to estimate the ARI-induced changes of
55 radiative forcing and the associated uncertainties in the analysis. Yoon et al. (2019) analyzed the
56 effects of aerosols on the radiative forcing based on the Aerosol Robotic Network observations and

删除的内容: and

删除的内容: 157

删除的内容: 81

60 demonstrated that these effects depended on aerosol types. On the other hand, since the uncertainties
61 in ARI estimations were associated with ACI (Kuniyal and Guleria, 2019), the simultaneous
62 assessments of both ARI and ACI effects were needed and had gradually been conducted via satellite
63 observations (Illingworth et al., 2015; Kant et al., 2019; Quaas et al., 2008; Sekiguchi et al., 2003).
64 In the early stages, observational studies of ACI effects were based on several cloud parameters
65 mainly derived from surface-based microwave radiometer (Kim et al., 2003; Liu et al., 2003) and
66 cloud radar (Feingold et al., 2003; Penner et al., 2004). Later on, with the further development of
67 satellite observation technology and enhanced spatial resolution of satellite measurement comparing
68 against traditional ground observations, the satellite-retrieved cloud parameters (effective cloud
69 droplet radius, liquid water path (LWP) and cloud cover) were utilized to identify the ACI effects
70 studies on cloud scale. (Goren and Rosenfeld, 2014; Rosenfeld et al., 2014). Moreover, in order to
71 clarify whether aerosols affect precipitation positively or negatively, the effects of ACI on cloud
72 properties and precipitation were widely investigated but with various answers (Andreae and
73 Rosenfeld, 2008; Casazza et al., 2018; Fan et al., 2018; Rosenfeld et al., 2014). Analyses of satellite
74 and/or ground observations revealed that increased aerosols could suppress (enhance) precipitation
75 in drier (wetter) environments (Donat et al., 2016; Li et al., 2011; Rosenfeld, 2000; Rosenfeld et al.,
76 2008). Most recently, Rosenfeld et al. (2019) further used satellite-derived cloud information
77 (droplet concentration and updraft velocity at cloud base, LWP at cloud cores, cloud geometrical
78 thickness and cloud fraction) to single out ACI under a certain meteorological condition, and found
79 that the cloudiness change caused by aerosol in marine low-level clouds was much greater than
80 previous analyses (Sato and Suzuki, 2019). Despite the fact that aforementioned studies had
81 significantly improved our understanding of aerosol effects, many limitations still exist, such as low
82 temporal resolution of satellite data, low spatial resolution of ground monitoring sites and lack of
83 vertical distribution information of aerosol and cloud (Rosenfeld et al., 2014; Sato and Suzuki, 2019;
84 Yu et al., 2006).

85 Numerical models can also be used to study the interactions between air pollutants and
86 meteorology. Air quality models simulate physical and chemical processes in the atmosphere (ATM)
87 and are classified as offline and online models (El-Harbawi, 2013). Offline models (also known as
88 traditional air quality models) require outputs from meteorological models to subsequently drive
89 chemical models (Byun and Schere, 2006; ENVIRON, 2008; Seaman, 2000). Comparing to online
90 models, offline models usually are computationally efficient but incapable of capturing two-way
91 feedbacks between chemistry and meteorology (North et al., 2014). Online models or coupled
92 models are designed and developed to consider the two-way feedbacks and attempted to accurately
93 simulate both meteorology and air quality (Briant et al., 2017; Grell et al., 2005; Wong et al., 2012).
94 Two-way coupled models can be generally categorized as integrated and access models based on
95 whether using a coupler to exchange variables between meteorological and chemical modules
96 (Baklanov et al., 2014). As Zhang (2008) pointed out, Jacobson (1994, 1997) and Jacobson et al.
97 (1996) pioneered the development of a fully-coupled model named Gas, Aerosol, Transport,
98 Radiation, General Circulation, Mesoscale, and Ocean Model (GATOR-GCMOM) in order to
99 investigate all the processes related to ARI and ACI. Currently, there are three representative two-
100 way coupled meteorology and air quality models, namely the Weather Research and Forecasting-
101 Chemistry (WRF-Chem) (Grell et al., 2005), WRF coupled with Community Multiscale Air Quality
102 (CMAQ) (Wong et al., 2012) and WRF coupled with a multi-scale chemistry-transport model for
103 atmospheric composition analysis and forecast (WRF-CHIMERE) (Briant et al., 2017). The WRF-
104 Chem is an integrated model that includes various chemical modules in the meteorological model
105 (i.e., WRF) without using a coupler. For the remaining two models, which belong to access model,
106 the WRF-CMAQ uses a subroutine called *aqprep* (Wong et al., 2012) as its coupler while the WRF-
107 CHIMERE a general coupling software named Ocean Atmosphere Sea Ice Soil-Model Coupling
108 Toolkit (Craig et al. 2017). With more growing interest in coupled models and their developments,
109 applications and evaluations, two review papers thoroughly summarized the related works published
110 before 2008 (Zhang, 2008) and 2014 (Baklanov et al., 2014). Zhang (2008) overviewed the
111 developments and applications of five coupled models in the United States (US) and the treatments
112 of chemical and physical processes in these coupled models with emphasis on the ACI related
113 processes. Another paper presented a systematic review on the similarities and differences of
114 eighteen integrated or access models in Europe and discussed the descriptions of interactions
115 between meteorological and chemical processes in these models as well as the model evaluation
116 methodologies involved (Baklanov et al., 2014). Some of these coupled models can not only be used

删除的内容: (WRF-Chem; Gas, Aerosol, Transport, Radiation, General Circulation, Mesoscale, and Ocean Model; Community Atmosphere Model version3; the Model for Integrated Research on Atmospheric Global Exchanges; Caltech unified General Circulation Model)

122 to investigate the interactions between air quality and meteorology at regional scales but also at
123 global and hemispheric scales (Grell et al., 2011; Jacobson, 2001; Mailler et al., 2017; Xing et al.,
124 2015a), but large scale studies were not included in the two review papers by Zhang (2008) and
125 Baklanov et al. (2014). These reviews only focused on application and evaluation of coupled models
126 in US and Europe but there is still no systematic review targeting two-way coupled model
127 applications in Asia.

128 Compared to US and Europe, Asia has been suffering more severe air pollution in the past three
129 decades (Bollasina et al., 2011; Gurjar et al., 2016; Rohde and Muller, 2015) due to the rapid
130 industrialization, urbanization and population growth together with unfavorable meteorological
131 conditions (Jeong and Park, 2017; Lelieveld et al., 2018; Li M. et al., 2017). Then, the interactions
132 between atmospheric pollution and meteorology in Asia, which have received a lot of attention from
133 scientific community, are investigated using extensive observations and a certain number of
134 numerical simulations (Li et al., 2016; Nguyen et al., 2019a; Wang et al., 2010). Based on airborne,
135 ground-based, and satellite-based observations, multiple important experiments have been carried
136 out to analyze properties of radiation, cloud and aerosols in Asia, as briefly reviewed by Lin N. et
137 al. (2014). Recent observational studies confirmed that increasing aerosol loadings play important
138 roles in radiation budget (Benas et al., 2020; Eck et al., 2018), cloud properties (Dahutia et al., 2019;
139 Yang et al., 2019), precipitation intensity along with vertical distributions of precipitation types
140 (Guo et al., 2018, 2014). According to previous observational studies in Southeast Asia (SEA), Tsay
141 et al. (2013) and Lin N. et al. (2014) comprehensively summarized the spatiotemporal characteristics
142 of biomass burning (BB) aerosols and clouds as well as their interactions. Li et al. (2016) analyzed
143 how ARI or ACI influenced climate/meteorology in Asia utilizing observations and climate models.
144 With regard to the impacts of aerosols on cloud, precipitation and climate in East Asia (EA), a
145 detailed review of observations and modeling simulations has also been presented by Li Z. et al.
146 (2019). Since the 2000s, substantial progresses have been made in the climate-air pollution
147 interactions in Asia based on regional climate models simulations, which have been summarized by
148 Li et al. (2016). Moreover, starting from year of 2010, with the development and availability of two-
149 way coupled meteorology and air quality models, more and more modeling studies have been
150 conducted to explore the ARI or/and ACI effects in Asia (Nguyen et al., 2019a; Sekiguchi et al.,
151 2018; Wang et al., 2010; Wang J. et al., 2014). In recent studies, a series of WRF-Chem and WRF-
152 CMAQ simulations were performed to assess the consequences of ARI on radiative forcing,
153 planetary boundary layer height (PBLH), precipitation, and fine particulate matter (PM_{2.5}) and ozone
154 concentrations (Huang et al., 2016; Nguyen et al., 2019a; Sekiguchi et al., 2018; J. Wang et al.,
155 2014). Different from current released version of WRF-CMAQ model (based on WRF version 4.3
156 and CMAQ version 5.3.3) that only includes ARI, WRF-Chem with ACI (starting from WRF-Chem
157 version 3.0, Chapman et al., 2009) has been implemented for analyzing the complicated aerosol
158 effects that lead to variations of cloud properties, precipitations and PM_{2.5} concentrations (Bai et al.,
159 2020; Liu Z. et al., 2018; Park et al., 2018; Zhao et al., 2017). To quantify the individual or joint
160 effects of ARI or/and ACI on meteorological variables and pollutants concentrations, several
161 modeling studies have been performed in Asia (Chen et al., 2019a; Ma et al., 2016; Zhang B. et al.,
162 2015; Zhang et al., 2018). In addition, model comparisons (including offline and online models)
163 targeting EA have been carried out recently under the Model Inter-Comparison Study for Asia
164 (MICS-Asia) phase III (Chen et al., 2019b; Gao M. et al., 2018a; Li J. et al., 2019). As mentioned
165 above, even though there are already several reviews regarding the observational studies of ARI
166 or/and ACI (Li et al., 2016; Li Z. et al., 2019S; Lin N. et al., 2014; Tsay et al., 2013) it is necessary
167 to conduct a systematic review in Asia focusing on applications of two-way coupled meteorology
168 and air quality models as well as simulated variations of meteorology and air quality induced by
169 aerosol effects.

170 This paper is constructed as follows: Section 2 describes the methodology for literature
171 searching, paper inclusion, and analysis; Section 3 summarizes the basic information about
172 publications as well as developments and applications of coupled models in Asia and Section 4
173 provides the recent overviews of their research points. Sections 5 to 6 present systematic review and
174 meta-analysis of the effects of aerosol feedbacks on model performance, meteorology and air quality
175 in Asia. The summary and perspective are provided in Section 7.

176

177 2 Methodology

178 2.1 Criteria and synthesis

179 Since 2010, in Asia, regional studies of aerosol effects on meteorology and air quality based
180 on coupled models have been increasing gradually, therefore in this study we performed a systematic
181 search of literatures to identify relevant studies from January 1, 2010 to December 31, 2019. In
182 order to find all the relevant papers in English, Chinese, Japanese and Korean, we deployed several
183 science-based search engines, including Google Scholar, the Web of Science, the China National
184 Knowledge Infrastructure, the Japan Information Platform for S&T Innovation, the Korean Studies
185 Information Service System. The different keywords and their combinations for paper searching are
186 as follows: (1) model-related keywords including “coupled model”, “two-way”, “WRF”, “NU-
187 WRF”, “WRF-Chem”, “CMAQ”, “WRF-CMAQ”, “CAMx”, “CHIMERE”, “WRF-CHIMERE”
188 and “GATOR-GCMOM”; (2) effect-related keywords including “aerosol radiation interaction”,
189 “ARI”, “aerosol cloud interaction”, “ACI”, “aerosol effect” and “aerosol feedback”; (3) air
190 pollution-related keywords including “air quality”, “aerosol”, “PM2.5”, “O3”, “CO”, “SO2”,
191 “NO2”, “dust”, “BC”, “black carbon”, “blown carbon”, “carbonaceous”, “primary pollutants”; (4)
192 meteorology-related keywords including “meteorology”, “radiation”, “wind”, “temperature”,
193 “specific humidity”, “relative humidity”, “planetary boundary layer”, “cloud” and “precipitation”;
194 (5) region-related keywords including “Asia”, “East Asia”, “Northeast Asia”, “South Asia”,
195 “Southeast Asia”, “Far East”, “China”, “India”, “Japan”, “Korea”, “Singapore”, “Thailand”,
196 “Malaysia”, “Nepal”, “North China Plain”, “Yangtze River Delta”, “Pearl River Delta”, “middle
197 reaches of the Yangtze River”, “Sichuan Basin”, “Guanzhong Plain”, “Northeast China”,
198 “Northwest China”, “East China”, “Tibet Plateau”, “Taiwan”, “northern Indian”, “southern Indian”,
199 “Gangetic Basin”, “Kathmandu Valley”.

200 After applying the search engines and the keywords combinations mentioned above, we found
201 946 relevant papers. In order to identify which paper should be included or excluded in this paper,
202 following criteria were applied: (1) duplicate literatures were deleted; (2) studies of using coupled
203 models in Asia with aerosol feedbacks turned on were included, and observational studies of aerosol
204 effects were excluded; (3) publications involving coupled climate model were excluded. According
205 to these criteria, not only regional studies, but also studies using the coupled models at global or
206 hemispheric scales involving Asia or its subregions were included. Then, we carefully examined all
207 the included papers and further checked the listed reference in each paper to make sure that no
208 related paper was neglected. A flowchart that illustrated the detailed procedures applied for article
209 identification is presented in [Appendix Figure A1](#) (Note: Although the deadline for literature
210 searching is 2019, any literature published in 2020 is also included.). There was a total of 160
211 publications included in our study.

212 2.2 Analysis method

214 To summarize the current status of coupled models applied in Asia and quantitatively analyze
215 the effects of aerosol feedbacks on model performance as well as meteorology and air quality, we
216 carried out a series of analyses based on data extracted from the selected papers. We firstly compiled
217 the publication information of the included papers as well as the information regarding model name,
218 simulated time period, study region, simulation design, and aerosol effects. Secondly, we
219 summarized the important findings of two-way coupled model applications in Asia according to
220 different aerosol sources and components to clearly acquire what are the major research focuses in
221 past studies. Finally, we gathered all the simulated results of meteorological and air quality variables
222 with/without aerosol effects and their statistical indices (SI). For questionable results, the quality
223 assurance was conducted after personal communications with original authors to decide whether
224 they were deleted and/or corrected. All the extracted publication and statistical information were
225 exported into an Excel file, which was provided in Table S1. Moreover, we performed quantitative
226 analyses of the effects of aerosol feedbacks through following steps. (1) We discussed whether
227 meteorological and air quality variables were overestimated or underestimated based on their SI.
228 Then, variations of the SI of these variables were further analyzed in detail with/without turning on ARI
229 or/and ACI in two-way coupled models. (2) We investigated the SI of simulation results at different
230 simulation time lengths and spatial resolutions in coupled models. (3) More detailed inter-model
231 comparisons of model performance based on the compiled SI among different coupled models are
232 conducted. (4) Differences in simulation results with/without aerosol feedbacks were grouped by study

删除的内容: Appendix A

234 regions and time scales (yearly, seasonal, monthly, daily and hourly). Toward a better understanding
235 of the complicated interactions between air quality and meteorology in Asia, the results sections in
236 this paper are organized following above analysis methods (1) - (3) and represented in Section 5,
237 and the results following method (4) were represented in Section 6. In addition, Excel and Python
238 were used to conduct data processing and plotting in this study.

240 3 Basic overview,

241 3.1 Summary of applications of coupled models in Asia

242 A total of 160 articles were selected according to the inclusion criteria, and their basic
243 information was compiled in Table 1. In Asia, five two-way coupled models are applied to study the
244 ARI and ACI effects. These include GATOR-GCMOM, two commonly used models, i.e., WRF-
245 Chem and WRF-CMAQ, and two locally developed models, i.e., the global-regional assimilation
246 and prediction system coupled with the Chinese Unified Atmospheric Chemistry Environment
247 forecasting system (GRAPES-CUACE) and WRF coupled with nested air-quality prediction
248 modeling system (WRF-NAQPMS). 127 out of total 160 papers involved the applications of WRF-
249 Chem in Asia since its two-way coupled version was publicly available in 2006 (Fast et al., 2006).
250 WRF-CMAQ was applied in only 16 studies due to its later initial release in 2012 (Wong et al.,
251 2012). GRAPES-CUACE was developed by the China Meteorological Administration and
252 introduced in details in Zhou et al. (2008, 2012, 2016), then firstly utilized in Wang et al. (2010) to
253 estimate impacts of aerosol feedbacks on meteorology and dust cycle in EA. The coupled version
254 of WRF-NAQPMS was developed by the Institute of Atmospheric Physics, Chinese Academy of
255 Sciences and could improve the prediction accuracy of haze pollution in the North China Plain (NCP)
256 (Wang Z.F. et al., 2014). Note that GRAPES-CUACE and WRF-NAQPMS were only applied in
257 China. There were only three published papers about the applications of GATOR-GCMOM in
258 Northeast Asia (NEA), NCP and India. In the included papers, 93, 33, 31 studies targeted various
259 areas in China, EA and India, respectively. There were 79 papers regarding effects of ARI (7 health),
260 63 both ARI and ACI (1 health) and 18 ACI. ACI studies were much less than ARI related ones,
261 which indicated that ACI related studies need to be paid with more attention in the future.
262 Considering that the choices of cloud microphysics and radiation schemes can affect coupled models'
263 results (Baró et al., 2015; Jimenez et al., 2016), these schemes used in the selected studies were also
264 summarized in Table 1. This table presents a concise overview of coupled models' applications in
265 Asia with the purpose of providing basic information regarding models, study periods and areas,
266 aerosol effects, scheme selections, and reference. More complete information is summarized Table
267 S1 including model version, horizontal resolution, vertical layer, aerosol and gas phase chemical
268 mechanisms, photolysis rate, PBL, land surface, surface layer, cumulus, urban canopy schemes,
269 meteorological initial and boundary conditions (ICs and BCs), chemical ICs and BCs, spin-up time,
270 and anthropogenic natural emissions.

271 It should be noted that in Table 1 there were four model inter-comparison studies that aimed at
272 evaluating model performance, identifying error sources and uncertainties, and providing optimal
273 model setups. By comparing simulations from two coupled models (WRF-Chem and Spectral
274 Radiation-Transport Model for Aerosol Species) (Takemura et al., 2003) in India (Govardhan et al.,
275 2016), it was found that the spatial distributions of various aerosol species (black carbon (BC),
276 mineral dust and sea salt) were similar with the two models. Based on the intercomparisons of WRF-
277 Chem simulations in different areas, Yang et al. (2017) revealed that aerosol feedbacks could
278 enhance PM_{2.5} concentrations in the Indo-Gangetic Plain but suppress the concentrations in the
279 Tibetan Plateau (TP). Targeting China and India, Gao M. et al. (2018b) also applied the WRF-Chem
280 model to quantify the contributions of different emission sectors to aerosol radiative forcings,
281 suggesting that reducing the uncertainties in emission inventories were critical, especially for India.
282 Moreover, for the NCP region, Gao M. et al. (2018a) presented a comparison study with multiple
283 online models under the MICS-Asia Phase III and pointed out noticeable discrepancies in the
284 simulated secondary inorganic aerosols under heavy haze conditions and the importance of accurate
285 wind speed at 10 meters above surface (WS10) predictions by these models. Comprehensive
286 comparative studies for Asia have been emerging lately but are still limited, comparing to those for
287 North America and Europe, such as the Air Quality Model Evaluation International Initiative Phase
288 II (Brunner et al., 2015; Campbell et al., 2015; Forkel et al., 2016; Im et al., 2015a, 2015b; Kong et
289 al., 2015; Makar et al., 2015a, 2015b; Wang K. et al., 2015).

290

带格式的: 缩进: 左侧: 0 厘米, 首行缩进: 0 厘米

删除的内容: Statistics of published literature

42	WRF-Chem	04/17/2010 to 04/22/2010	India	ARI	RRTM	Thompson	Kumar et al. (2014)
43	WRF-Chem	01/11/2013 to 01/14/2013	NCP	ARI	Goddard/RRTM	Lin	Li and Liao (2014)
44	WRF-Chem	03/15/2008 to 03/18/2008	EA	ARI	RRTMG	Morrison	Lin C. et al. (2014)
45	WRF-Chem	07/21/2006 to 07/30/2006	NWC	ARI	RRTMG	Morrison	Chen et al. (2013)
46	WRF-Chem	05/12/2009 to 05/22/2009	India	ARI	Goddard/RRTM	Milbrandt-Yau	Dipu et al. (2013)
47	WRF-Chem	2008	India	ARI	Goddard/RRTM	Thompson	Kumar et al. (2012a)
48	WRF-Chem	2008	India	ARI	Goddard/RRTM	Thompson	Kumar et al. (2012b)
49	WRF-Chem	1999	India	ARI	Goddard/*	Lin	Seethala et al. (2011)
50	WRF-Chem	2006	China	ARI	†	†	Zhuang et al. (2011)
51	WRF-Chem	12/14/2013 to 12/16/2013	PRD	ARI & ACI	RRTMG	Morrison	Liu et al. (2020)*
52	WRF-Chem	11/30/2009 to 12/01/2009	NCP	ARI & ACI	Goddard/RRTM	Morrison	Jia et al. (2019)
53	WRF-Chem	11/25/2013 to 12/26/2013	EC	ARI & ACI	RRTMG	Lin	Wang Z. et al. (2019)
54	WRF-Chem	01/2014	China	ARI & ACI	RRTMG	Morrison	Archer-Nichols et al. (2019)
55	WRF-Chem	12/09/2016 to 12/24/2016	YRD	ARI & ACI	RRTMG	Lin	Li M. et al. (2019)
56	WRF-Chem	05/06/2013 to 20/06/2013 & 24/08/2014 to 08/09/2014	India	ARI & ACI	RRTM	Lin	Kedia et al. (2019a)
57	WRF-Chem	06/2010 to 09/2010	India	ARI & ACI	RRTM	Lin, Morrison, Thompson	Kedia et al. (2019b)
58	WRF-Chem	04/2013	PRD	ARI & ACI	RRTMG	Lin	Huang et al. (2019)
59	WRF-Chem	11/30/2013 to 12/10/2013	EC	ARI & ACI	RRTMG	Morrison	Ding et al. (2019)
60	WRF-Chem	12/01/2015	NCP	ARI & ACI	RRTMG	Lin	Chen et al. (2019)
61	WRF-Chem	04/12/2015 to 27/12/2015	EA	ARI & ACI	Goddard	WSM 6-class-graupel	An et al. (2019)
62	WRF-Chem	06/2015 to 02/2016	MRYR	ARI & ACI	Goddard/RRTM	WSM 6-class-graupel	Liu L. et al. (2018)
63	WRF-Chem	06/2008, 06/2009, 06/2010, 06/2011, 06/2012	PRD	ARI & ACI	RRTMG	Morrison	Liu Z. et al. (2018)
64	WRF-Chem	01/2014, 04/2014, 07/2014, 10/2014	China	ARI & ACI	RRTMG	Lin	Zhang et al. (2018)
65	WRF-Chem	10/01/2015 to 10/26/2015	YRD	ARI & ACI	RRTMG	Lin	Gao J. et al. (2018)
66	WRF-Chem	2001, 2006, 2011	EA	ARI & ACI	RRTMG	Morrison	Zhang et al. (2017)
67	WRF-Chem	06/01/2011 to 06/06/2011	EC	ARI & ACI	Goddard/RRTM	Lin	Wu et al. (2017)
68	WRF-Chem	11/27/2013 to 12/12/2013	YRD	ARI & ACI	Goddard/RRTM	Single-Moment 5-class	Sun et al. (2017)
69	WRF-Chem	2005 & 2009	YRD	ARI & ACI	RRTMG	Morrison	Zhong et al. (2017)
70	WRF-Chem	11/05/2014 to 11/11/2014	NCP	ARI & ACI	Goddard/RRTM	Lin	Gao et al. (2017b)
71	WRF-Chem	01/2013	NCP	ARI & ACI	Goddard/RRTM	Lin	Gao et al. (2017c)
72	WRF-Chem	01/2010, 07/2010	China	ARI & ACI	†	†	Ma and Wen (2017)
73	WRF-Chem	06/01/2008 to 07/05/2008	India	ARI & ACI	†	†	Lau et al. (2017)
74	WRF-Chem	01/2013	NCP	ARI & ACI	Goddard/RRTM	Morrison	Kajino et al. (2017)
75	WRF-Chem	03/01/2009 to 03/31/2009	TP & India	ARI & ACI	RRTMG	Morrison	Yang et al. (2017)
76	WRF-Chem	2001, 2006, 2011	EA	ARI & ACI	RRTMG	Morrison	He et al. (2017)
77	WRF-Chem	05/2008 to 08/2008	YRD	ARI & ACI	†	†	Campbell et al. (2017)
78	WRF-Chem	12/07/2013 to 12/09/2013	EC	ARI & ACI	Goddard/RRTM	Morrison	Zhang Yue et al. (2016)
79	WRF-Chem	01/2006, 04/2006, 07/2006, 10/2006	China	ARI & ACI	Goddard/RRTM	Lin	Ma et al. (2016)
80	WRF-Chem	01/2005, 04/2005, 07/2005, 10/2005	EC	ARI & ACI	Goddard/RRTM	Lin	Zhang Yang et al. (2016a)
81	WRF-Chem	01/2005, 04/2005, 07/2005, 10/2005	EC	ARI & ACI	Goddard/RRTM	Lin	Zhang Yang et al. (2016b)
82	WRF-Chem	06/2012	EC	ARI & ACI	RRTMG	Lin	Huang et al. (2016)
83	WRF-Chem	01/2010, 07/2010	YRD	ARI & ACI	Goddard/RRTM	Lin	Xie et al. (2016)
84	WRF-Chem	11/12/2012 to 11/16/2012, 11/02/2013 to 11/06/2013	India	ARI & ACI	Goddard/RRTM	Lin	Srinivas et al. (2016)
85	WRF-Chem	07/2010	India	ARI & ACI	RRTMG	Lin	Kedia et al. (2016)

带格式的: 字体颜色: 文字 1

带格式的: 字体颜色: 文字 1

带格式的: 字体颜色: 文字 1

带格式的: 字体颜色: 文字 1

带格式的: 字体颜色: 文字 1

带格式的: 字体颜色: 文字 1

带格式的: 字体颜色: 文字 1

带格式的: 字体颜色: 文字 1

带格式的: 字体颜色: 文字 1

带格式的: 字体颜色: 文字 1

带格式的: 字体颜色: 文字 1

带格式的: 字体颜色: 文字 1

带格式的: 字体颜色: 文字 1

带格式的: 字体颜色: 文字 1

带格式的: 字体颜色: 文字 1

带格式的: 字体颜色: 文字 1

带格式的: 字体颜色: 文字 1

带格式的: 字体颜色: 文字 1

带格式的: 字体颜色: 文字 1

带格式的: 字体颜色: 文字 1

带格式的: 字体颜色: 文字 1

带格式的: 字体颜色: 文字 1

带格式的: 字体颜色: 文字 1

带格式的: 字体颜色: 文字 1

带格式的: 字体颜色: 文字 1

带格式的: 字体颜色: 文字 1

带格式的: 字体颜色: 文字 1

带格式的: 字体颜色: 文字 1

带格式的: 字体颜色: 文字 1

带格式的: 字体颜色: 文字 1

带格式的: 字体颜色: 文字 1

带格式的: 字体颜色: 文字 1

带格式的: 字体颜色: 文字 1

带格式的: 字体颜色: 文字 1

带格式的: 字体颜色: 文字 1

带格式的: 字体颜色: 文字 1

带格式的: 字体颜色: 文字 1

带格式的: 字体颜色: 文字 1

带格式的: 字体颜色: 文字 1

带格式的: 字体颜色: 文字 1

带格式的: 字体颜色: 文字 1

带格式的: 字体颜色: 文字 1

带格式的: 字体颜色: 文字 1

带格式的: 字体颜色: 文字 1

带格式的: 字体颜色: 文字 1

带格式的: 字体颜色: 文字 1

带格式的: 字体颜色: 文字 1

带格式的: 字体颜色: 文字 1

带格式的: 字体颜色: 文字 1

带格式的: 字体颜色: 文字 1

带格式的: 字体颜色: 文字 1

带格式的: 字体颜色: 文字 1

带格式的: 字体颜色: 文字 1

带格式的: 字体颜色: 文字 1

带格式的: 字体颜色: 文字 1

带格式的: 字体颜色: 文字 1

带格式的: 字体颜色: 文字 1

带格式的: 字体颜色: 文字 1

带格式的: 字体颜色: 文字 1

带格式的: 字体颜色: 文字 1

带格式的: 字体颜色: 文字 1

带格式的: 字体颜色: 文字 1

带格式的: 字体颜色: 文字 1

带格式的: 字体颜色: 文字 1

带格式的: 字体颜色: 文字 1

130	WRF-CMAQ	2014	EA	ARI	RRTMG	Morrison	Nguyen et al. (2019a)
131	WRF-CMAQ	2014	SEA	ARI	RRTMG	Morrison	Nguyen et al. (2019b)
132	WRF-CMAQ	02/2015	NEA	ARI	RRTMG	Single-Moment 5-class	Yoo et al. (2019)
133	WRF-CMAQ	01/2014, 02/2014, 03/2014	EA	ARI	RRTMG	Morrison	Seikiguchi et al. (2018)
134	WRF-CMAQ	2006 to 2010, 2013	EA	ARI	RRTMG	Morrison	Hong et al. (2017)
135	WRF-CMAQ	01/2013, 07/2013	China	ARI	RRTMG	Morrison	Xing et al. (2017)
136	WRF-CMAQ	1990 to 2010	EA	ARI	RRTMG	Morrison	Xing et al. (2016)
137	WRF-CMAQ	1990 to 2010	EC	ARI	RRTMG	Morrison	Xing et al. (2015a)
138	WRF-CMAQ	1990 to 2010	EC	ARI	RRTMG	Morrison	Xing et al. (2015b)
139	WRF-CMAQ	1990 to 2010	EC	ARI	RRTMG	Morrison	Xing et al. (2015c)
140	WRF-CMAQ	01/2013	China	ARI	RRTMG	Morrison	J. Wang et al. (2014)
141	WRF-CMAQ	01/2013, 04/2013, 07/2013, 10/2013	China	ACI	RRTMG	Morrison	Chang (2018)
142	WRF-CMAQ	2050	China	ARI (Health)	RRTMG	Morrison	Hong et al. (2019)
143	WRF-CMAQ	1990 to 2010	EA & India	ARI (Health)	RRTMG	Morrison	Wang et al. (2017)
144	GRAPES-CUACE	12/15/2016 to 12/24/2016	NCP	ARI	Goddard	†	H. Wang et al. (2018)
145	GRAPES-CUACE	07/07/2008 to 07/11/2008	EC	ARI	CLIRAD	†	H. Wang et al. (2015)
146	GRAPES-CUACE	04/26/2006	EA	ARI	Goddard/†	†	Wang and Niu. (2013)
147	GRAPES-CUACE	04/26/2006	EA	ARI	Goddard/†	†	Wang et al. (2013)
148	GRAPES-CUACE	07/13/2008 to 07/31/2008	NCP	ARI	†	†	Zhou et al. (2012)
149	GRAPES-CUACE	04/26/2006	EA	ARI	Goddard/†	†	Wang et al. (2010)
150	GRAPES-CUACE	01/2013	EC	ACI	†	Single-Moment 6-class	Zhou et al. (2016)
151	WRF-NAQPMS	2013	EA	ARI	†	†	Li J. et al. (2018)
152	WRF-NAQPMS	09/27/2013 to 10/01/2013	NCP	ARI	Goddard/RRTM	Lin	Wang Z. et al. (2019)
153	WRF-NAQPMS	01/01/2013	EC	ARI	Goddard/RRTM	Lin	Wang Z. F. et al. (2014)
154	GATOR-GCMOM	2000 & 2009	NEA	ARI & ACI	†	†	Ten Hoeve and Jacobson, 2012
155	GATOR-GCMOM	2002 & 2009	India	ARI & ACI	†	†	Jacobson et al. (2019)
156	GATOR-GCMOM	2000 & 2009	NCP	ARI & ACI	†	†	Jacobson et al. (2015)
157	Multi-model comparison	†	EA	ARI & ACI	†	†	Chen et al. (2019b)
158	Multi-model comparison	2010	EA	ARI & ACI	†	†	Li J. et al., (2019)
159	Multi-model comparison	01/2010	NCP	ARI & ACI	†	†	Gao et al. (2013a)
160	Multi-model comparison	05/2011	India	ARI & ACI	†	†	Govardhan et al. (2016)

†: Unclear *: A preprint version of this study was available online on October 31, 2019, and was formally published on January 1, 2020. (EA: East Asia, NEA: Northeast Asia, SEA: Southeast Asia, EC: East China, NCP: North China Plain, YRD: Yangtze River Delta, SEC: Southeast China, NWC: Northwest China, TP: Tibetan Plateau, MRYR: middle reaches of the Yangtze River, SWC: Southwest China, PRD: Pearl River Delta).

3.2 Spatiotemporal distribution of publications

To gain an overall understanding of applications of coupled models in Asia, the spatial distributions of study areas of the selected literatures and the temporal variations of the annual publication numbers were extracted from Table 1 and summarized. Figure 1 illustrates the spatial distributions of study regions as well as the number of papers involving coupled models in Asia (Fig. 1a) and China (Fig. 1b). In this figure, the color and number in the pie charts represent individual (WRF-Chem, WRF-CMAQ, GRAPES-CUACE, WRF-NAQPMS, and GATOR-GCMOM) or multiple coupled models and the quantity of corresponding articles, respectively. At subregional scales, most studies targeted EA where high anthropogenic aerosol loading occurred in recent decades, mainly using WRF-Chem and WRF-CMAQ (Fig. 1a). For other subregions, such as NEA, SEA, Central Asia (CA), and West Asia (WA), there were rather limited research activities taking into account aerosol feedbacks with two-way coupled models. National scale applications of two-

带格式的: 字体颜色: 文字 1

带格式的: 字体颜色: 文字 1

带格式的: 字体颜色: 文字 1

带格式的: 字体颜色: 文字 1

带格式的: 字体颜色: 文字 1

带格式的: 字体颜色: 文字 1

带格式的: 字体颜色: 文字 1

带格式的: 字体颜色: 文字 1

带格式的: 字体颜色: 文字 1

带格式的: 字体颜色: 文字 1

带格式的: 字体颜色: 文字 1

带格式的: 字体颜色: 文字 1

带格式的: 字体颜色: 文字 1

带格式的: 字体颜色: 文字 1

带格式的: 字体颜色: 文字 1

带格式的: 字体颜色: 文字 1

带格式的: 字体颜色: 文字 1

带格式的: 字体颜色: 文字 1

带格式的: 字体颜色: 文字 1

带格式的: 字体颜色: 文字 1

带格式的: 字体颜色: 文字 1

带格式的: 字体颜色: 文字 1

带格式的: 字体颜色: 文字 1

带格式的: 字体颜色: 文字 1

带格式的: 字体颜色: 文字 1

带格式的: 字体颜色: 文字 1

带格式的: 字体颜色: 文字 1

带格式的: 字体颜色: 文字 1

带格式的: 字体颜色: 文字 1

带格式的: 字体颜色: 文字 1

带格式的: 字体颜色: 文字 1

带格式的: 字体颜色: 文字 1

带格式的: 字体颜色: 文字 1

带格式的: 字体颜色: 文字 1

带格式的: 字体颜色: 文字 1

带格式的: 字体颜色: 文字 1

带格式的: 字体颜色: 文字 1

带格式的: 字体颜色: 文字 1

带格式的: 字体颜色: 文字 1

带格式的: 字体颜色: 文字 1

带格式的: 字体颜色: 文字 1

带格式的: 字体颜色: 文字 1

带格式的: 字体颜色: 文字 1

带格式的: 字体颜色: 文字 1

带格式的: 字体颜色: 文字 1

带格式的: 字体颜色: 文字 1

带格式的: 字体颜色: 文字 1

带格式的: 字体颜色: 文字 1

带格式的: 字体颜色: 文字 1

带格式的: 字体颜色: 文字 1

带格式的: 字体颜色: 文字 1

带格式的: 字体颜色: 文字 1

带格式的: 字体颜色: 文字 1

带格式的: 字体颜色: 文字 1

带格式的: 字体颜色: 文字 1

带格式的: 字体颜色: 文字 1

带格式的: 字体颜色: 文字 1

带格式的: 字体颜色: 文字 1

带格式的: 字体颜色: 文字 1

带格式的: 字体颜色: 文字 1

带格式的: 字体颜色: 文字 1

带格式的: 字体颜色: 文字 1

带格式的: 字体颜色: 文字 1

带格式的: 字体颜色: 文字 1

带格式的: 字体颜色: 文字 1

带格式的: 字体颜色: 文字 1

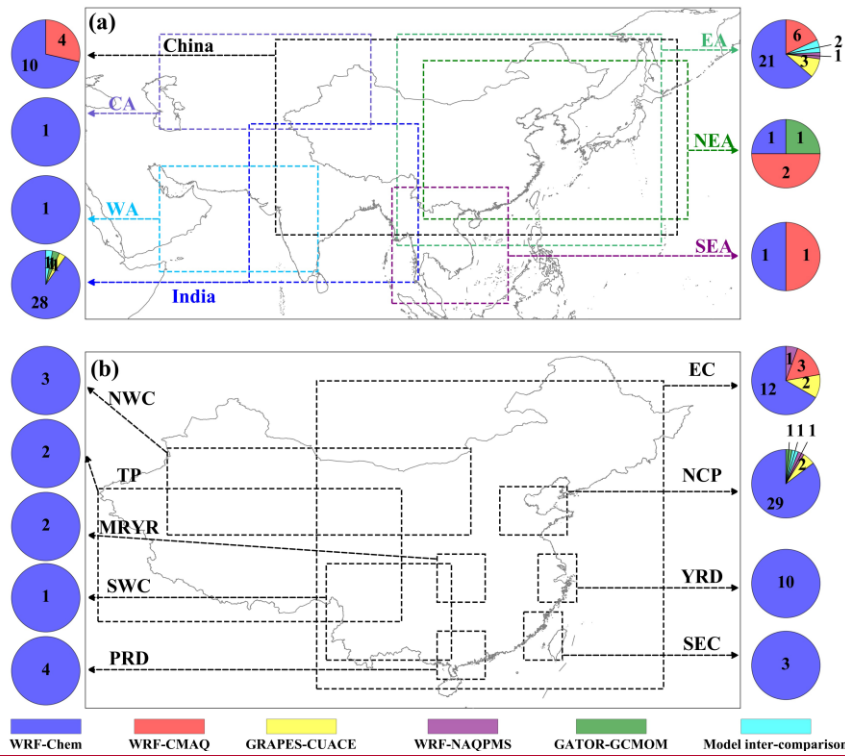
带格式的: 字体颜色: 文字 1

带格式的: 字体颜色: 文字 1

323 way coupled models targeted mostly modeling domains covering India and China but much less
 324 work were carried out in other countries, such as Japan and Korea, where air pollution levels are
 325 much lower. With respect to various areas in China (Fig. 1b), the research activities concentrated
 326 mostly in NCP and secondly in the East China (EC), then in the Yangtze River Delta (YRD) and
 327 Pearl River Delta (PRD) areas. WRF-Chem was the most popular model applied in all areas, but
 328 there were a few applications of GPRAPES-CUACE and WRF-NAQPMS in EC and NCP.

329 Figure 2 depicts the temporal variations of research activities with two-way coupled models in
 330 Asia over the period of 2010 to 2019. The total number of papers related to two-way coupled models
 331 had an obvious upward trend in the past decade. Prior to 2014, applications of two-way coupled
 332 models in Asia were scarce, with about 1 to 6 publications per year. A noticeable increase of research
 333 activities emerged starting from 2014 and the growth was rapid from 2014 to 2016, at a rate of 7-9
 334 more papers per year, especially in China. It could be related to the Action Plan on Prevention and
 335 Control of Atmospheric Pollution (2013-2017) implemented by the Chinese government. The
 336 growth was rather flat during 2016-2018 before reaching a peak of 31 articles in 2019. In addition,
 337 the pie charts in Fig. 2 indicates that modeling activities had been picking up with a diversified
 338 pattern in study domain from 2010 to 2019. The modeling domains extended from EA to China and
 339 India and then several subregions in Asia and various areas in China. For EA and India,
 340 investigations of aerosol feedbacks based on two-way coupled models rose from 1-2 papers per year
 341 during 2010-2013 to 4-8 during 2014-2019. Since 2014, most model simulations were carried out
 342 towards areas with severe air pollution in China, especially the NCP area where attracted 5-7
 343 publications per year.

344



345

346

347 Figure 1. The spatial distributions of study domains as well as the two-way coupled modeling publication numbers
 348 in different subregions or countries of Asia (a) and areas of China (b). (EA: East Asia, NEA: Northeast Asia, SEA:
 349 Southeast Asia, EC: East China, NCP: North China Plain, YRD: Yangtze River Delta, SEC: Southeast China, NWC:
 350 Northwest China, TP: Tibetan Plateau, MRYS: middle reaches of the Yangtze River, SWC: Southwest China; PRD:
 351 Pearl River Delta).

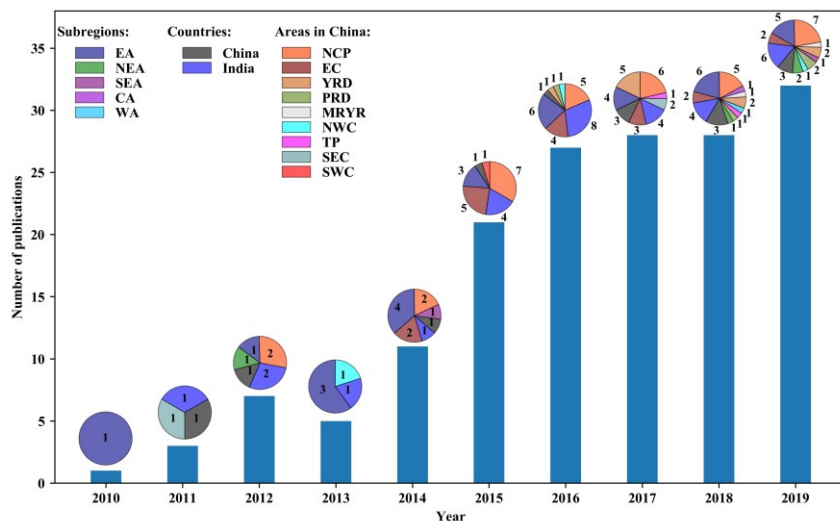


Figure 2. The temporal variations of study activities adopting two-way coupled models in Asia during 2010-2019. (EA: East Asia, NEA: Northeast Asia, SEA: Southeast Asia, EC: East China, NCP: North China Plain, YRD: Yangtze River Delta, SEC: Southeast China, NWC: Northwest China, TP: Tibetan Plateau, MRYS: middle reaches of the Yangtze River, SWC: Southwest China; PRD: Pearl River Delta).

3.3 Summary of modeling methodologies

The physiochemical processes involved with ARI and ACI are sophisticated in actual conditions of atmospheric environment but their representations in two-way coupled models can be rather different. Also, simulation results depend on how these models are configured and set up. Therefore, the treatments of aerosol and cloud microphysics, and aerosol-radiation-cloud interactions in WRF-Chem, WRF-CMAQ, GRAPES-CUACE, WRF-NAQPMS and GATOR-GCMOM applied in Asia, as well as the various aspects of how the modeling studies being set up in the selected papers are summarized in Tables 2-5, respectively, and outlined in this section.

Aerosol microphysics processes consist of particle nucleation, coagulation, condensation/evaporation, gas/particle mass transfer, inorganic aerosol thermodynamic equilibrium, aqueous chemistry and formation of secondary organic aerosol (SOA). Their representations in a variety of aerosol mechanisms offered in the five two-way coupled models applied in Asia and relevant references are compiled in Table 2. Note that the GOCART scheme in WRF-Chem is based on a bulk aerosol mechanism that is not able to consider the details of these microphysics processes. The binary homogeneous nucleation schemes with/out hydration developed by different authors are applied in the five coupled models for simulating the new particle formation and GATOR-GCMOM also adopts the ternary nucleation parameterization scheme for H_2SO_4 , NH_3 and H_2O vapors. All the five coupled models calculate the aerosol-aerosol coagulation rate coefficients based the Brownian coagulation theory, with certain enhancements in GATOR-GCMOM as stated in details by Jacobson (1999). The dynamic condensation/evaporation approaches of inorganic gases (e.g., H_2SO_4 , NH_3 , HNO_3 , and HCl) and organic gases (VOCs) based on the Fuchs-Sutugin expression are implemented in various aerosol mechanisms offered by WRF-Chem, WRF-CMAQ, GRAPES-CUACE, and WRF-NAQPMS, while GATOR-GCMOM deploys the condensation/evaporation approach in which several terms of processes are factored in the 3-D equations of discrete size-resolved aerosol growth (Jacobson, 2012). The mass transfer between gaseous and aerosol particles are treated via two typical methods (i.e., bulk equilibrium and kinetic) in most coupled models, and the hybrid and Henry's law equilibrium methods are also applied in the MADRID (WRF-Chem) and the 6th/7th generation CMAQ aerosol modules (AERO6/AERO7) (WRF-CMAQ), respectively. Different versions of the ISORROPIA module, the Model for an Aerosol Reacting System-version A (MARS-A), the Multicomponent Equilibrium Solver for Aerosols with the Multicomponent Taylor Expansion Method (MESA-MTEM), and the EQUilibrium SOLVER version 2 (EQUISOLV

批注 [g1]: Jacobson M Z. History of, processes in, and numerical techniques in GATOR-GCMOM[J]. 2012.

带格式的: 字体颜色: 文字 1

带格式的: 字体颜色: 文字 1

- 批注 [g71]: Jacobson M Z. Analysis of aerosol interaction ...
- 带格式的
- 批注 [g62]: Knote C, Hodzic A, Jimenez J L, et al. Simulat ...
- 批注 [g67]: Appel K W, Bash J O, Fahey K M, et al. The ...
- 带格式的
- 批注 [g59]: Ahmadvor R, McKeen S A, Robinson A L, et al ...
- 带格式的
- 批注 [g63]: Zhang Y, Pun B, Vijayaraghavan K, et al. ...
- 带格式的
- 批注 [g72]: Jacobson M Z. Investigating cloud absorptio ...
- 带格式的
- 批注 [g73]: Marelle L, Raut J C, Law K S, et al. Improvem ...
- 带格式的
- 带格式的: 字体颜色: 文字 1
- 带格式的: 字体颜色: 文字 1
- 带格式的: 字体颜色: 文字 1
- 批注 [g74]: Jacobson M Z, Kaufman Y J, Rudich Y. Examin ...
- 带格式的
- 带格式的: 字体颜色: 文字 1
- 批注 [g75]: Jacobson M Z, Jadhav V. World estimate ...
- 带格式的
- 带格式的: 字体颜色: 文字 1
- 批注 [g76]: Ghan S J, Zaveri R A. Parameterization of opt ...
- 批注 [g77]: Martin S T, Schlenker J C, Malinowski A, et al ...
- 带格式的
- 带格式的
- 批注 [g78]: Nenes A, Pandis S N, Pilinis C. ISORROPIA: A ...
- 批注 [g79]: Jacobson M Z, Tabazadeh A, Turco R P. Simul ...
- 带格式的
- 带格式的
- 带格式的: 字体颜色: 文字 1
- 批注 [g84]: Gong S L, Barrie L A, Blanchet J P, et al. Cana ...
- 批注 [g85]: Giorgi F, Chameides W L. Rainout lifetimes of ...
- 批注 [g86]: Giorgi, F., and W. L. Chameides, Rainout lifeti ...
- 带格式的: 字体颜色: 文字 1
- 带格式的: 字体颜色: 文字 1
- 批注 [g87]: Seinfeld J, Pandis S. Atmospheric chemistry a ...
- 批注 [g89]:
- 批注 [g90]: Jacobson M Z. Development of mixed - phas ...
- 带格式的
- 带格式的: 字体颜色: 文字 1
- 带格式的: 字体颜色: 文字 1
- 批注 [g88]: Chen X, Wang Z, Yu F, et al. Estimation of ...
- 带格式的
- 批注 [g80]: Easter R C, Ghan S J, Zhang Y, et al. MIRAGE: ...
- 批注 [g81]: Easter R C, Ghan S J, Zhang Y, et al. MIRAGE: ...
- 批注 [g82]: Binkowski F S, Roselle S J. Models - 3 Comm ...
- 带格式的: 字体颜色: 文字 1
- 带格式的: 字体颜色: 文字 1
- 带格式的
- 批注 [g83]: Fahey K M, Carlton A G, Pye H O T, et al. A ...
- 带格式的

al., 1997; Griffin et al., 1999)
 2. Based on volatility basis set approach (Ahmadvor et al., 2012)

(Knote et al., 2012)

dissolution approaches for 42 hydrophilic and hydrophobic VOCs (Zhang et al., 2004)

(Foley et al., 2012)

*CUACE is the aerosol mechanism implemented in the GRAPES-CUACE model (Zhou et al., 2012).
 *GATOR2012 is the aerosol mechanism implemented in the GATOR-GCMOM model (Jacobson et al., 2012).

In addition to aerosol microphysics processes, the cloud properties included in cloud microphysics schemes and the treatment of aerosol-cloud processes in the five two-way coupled models are different in terms of hydrometeor classes, cloud droplet size distribution, aerosol water uptake, in-/below-cloud scavenging, hydrometeor-aerosol coagulations, and sedimentation of aerosols and cloud droplets (Table 3). Among the microphysics schemes implemented in the five coupled models, mass concentrations of different hydrometeors (including cloud water, rain, ice, snow or graupel) are included but their number concentrations are only considered if the cloud microphysics schemes are two-moment or three-moment. The single modal approach with either lognormal or gamma distribution and the sectional approach with discrete size distributions for cloud droplets are applied in different microphysics schemes. Based on the Mie theory, WRF-Chem, WRF-CMAQ, GRAPES-CUACE, WRF-NAQPMS and GATOR-GCMOM calculate cloud radiative properties (including extinction/scattering/absorption coefficient, single scattering albedo and asymmetry factor of liquid and ice clouds) in their radiation schemes (e.g., RRTMG, GODDARD, GATOR2012). In atmosphere, the hygroscopic growth of aerosols due to water uptake is parameterized based on the Köhler or Zdanovskii-Stokes-Robinson theory and the hysteresis effects depending on the deliquescence and crystallization RH are taken into account in the five coupled models. The removal processes of aerosol particles include wet removal and sedimentation. Aerosol particles in accumulation and coarse modes can act as CCN or IN via activations in cloud, which can further develop to different types of hydrometeors (cloud water, rain, ice, snow and graupel), and then gradually form precipitations. These processes are named as in-cloud scavenging or rainout. The aerosol particles below cloud base also can be coagulated with the falling hydrometeors, which are known as below-cloud scavenging or wash out. Both representations of in- and below-cloud scavenging processes are based on scavenging rate approach in aerosol mechanisms of WRF-Chem, WRF-CMAQ, GRAPES-CUACE and WRF-NAQPMS except GATOR-GCMOM. Size-resolved sedimentation of aerosols are computed from one model layer to layers below down to the surface layer using settling velocity in most coupled models and the MOSAIC aerosol mechanism in WRF-Chem only considers the sedimentation in the lowest model level (Marelle et al., 2017).

Table 3. Compilation of cloud properties and aerosol-cloud processes in two-way coupled models (WRF-Chem, WRF-CMAQ, GRAPES-CUACE, WRF-NAQPMS and GATOR-GCMOM) applied in Asia.

	WRF-Chem	WRF-CMAQ	GRAPES-CUACE	WRF-NAQPMS	GATOR-GCMOM
Hydrometeor (Cloud microphysics scheme)	Mass concentrations: Cloud water, rain, ice, snow and graupel (Morrison, Lin, Thompson, WSM 6 class and Milbrandt-Yau) Cloud water, rain, ice and snow (WSM 5 class) Number concentrations: Rain, ice, snow and graupel (Morrison and Milbrandt-Yau) Rain and ice (Thompson) None (Lin, WSM 5 class and WSM 6 class)	Mass concentrations: Cloud water, rain, ice, snow and graupel (Morrison) Cloud water, rain, ice and snow (WSM 5 class) Cloud water and rain (WSM 3 class) Number concentrations: Rain, ice, snow and graupel (Morrison) None (WSM 3 class and WSM 5 class)	Mass concentrations: Cloud water, rain, ice, snow and graupel (WSM 6 class) Number concentrations: None (WSM 6 class)	Mass concentrations: Cloud water, rain, ice, snow and graupel (Lin) Number concentrations: None (Lin)	Mass concentrations: Cloud water, rain, ice, snow and graupel Number concentrations: Cloud water, rain, ice, snow and graupel
Cloud droplet size distribution (Cloud microphysics scheme)	1. Single modal approach with lognormal distribution (Morrison and Lin) 2. Gamma distribution (Thompson, WSM 5 class and WSM 6 class)	1. Single modal approach with lognormal distribution (Morrison) 2. Gamma distribution (WSM 3 class and WSM 5 class)	Gamma distribution (WSM 6 class)	Single modal approach with lognormal distribution (Lin)	Sectional approach with (GATOR2012) 2 size bins
Cloud radiative properties (Radiation scheme)	Extinction coefficient, single scattering albedo and asymmetry factor of liquid and ice clouds based on Mie scattering theory (RRTMG SW) Absorption coefficient of liquid and ice clouds using constant values (RRTMG LW) Extinction coefficient, single scattering albedo and asymmetry factor of liquid and ice clouds from lookup tables (Goddard SW and LW)	Extinction coefficient, single scattering albedo and asymmetry factor of liquid and ice clouds based on Mie scattering theory (RRTMG SW) Absorption coefficient of liquid and ice clouds using constant values (RRTMG LW)	Extinction coefficient, single scattering albedo and asymmetry factor of liquid and ice clouds using lookup tables (Goddard SW) Extinction coefficient, single scattering albedo and asymmetry factor of liquid and ice clouds from lookup tables (Goddard LW)	Extinction coefficient, single scattering albedo and asymmetry factor of liquid and ice clouds using lookup tables (Goddard SW) Clear sky optical depth from lookup table (RRTM LW)	Integration over particle size bin of Mie theory distribution (Ghan S J, Zdanovskii, Stokes-Robinson, and hysteresis is treated (Jadhav, 2012))
Aerosol water uptake	Equilibrium with RH based on Köhler theory and hysteresis is treated (Fkan and Zaveri, 2006)	The empirical equations of deliquescence and crystallization RH developed by Martin et al (2003) and hysteresis is treated (CMAQ source code)	Equilibrium with the mutual deliquescence and crystallization RH using the Zdanovskii-Stokes-Robinson equation, and hysteresis is treated (Personal communication)	Equilibrium with the mutual deliquescence and crystallization RH using the Zdanovskii-Stokes-Robinson equation, and hysteresis is treated (Nenes et al., 1998; Li et al., 2011)	Size-resolved deliquescence and crystallization RH using the Zdanovskii-Stokes-Robinson equation, and hysteresis is treated (Easter et al., 2007)
In-cloud scavenging (Aerosol mechanism)	Scavenging via nucleation, Brownian diffusion, collection and autoconversion in both grid-scale and sub-grid clouds with a first-order removal rate (MADE-SORGAM, MOSAIC, MAM0 and MAM7) (Fahey et al., 2004)	Scavenging of interstitial aerosol in the Aitken mode and nucleation scavenging of aerosol in the accumulation and coarse modes by the cloud droplets in both grid-scale and sub-grid clouds (AEROS, AEROC and AEROT) (Binkowski and Roselle, 2004; Fahey et al., 2012)	Algorithm of rainout removal tendency by Giorgi and Chameides (1986)	Employing a scavenging coefficient approach based on relationships described by Seinfeld and Pandis (1998) only hydrophilic particles can be scavenged (Easter et al., 2007)	Size-resolved aerosol scavenging and cloud droplet scavenging (GATOR-GCMOM)

Below-cloud scavenging (Aerosol mechanism)	Scavenged aerosols are instantly removed by interception and impaction but not resuspended by evaporating rain. (MADE/SORGAM, MOSAIC, MAM3 and MAM7) (Slinn, 1984; Easter et al., 2004)	All aqueous species are scavenged from the cloud top to the ground in both grid-scale and sub-grid clouds (AEROS, AEROS6 and AEROS7) (CMAQ User's Guide; Fahey et al., 2012)	Aerosol particles between sizes ranging from 0.5 to 1 μm radius are instantly removed with considering cloud fraction, and scavenged rate depends on aerosol and hydrometeor sizes (Slinn, 1984; Essig et al., 2005)	Employing a scavenging coefficient approach based on relationships described by Scirefield and Pandis (1998), considering accretion of in-cloud droplets particles into precipitation and impaction of ambient particles into precipitation.	Discrete size-resolved hydrometeors and wet liquid aerosol-ice are (GATOR2012) (Jacobson et al., 2012)
Sedimentation of aerosols (Aerosol mechanism)	Sedimentation with considering mass and number concentrations of aerosols at surface. (MOSAIC) (Mareille et al., 2017)	Only considering gravitational sedimentation for aerosols (AEROS, AEROS6 and AEROS7)	Size-resolved sedimentation of aerosol particles above surface layer is computed with the settling velocity (CUACE) (Fahey et al., 2012)	Using size-resolved sedimentation velocity to simulate sedimentation of aerosols (AEROS)	Sedimentation of size computed from one down to the surface velocities (GATOR2012) (Jacobson et al., 1997, 2012)

- 带格式的: 字体颜色: 文字 1
- 批注 [g94]: Jacobson M Z. Development of mixed - phase clouds from multiple aerosol size distributions and the effect of the clouds on aerosol removal[J]. Journal of Geophysical Research: Atmospheres, 2003, 108(D8).
- 带格式的
- 批注 [g91]: Slinn W G N. Precipitation scavenging, in atmospheric sciences and power production-1979[J]. Division of Biomedical Environmental Research, US
- 批注 [g92]: Fahey K M, Carlton A G, Pye H O T, et al. A
- 批注 [g93]: Gong S L, Barrie L A, Blanchet J P, et al. Cana
- 带格式的
- 带格式的
- 带格式的
- 带格式的: 字体颜色: 文字 1
- 批注 [g95]: Gong S L, Barrie L A, Blanchet J P, et al. Cana
- 带格式的
- 批注 [g96]: Jacobson M Z. Development of mixed - phas
- 批注 [g97]:
- 带格式的
- 带格式的
- 带格式的: 字体颜色: 文字 1
- 删除的内容: .
- 删除的内容: Table 3. Treatments of relevant aerosol
- 带格式的
- 带格式的: 字体: 非倾斜
- 带格式的: 字体: 小五, 字体颜色: 文字 1
- 带格式的: 字体颜色: 文字 1
- 带格式的: 两端对齐
- 带格式表格
- 带格式的: 字体颜色: 文字 1
- 带格式的: 字体颜色: 文字 1
- 带格式的: 两端对齐
- 带格式的: 字体颜色: 文字 1
- 带格式的: 两端对齐
- 带格式的: 字体颜色: 文字 1
- 带格式的: 两端对齐
- 带格式的: 字体颜色: 文字 1
- 带格式的: 两端对齐
- 带格式的: 字体颜色: 文字 1
- 带格式的: 两端对齐
- 带格式的: 字体颜色: 文字 1
- 带格式的: 两端对齐

435 * GATOR2012 refers to either the aerosol or cloud microphysics scheme used in Jacobson (2012).

436

437 Table 4 further lists various aspects with regards to how ARI and ACI being calculated in the

438 five two-way coupled models (WRF-Chem, WRF-CMAQ, GRAPES-CUACE, WRF-NAQPMS,

439 and GATOR-GCMOM) applied in Asia. Note that the information in this table was extracted from

440 the latest released version of WRF-Chem (version 4.3.3) and WRF-CMAQ (based on WRF v4.3

441 and CMAQ v5.3.3) as well as relevant references for GRAPES-CUACE (Wang et al., 2015), WRF-

442 NAQPMS (Wang et al., 2014) and GATOR-GCMOM (Jacobson et al., 2010; 2012). These models

443 all use the Mie theory to compute ARI effects but differ in representations of aerosol optical

444 properties and radiation schemes. To simplify the calculation, aerosol species simulated by the

445 chemistry module/model are put into different groups (Table 4) and the refractive indices of these

446 groups are directly from the Optical Properties of Aerosols and Clouds (OPAC) database (Hess et

447 al., 1998) in WRF-Chem and WRF-CMAQ (Table B6 in Appendix B). In WRF-Chem, the aerosol

448 optical properties (AOD, extinction/scattering/absorption coefficient, single scattering albedo and

449 asymmetry factor) are calculated in terms of four spectral intervals (listed in Table B6 in Appendix

450 B) and then inter/extrapolated to 11 (14) SW intervals defined in the GODDARD (RRTMG) scheme.

451 For SW and LW radiation in both WRF-CMAQ and WRF-Chem, these optical parameters are

452 computed at each of corresponding spectral intervals in the RRTMG scheme. The aerosol optical

453 property for LW radiation is considered only at 5 thermal windows (listed in Table B6) in WRF-

454 CMAQ. No detailed information regarding how aerosol optical property and relevant parameters

455 being calculated in GRAPES-CUACE and WRF-NAQPMS can be found from the relevant

456 references.

457 With respect to ACI effects, the simulated aerosol characteristics (such as mass, size

458 distribution and species) are utilized for the calculation of cloud droplet activation and aerosol

459 resuspension based on the Köhler theory (Abdul-Razzak and Ghan, 2002) in several (one)

460 microphysics schemes (scheme) in WRF-Chem (GRAPES-CUACE). GATOR-GCMOM is the first

461 two-way coupled model adding IN activation processes including heterogeneous and homogeneous

462 freezing (Jacobson et al., 2003). None of the other four two-way coupled models considers the IN

463 formation processes (including immersion freezing, deposition freezing, contact freezing, and

464 condensation freezing) but they have been included in some specific versions of WRF-Chem (Keita

465 et al., 2020; Lee et al., 2020), which are not yet in the latest release version 4.3.3 of WRF-Chem.

466

467 Table 4. Summary of relevant information regarding calculations of aerosol-radiation interactions (ARI) and aerosol-

468 cloud interactions (ACI) in two-way coupled models (WRF-Chem, WRF-CMAQ, GRAPES-CUACE, WRF-

469 NAQPMS and GATOR-GCMOM) applied in Asia.

Model	ARI	ACI					
	Aerosol species groups	Aerosol size distribution (Aerosol mechanism)	Mixing state	SW scheme (# of spectral intervals)	LW scheme (# of spectral intervals)	CCN (Microphysics scheme)	IN (Microphysics scheme)
WRF-Chem	1. Water 2. Dust 3. BC 4. OC 5. Sea-salt 6. Sulfate	1. Bulk (GOCART) 2. Modal (MADE/SORGAM, AEROS, MAM3 and MAM7) 3. Sectional (MOSAIC (4bins and 8 bins) and MADRID (8bins))	Internal mixing (Volume averaging, Core-shell, and Maxwell-Garnett)	1. Goddard (11) 2. RRTMG (14)	RRTMG (16)	Activation under a certain supersaturation in an air parcel based on Köhler theory (Morrison, Liu, Thompson, WSM 6.5/3 class and Milbrandt-Yau)	Ice liquid water mixed phase (classical) and Diffusion
WRF-CMAQ	1. Water 2. Water-soluble 3. BC 4. Insoluble 5. Sea-salt 6. Sulfate	Modal (AEROS, AEROS6 and AEROS7)	Internal mixing (Core-shell)	RRTMG (14)	RRTMG (16)	None	None
GRAPES-CUACE	1. Nitrate 2. Dust 3. BC 4. OC 5. Sea-salt 6. Sulfate 7. Ammonium	Sectional (CUACE (12 bins))	External mixing	Goddard (11)	Goddard (14)	Activation under a certain supersaturation in an air parcel based on Köhler theory (WSM 6-class)	None
WRF-NAQPMS	1. Nitrate 2. Dust 3. BC 4. OC 5. Sea-salt 6. Sulfate	Modal (AEROS)	External mixing	Goddard (11)	RRTMG (16)	Activation under a certain supersaturation in an air parcel based on Köhler theory (Lin)	None

538 schemes, most studies selected YSU in WRF-Chem and ACM2 in WRF-CMAQ. Regarding to
539 meteorological ICs and BCs, the FNL data were the first choice, and outputs from the Model for
540 Ozone and Related Chemical Tracer (MOZART) were used to generate chemical ICs and BCs by
541 most researchers. Georgiou et al. (2018) also unraveled that boundary conditions of dust and O₃
542 played an important role in WRF-Chem simulations. The modeling applications in Asia utilized
543 global (EDGAR), regional (e.g., MIX, INTEX-B, and REAS), and national (e.g., MEIC and JEL-
544 DB) anthropogenic emission inventories. Natural emission sources, such as mineral dust (Shao,
545 2004), biomass burning (FINN (Wiedinmyer et al., 2011) and GFED (Guido et al., 2010)), biogenic
546 VOCs (MEGAN (Guenther et al., 2006)), and sea salt (Gong et al., 1997) were also considered. It
547 should be noted that only one paper by Gao et al. (2017) reported that the WRF-Chem model with
548 the Gridpoint Statistical Interpolation (GSI) data assimilation could improve the simulation
549 accuracy during a wintertime pollution period.

551 **4 Overview of research focuses in Asia**

552 **4.1 Feedbacks of natural aerosols**

553 **4.1.1 Mineral dust aerosols**

555 Due to the fact that dust storm events frequently occurred over Asia during 2000-2010, the
556 research community has focused on dust transportation and associated climatic effects (Choobari et
557 al., 2014; Gong et al., 2003; Lee et al., 2010; Yasunari and Yamazaki, 2009; Zhang et al., 2003a,
558 2003b). Also the detailed processes and physiochemical mechanisms of dust storms had been well
559 understood and reviewed in detail (Chen et al., 2017a; Huang et al., 2014; Shao and Dong, 2006;
560 Uno et al., 2006). To probe into the radiative feedbacks of dust aerosols in Asia, Wang et al. (2013,
561 2010) initiated modeling studies by a two-way coupled model, i.e., the GRAPES-CUAUE model,
562 to simulate direct radiative forcing (DRF) of dust, and revealed that the feedback effects of dust
563 aerosols could lead to decreasing of surface wind speeds and then suppress dust emissions. Further
564 modeling simulations by the same model (Wang and Niu, 2013) indicated that considering dust
565 radiative effects did not substantially improve the model performance of the air temperature at 2
566 meters above the surface (T2), even with assimilating data from in-situ and satellite observations
567 into the model. Subsequently, several similar studies based on another two-way coupled model
568 (WRF-Chem with The Georgia Tech/Goddard Global Ozone Chemistry Aerosol Radiation and
569 Transport scheme) were conducted to investigate dust radiative forcing (including shortwave
570 radiative forcing (SWRF) and longwave radiative forcing (LWRF)) and ARI effects of dust on
571 meteorological variables (PBLH, T2 and WS10) in different regions of Asia (Bran et al., 2018; Chen
572 et al., 2014; Jin et al., 2016a, 2015; Kumar et al., 2014; Liu L. et al., 2016; Su and Fung, 2018a,
573 2018b; Zhou et al., 2018). These studies demonstrated that dust aerosols could induced negative
574 radiative forcing (cooling effect) at top of atmosphere (TOA) as well as the surface (including both
575 Earth's and sea surfaces) and positive radiative forcing (warming effect) in the ATM (Bran et al.,
576 2018; Chen et al., 2014; Kumar et al., 2014; Li and Sokolik, 2018; Li M.M. et al., 2017a; Su and
577 Fung, 2018a; Wang et al., 2013). More thorough analyses of the radiative effects of dust in Asia (Li
578 and Sokolik, 2018; Wang et al., 2013) pointed out that dust aerosols played opposite roles in the
579 shortwave and longwave bands, so that the dust SWRF at TOA and the surface (cooling effects) as
580 well as in the ATM (warming effects) was offset partially by the dust LWRF (warming effects at
581 TOA and the surface but cooling effects in the ATM). It was noteworthy that adding more detailed
582 mineralogical composition into the dust emission for WRF-Chem could alter the dust SWRF at TOA
583 from cooling to warming and then lead to a positive net radiative forcing at TOA (Li and Sokolik,
584 2018). These different conclusions showed some degrees of uncertainties in the coupled model
585 simulations of dust aerosols' radiative forcing that need to be further investigated in the future.

586 Dust aerosols can act not only as water-insoluble cloud condensation nuclei (CCN) (Kumar et
587 al., 2009) but also as ice nuclei (IN) (Lohmann and Diehl, 2006) since they are referred to as ice
588 friendly (Thompson and Eidhammer, 2014). Therefore, activation and heterogeneous ice nucleation
589 parameterizations (INPs) with respect to dust aerosols were developed and incorporated into WRF-
590 Chem to explore ACI effects as well as both ARI and ACI effects of dust aerosols in Asia (Jin et al.,
591 2016a, 2015; Su and Fung, 2018a, 2018b; Wang K. et al., 2018; Zhang Y. et al., 2015b). During dust
592 storms, including the adsorption activation of dust particles played vital roles in the simulations of
593 ACI-related cloud properties and a 45 % of increase of cloud droplet number concentration (CDNC),
594 comparing to a simpler aerosols activation scheme in WRF-Chem (Wang K. et al., 2018). More
595 sophisticated INPs implemented in WRF-Chem that taking dust particles into account as IN resulted

带格式的: 字体颜色: 文字 1

带格式的: 字体: 非倾斜, 字体颜色: 文字 1, 非上标/
下标

带格式的: 字体: 五号, 字体颜色: 文字 1

596 in substantial modifications of cloud and ice properties as well as surface meteorological variables
597 and air pollutant concentrations in model simulations (Su and Fung, 2018b; Zhang Y. et al., 2015b).
598 Zhang Y. et al. (2015b) delineated that dust aerosols acting either as CCN or IN made model results
599 rather different regarding radiation, T2, precipitation, and number concentrations of cloud water and
600 ice. Su and Fu (2018b) described that the ACI effects of dust had less impacts on the radiative forcing
601 than its ARI effects and dust particles could promote (demote) ice (liquid) clouds in mid-upper (low-
602 mid) troposphere over EA. With turning on both ARI and ACI effects of dust, less low-level clouds
603 and more mid- and high-level clouds were detected that contributed to cooling at the Earth's surface
604 and in the lower atmosphere and warming in the mid-upper troposphere (Su and Fung, 2018b).
605 Mineral dust particles transported by the westerly and southwesterly winds from the Middle East
606 (ME) affected the radiative forcing at TOA and the Earth's surface and in the ATM by the dust-
607 induced ARI and ACI in the Arabian Sea and the India subcontinent, and subsequently changed the
608 circulation patterns, cloud properties, and characteristics related to the India summer monsoon (ISM;
609 Jin et al., 2015, 2016b). Moreover, the effects of dust on precipitation are not only complex but also
610 highly uncertain, evidencing from several modeling investigations targeting a variety of areas in
611 Asia (Jin et al., 2016a, 2016b, 2015; Su and Fung, 2018b; Zhang Y. et al., 2015b). Less precipitation
612 from model simulations including dust effects was found at EA and dust particles acting mainly as
613 CCN or IN influenced precipitation in a rather different way (Zhang Y. et al., 2015b). A positive
614 response of ISM rainfall to dust particles from the ME was reported by Jin et al. (2015) and less
615 affected by dust storms from the local sources and NWC (Jin et al., 2016a). Jin et al. (2016b) further
616 elucidated that the impacts of ME dust on ISM rainfall were highly sensitive to the imaginary
617 refractive index of dust setting in the model, so that accurate simulations of the dust-rainfall
618 interaction depended on more precise representation of radiative absorptions of dust in two-way
619 coupled models. About 20 % of increase or decrease in rainfall due to the dust effects were detected
620 in different areas over EA from the WRF-Chem simulations (Su and Fung, 2018b). However, it
621 should be mentioned that a few studies that targeting DRF of dust in Asia based on WRF-Chem
622 simulations but without enabling aerosol-radiation feedbacks (Ashrafi et al., 2017; Chen S. et al.,
623 2017b; Tang et al., 2018) were not included in this paper.

624 Along with the modeling research on the effects of dust aerosols on meteorology, their impacts
625 on air quality in Asia were explored using two-way coupled models (Chen et al., 2014; Kumar
626 et al., 2014; Li and Sokolik, 2018; Li M. M. et al., 2017a; Wang et al., 2013). Many early modeling
627 research work involving two-way coupled models with dust only looked into the ARI or direct
628 radiative effects of dust particles, which are described as follows. Taking a spring-time dust storm
629 from the Thar Desert into consideration in WRF-Chem, the modeled aerosol optical depth (AOD)
630 and Angstrom exponent (as indicators of aerosol optical properties and unique proxies of the surface
631 particulate matter pollution) demonstrated that turning on the ARI effects of dust could reduce biases
632 in their simulations, but were underestimated in North India (Kumar et al., 2014). Wang et al. (2013)
633 pointed out that in EA, including the longwave radiative effects of dust in the GRAPES-
634 CUACE/dust model lowered relative errors of the modeled AOD by 15 %, as compared to
635 simulations that only considering shortwave effects of dust. Comparisons against both satellite and
636 in situ observations depicted that the WRF-Chem model was able to capture the general
637 spatiotemporal variations of the optical properties and size distribution of dust particles over the
638 main dust sources in EA, such as the Taklimakan Desert and Gobi Desert, but overestimated AOD
639 during summer and fall and also exhibited positive (negative) biases in the fine (coarse) mode of
640 dust particles (Chen et al., 2014). Besides the ARI effects of dust, the heterogeneous chemistry on
641 dust particles' surface added in WRF-Chem was accounted for 80 % of the net reductions of O₃,
642 NO₂, NO₃, N₂O₅, HNO₃, ·OH, HO₂· and H₂O₂ when a springtime dust storm striking the Nanjing
643 megacity of EC (Li M. M. et al., 2017a). In CA, AOD was overestimated by WRF-Chem model but
644 its simulation was improved when more detailed mineral components of dust particles were
645 incorporated in the model (Li and Sokolik, 2018). Later on, more investigations started to focus on
646 both ARI and ACI effects of dust aerosols. With consideration of ARI as well as both ARI and ACI
647 of dust particles from the ME, during the ISM period, the WRF-Chem model reproduced AOD's
648 spatial distributions but underpredicted (overpredicted) AOD over the Arabian Sea (the Arabian
649 Peninsula) comparing with satellite observations and AOD reanalysis data (Jin et al., 2016a, 2016b,
650 2015). In EA, Wang K. et al. (2018) demonstrated that including both ARI and ACI effects of dust
651 in WRF-Chem caused lower O₃ concentrations and by incorporating INPs, the WRF-Chem model
652 well simulated the surface PM₁₀ concentrations (Su and Fung, 2018a) with reduced (elevated)

653 surface concentrations of OH, O₃, SO₄²⁻, and PM_{2.5} (CO, NO₂, and SO₂) (Zhang Y. et al., 2015b). It
654 is worth noting that how to partition dust particles into fine mode and coarse mode or initialize their
655 size distribution in coupled models can affect simulations in many ways and requires more detailed
656 measurements at the source areas and further modeling studies.

657

658 4.1.2 Wildfire, sea salt and volcanic ash

659 [In the Maritime SEA region, peat and forest fire triggered by El Niño induced drought](#)
660 [conditions released huge amount of smoke particles, which promoted dire air pollution problems in](#)
661 [the downstream areas, and their ARI effects simulated by WRF-Chem enhanced radiative forcing at](#)
662 [the TOA and the atmospheric stability \(Ge et al., 2014\)](#). Ge et al. (2014) also pointed out the ARI
663 effects of these fires impaired (intensified) sea breeze at daytime (land breeze at nighttime) over this
664 region so that their impacts on cloud cover could be positive or negative in different areas and time
665 period (day or night). Sea salt and volcanic ash are also important natural aerosols for regions near
666 seashores and active volcanoes and surrounding areas but modeling studies of their ARI and ACI
667 effects are relatively scarce in Asia. Based on WRF-Chem simulations, Kedia et al. (2019a)
668 demonstrated that the feedbacks of sea salt aerosols impacted convective and nonconvective
669 precipitation rather variously in different areas of the India subcontinent. Jiang et al. (2019a, 2019b)
670 also used WRF-Chem with/without sea-salt emissions to evaluate the effects of sea salt on rainfall
671 in Guangdong Province of China, but unfortunately, no feedbacks were considered in the
672 simulations. So far there is no investigation targeting aerosol effects of volcanic ash from volcano
673 eruptions in Asia using coupled models.

674

675 4.2 Feedbacks of anthropogenic aerosols

676 Atmospheric pollutants from anthropogenic sources are the leading causes of heavy pollution
677 events occurring in Asia due to the acceleration of urbanization, industrialization, and population
678 growth in recent decades, particularly in China and India, and their ARI or/and ACI effects on
679 meteorology and air quality had been quantitatively examined using two-way coupled models
680 (Archer-Nicholls et al., 2019; Bharali et al., 2019; Gao M. et al., 2016b; Kumar et al., 2012a, 2012b;
681 Li and Liao, 2014; Wang J. et al., 2014; Wang Z. et al., 2018; Zhang B. et al., 2015; Yao et al., 2017;
682 Zhong et al., 2016). These modeling research work had been primarily focused on the ARI or/and
683 ACI effects of anthropogenic aerosols, their specific chemical components (especially the light-
684 absorbing aerosols, i.e., BC and brown carbon (BrC)) and aerosols originated from different sources.
685 The major findings are outlined as follows, with respect to the effects of anthropogenic aerosol
686 feedbacks on meteorology and air quality.

687 Concerning the meteorological responses, most papers treated anthropogenic aerosols as a
688 whole to explore their effects on meteorological variables based on coupled model simulations with
689 enabling ARI or/and ACI in WRF-Chem, WRF-CMAQ, WRF-CMAQ, GRAPES-CUACE and
690 WRF-NAQPMS (Bai et al., 2020; Gao M. et al., 2016b; Kumar et al., 2012a; Nguyen et al., 2019a,
691 2019b; Wang H. et al., 2015; J. Wang et al., 2014; Wang Z. F. et al., 2014; Zhang B. et al., 2015;
692 Zhang et al., 2018; Zhao et al., 2017). Generally, the main ARI effects of anthropogenic aerosols
693 resulted in decreases of SWRF, T2 and WS10, and PBLH, as well as increases of surface relative
694 humidity (RH2) and temperature in the ATM, which further suppressed PBL development (Gao Y.
695 et al., 2015; Li M. M. et al., 2017b; Nguyen et al., 2019a, 2019b; Xing et al., 2015c; Zhang et al.,
696 2018). Wang H. et al. (2015) utilized GRAPES₂-CUACE with ARI to study a summer haze case in
697 the NCP area and discovered that the ARI effects made the subtropical high less intense (-14 hPa)
698 to help pollutants in the area to dissipate. In Asia, ACI effects of anthropogenic aerosols on cloud
699 properties and precipitation are relatively complex. On the one hand, anthropogenic aerosols, that
700 being activated as CCN, enhanced CDNC and LWP and then slowed down the precipitation onset,
701 but their impacts on precipitation amounts varied in different seasons and areas in China (Zhao et
702 al., 2017). Targeting a summertime rainstorm in the middle reaches of the Yangtze River (MRYR)
703 in China, sensitivity studies using WRF-Chem unveiled that CDNC, cloud water contents, and
704 precipitation decreased (increased) with low (high) anthropogenic emission scenarios due to the
705 ACI effects and these variations tended to depend on atmospheric humidity (Bai et al., 2020). The
706 modeling investigations with WRF-Chem aiming at the ISM (Kedia et al., 2019) and a disastrous
707 flood event in Southwest China (SWC) (Fan et al., 2015) pointed out that the simulated convective
708 process was suppressed and convective (nonconvective) precipitation was inhibited (enhanced) by

709 the ARI and ACI effects of accumulated anthropogenic aerosols, but these effects could invigorate
710 convection and rainfall in the downwind mountainous area at nighttime (Fan et al., 2015). On the
711 other hand, how anthropogenic aerosols act in the ice nucleation processes is still open to question
712 (Zhao et al., 2019) and these processes need to be represented accurately in two-way coupled models,
713 however until now no study had been performed to simulate the ACI effects of anthropogenic
714 aerosol serving as IN in Asia using two-way coupled models. Therefore, in Asia, further
715 investigations are needed that targeting cloud or/and ice processes involving anthropogenic aerosols
716 (including their size, composition, and mixing state) in two-way coupled models. Meanwhile,
717 several studies not only discussed aerosol feedbacks but also focused on the additional effects of
718 topography or urban heat island on meteorology (Wang D. et al., 2019; Zhong et al., 2017, 2015).
719 Utilizing the GATOR-GCMOM model at global and local scales, Jacobson et al. (2015, 2019)
720 explored the impacts of landuse changes due to the unprecedented expansions of megacities, such
721 as Beijing and New Delhi in Asia, from 2000 to 2009 on meteorology and air quality.

722 Hitherto there were several attempts to ascertain the effects of different chemical components
723 of anthropogenic aerosols on meteorology in Asia (Archer-Nicholls et al., 2019; Ding et al., 2019;
724 Ding et al., 2016; Gao J. et al., 2018; Huang et al., 2015; Wang Z. et al., 2018). First of all, Asia is
725 the region in the world with the highest BC emissions due to burning of large amount of fossil fuels
726 and biomass and this has increasingly attracted many researchers to probe into the ARI or/and ACI
727 effects of BC (Boucher et al., 2013). As the most important absorbing aerosol, BC induced the
728 largest positive, positive and negative mean DRF at the TOA, in the ATM, and at the surface,
729 respectively, over China during 2006 (Huang et al., 2015). Ding et al. (2016) and Wang Z. et al.
730 (2018) further applied WRF-Chem with feedbacks to investigate how aerosol-PBL interactions
731 involving BC suppressed the PBL development, which deteriorated air quality in Chinese cities and
732 was described as “dome effect” (namely BC warms the atmosphere and cools the surface, suppresses
733 the PBL development and eventually results in more accumulation of pollutants). This “dome effect”
734 of BC promoted the advection-radiation fog and fog-haze formation in the YRD area through
735 altering the land-sea circulation pattern and increasing the moisture level (Ding et al., 2019). Gao J.
736 et al. (2018) also pointed out BC in the ATM modified the vertical profiles of heating rate and
737 equivalent potential temperature in Nanjing, China. In India, the ARI effects of BC enhanced
738 convective activities, meridional flows, and rainfall in North-East India during the pre-monsoon
739 season but could either enhance or suppress precipitation during the monsoon season in different
740 parts of the India subcontinent (Soni et al., 2018). Moreover, the ARI effects of BC on surface
741 meteorological variables were larger than its ACI effects in EC (Archer-Nicholls et al., 2019; Ding
742 et al., 2019). Besides BC, the BrC portion of organic aerosols (OA) emitted from agriculture residue
743 burning (ARB) were included in WRF-Chem with the parameterization scheme suggested by Saleh
744 et al. (2014) and the model simulations in EC revealed that at the TOA, the net DRF of OA was -
745 0.22 W·m⁻² (absorption and scattering DRF were +0.21 W·m⁻² and -0.43 W·m⁻² respectively), but
746 the BC's DRF was still the highest (+0.79 W·m⁻²) (Yao et al., 2017). As mentioned above, it is
747 obvious that ARI and ACI effects of different aerosol components are substantially distinctive, and
748 many other aerosol compositions (e.g., sulfate, nitrate and ammonium) besides BC and BrC should
749 be taken into considerations in future modeling studies in Asia.

750 ARB is a common practice in many Asian countries after harvesting and before planting and
751 can deteriorate air quality quickly as one of the most important sources of anthropogenic aerosols,
752 so that it has been attracting much attention among the public and scientists worldwide (Chen J. et
753 al., 2017; Hodshire et al., 2019; Koch and Del Genio, 2010; Reid et al., 2005; Yan et al., 2018).
754 Recently, the effects of ARB aerosols on meteorology had widely been explored using the two-way
755 coupled model (WRF-Chem) in many Asian countries and regions, such as EC (Huang et al., 2016;
756 Li M. et al., 2018; Wu et al., 2017; Yao et al., 2017), South China (SC) (Huang et al., 2019), and
757 South Asia (SA) (Singh et al., 2020). In general, when ARB occurred, the WRF-Chem simulations
758 from all the studies showed that the changes in radiative forcing induced by ARB aerosols were
759 greater than by those from other anthropogenic sources, especially in the ATM. Also all the modeling
760 studies indicated that ARB aerosols reduced (increased) radiative forcing at the surface (in the ATM),
761 cooled (warmed) the surface (the atmosphere), and increased (decreased) atmospheric stability
762 (PBLH). Furthermore, the WRF-Chem simulations with ARI demonstrated that light-absorbing
763 carbonaceous aerosols (CAs) from ARB caused daytime (nighttime) precipitation decreased
764 (increased) over Nanjing in EC during a post-harvest ARB event (Huang et al., 2016). Yao et al.
765 (2017) pointed out their WRF-Chem simulations in EC exhibited larger DRE induced by BC from

删除的内容: As the most important absorbing aerosol, BC induced the largest positive, positive and negative mean DRF at the TOA (followed by sulfate and other types of aerosols with negative DRF), in the ATM (followed by mineral dust), and at the surface, respectively, over China during 2006 (Huang et al., 2015).

772 ARB at the TOA than previous studies. Lately, several modeling studies using WRF-Chem had
773 targeted the effects of ARI and both ARI and ACI due to ARB aerosols from countries in the
774 Indochina, SEA, and SA regions during the planting and harvesting time (Dong et al., 2019; Huang
775 et al., 2019; Singh et al., 2020; Zhou et al., 2018). Zhou et al. (2018) investigated how ARB aerosols
776 from SEA mixed with mineral dust and other anthropogenic aerosols while being lifted to the mid-
777 low troposphere over the source region and transported to the YRD area and then affected
778 meteorology and air quality there. The influences of ARI and ACI caused by ARB aerosols from
779 Indochina were contrary, namely, the ARI (ACI) effects made the atmosphere over SC warmer
780 (cooler) and drier (wetter), and the ARI effects hindered cloud formation and suppressed
781 precipitation there (Huang et al., 2019). Dong et al. (2019) found the warming ARI effects of ARB
782 aerosols were smaller over the source region (i.e., SEA) than the downwind region (i.e., SC) with
783 cloudier conditions. Annual simulations regarding the ARI effects of ARB aerosols from SA
784 (especially Myanmar and Punjab) indicated that CAs released by ARB reduced the radiative forcing
785 at the TOA but did not change the precipitation processes much when only the ARI effects were
786 considered in WRF-Chem (Singh et al., 2020).

787 Besides ARB, to our best knowledge, there were only a few research work quantitatively
788 assessing the effects of anthropogenic aerosols from different emission sources on meteorology
789 using WRF-Chem. Gao M. et al. (2018b) evaluated the responses of radiative forcing in China and
790 India to aerosols from five emission sectors (power, industry, residential, BB, and transportation),
791 and found that the power (residential) sector was the dominate contributor to the negative (positive)
792 DRF at the TOA over both countries due to high emissions of sulfate and nitrate precursors (BC
793 and the total sectoral contributions were in the order of power > residential > industry > BB >
794 transportation (power > residential > transportation > industry > BB) for China (India) during 2013.
795 To pinpoint the ARI and ACI effects, Archer-Nicholls et al. (2019) reported that during January
796 2014, the aerosols from the residential emission sector induced larger SWRF (+1.04 W·m⁻²) than
797 LWRF (+0.18 W·m⁻²) at the TOA and their DRF (+0.79 W·m⁻²) was the largest, followed by their
798 semidirect effects (+0.54 W·m⁻²) and indirect effects (-0.29 W·m⁻²) over EC. This study further
799 emphasized a realistic ratio of BC to total carbon from the residential emission was critical for
800 accurate simulations of the ARI and ACI effects with two-way coupled models.

801 In terms of anthropogenic aerosol effects on air quality, the responses of PM_{2.5} had been widely
802 investigated (Chen et al., 2019a; Gao J. et al., 2018; Gao M. et al., 2016b; Gao Y. et al., 2015;
803 Nguyen et al., 2019a, 2019b; Wang H. et al., 2015; Wang J. et al., 2014; Wang Z. F. et al., 2014;
804 Wu et al., 2019a; Zhang B. et al., 2015; Zhang et al., 2018; Zhao et al., 2017) but less studies
805 explored the responses of O₃ and other species (Kumar et al., 2012b; Li J. et al., 2018; Nguyen et
806 al., 2019a, 2019b; Xing et al., 2017; Zhang B. et al., 2015). As summarized by Wu et al. (2019a) in
807 their Table 1, observations and model simulations with WRF-Chem, WRF-CMAQ, WRF-CMAQ,
808 GRAPES-CUACE, and WRF-NAQPMS all pointed out that the ARI effects promoted higher PM_{2.5}
809 concentrations in China (Chen et al., 2019a; Gao M. et al., 2016b; Gao Y. et al., 2015; Wang H. et
810 al., 2015; Wang J. et al., 2014; Wang Z.F. et al., 2014; Zhang B. et al., 2015; Zhang et al., 2018) and
811 this was also true in other areas of Asia (e.g., India, EA, Continental SEA) (Gao M. et al., 2018b;
812 Nguyen et al., 2019a, 2019b) during different seasons. At the same time, all the modeling
813 investigations revealed that the positive aerosol-meteorology feedbacks could further exacerbate
814 pollution problems during heavy haze episodes. Based on WRF-Chem simulations, the ACI effects
815 on PM_{2.5} was negligible comparing to the ARI effects over EC (Zhang B. et al., 2015) but was
816 subject to a certain degree of uncertainty if no consideration of the ACI effects induced by cumulus
817 clouds in the model (Gao Y. et al., 2015). Annual WRF-Chem simulations for 2014 by Zhang et al.
818 (2018) indicated that even though the ARI effects had bigger impacts on PM_{2.5} during wintertime
819 than the ACI effects, the ARI and ACI impacts on PM_{2.5} were similar during other seasons and the
820 increase of PM_{2.5} due to the ACI effects was more noticeable in wet season than dry season. Using
821 the process analysis method to distinguish the contributions of different physical and chemical
822 processes to PM_{2.5} over the NCP area, Chen et al. (2019a) applied WRF-Chem with ARI and ACI
823 and found that besides local emissions and regional transport processes, vertical mixing contributed
824 the most to the accumulation and dispersion of PM_{2.5}, comparing to chemistry and advection, and
825 the ARI effects changed the vertical mixing contribution to daily PM_{2.5} variation from negative to
826 positive. Regarding surface O₃ concentrations, all the two-way coupled models with ARI, ACI, and
827 both ARI and ACI predicted reduced photolysis rate and O₃ concentrations under heavy pollution
828 conditions, through the radiation attenuation induced by aerosols and clouds. Further analyses

829 indicated that the ARI effects impacted O₃ positively through reducing vertical dispersions (WRF-
830 CMAQ, Xing et al., 2017), reduced O₃ more during wintertime than summertime in EC (WRF-
831 NAQPMS, Li J. et al., 2018), and suppressed (enhanced) O₃ in dry (wet) season in continental SEA
832 (WRF-CMAQ, Nguyen et al., 2019b). Xing et al. (2017) applied the process analysis method in
833 WRF-CMAQ with ARI and revealed that the impacts of ARI on the contributions of atmospheric
834 dynamics and photochemistry processes to O₃ over China varied in winter and summer months and
835 ARI induced largest changes in photochemistry (dry deposition) of surface O₃ at noon time in
836 January (July). The process analysis in WRF-Chem with ARI and ACI identified that the vertical
837 mixing process played the most important role among the other physical and chemical processes
838 (advection and photochemistry) in surface O₃ growth during 10-14 local time in Nanjing, China
839 (Gao J. et al., 2018). ARI and ACI not only affected PM_{2.5} and O₃, but also other chemical species.
840 For instance, CO and SO₂ increased due to ARI and ACI over EC (Zhang B. et al., 2015), ARI
841 caused midday (daily average) OH increased (decreased) in July (January) over China (Xing et al.,
842 2017), SO₂, NO₂, BC, SO₄²⁻, NO₃⁻ were enhanced but OH was reduced over China by ACI (Zhao
843 et al., 2017), and ARI impacted SO₂ and NO₂ positively over EA (Nguyen et al., 2019a). Wu et al.
844 (2019b) further analyzed how the aerosol liquid water involved in ARI and chemical processes (i.e.,
845 photochemistry and heterogeneous reactions) and influenced radiation and PM_{2.5} (esp. secondary
846 aerosols) over NCP during an intense haze event. Moreover, evaluations and sensitivity studies
847 indicated that turning on aerosol feedbacks could improve the model performance for surface PM_{2.5},
848 particularly during severe haze episodes (Li J. et al., 2018; Wang H. et al., 2018; Zhang B. et al.,
849 2015; Zhang et al., 2018).

850 With reference to the feedback effects of anthropogenic aerosol compositions on air quality,
851 most modeling research work with WRF-Chem had focused on the ARI and ACI effects of BC and
852 BrC, especially the “dome effect” that prompted the accumulation of pollutants (aerosols and O₃)
853 near surface and in PBL (Ding et al., 2016; Ding et al., 2019; Gao J. et al., 2018; Li and Liao, 2014;
854 Wang Z. et al., 2018). At the same time, the ARI effects of BC undermined the low-level wind
855 convergence and then led to decrease of aerosols (sulfate and nitrate) and O₃ (Li and Liao, 2014).
856 With the process analysis methodology in WRF-Chem, Gao J. et al. (2018) indicated that comparing
857 to simulations without BC, the BC and PBL interaction slowed the O₃ growth from late morning to
858 early afternoon somewhat before O₃ reaching its maximum value at noon due to less vertical mixing
859 in PBL.

860 Studies on the feedback effects of aerosols from different emission sectors on air quality were
861 relatively limited and mainly involved with ARB emissions and assessments of emission controls
862 during certain major air pollution events. Jena et al. (2015) applied WRF-Chem with aerosol
863 feedbacks and investigated O₃ and its precursors in SA due to regional ARB. Based on WRF-Chem
864 simulations with enabling ARI and ACI, Wu et al. (2017) denoted that aerosols emitted from ARB
865 could be mixed or/and coated with urban aerosols while being transported to cities and contributed
866 to heavy air pollution events there, such as in Nanjing, China. The ARI effects induced by ARB
867 aerosols on O₃ and NO₂ concentrations (-1 % and 2 %, respectively) were small compared to the
868 contribution of precursors emitted from ARB to O₃ chemistry (40 %) in the ARB zone (Li M. et al.,
869 2018). Pollutants emitted from natural and anthropogenic BB over Indochina affected pollution
870 levels over SC and their ACI effects removed aerosols more efficiently than the ARI effects that
871 could make BB aerosols last longer in the ATM (Huang et al., 2019). Gao et al. (2017a) and Zhou
872 et al. (2019) both utilized WRF-Chem to evaluate what role the ARI effects played when dramatic
873 emission reductions implemented during the week of Asia Pacific Economic Cooperation Summit
874 and concluded that the ARI reduction induced by decreased emission led to 6.7-10.9 % decline in
875 PM_{2.5} concentrations in Beijing.

876 877 4.3 Human health effects

878 Poor air quality posts risks to human health (Brunekreef and Holgate, 2002; Manisalidis et al.,
879 2020), therefore, in the past several decades, air quality models had been used in epidemiology
880 related research to establish quantitative relationships between concentrations of various pollutants
881 and burden of disease (including mortality or/and morbidity) as well as associated economic loss
882 (Conti et al., 2017). In Asia, there were several studies that applied coupled air quality models with
883 feedbacks to assess human health effects of air pollutants under historical and future scenarios
884 (Conibear et al., 2018a, 2018b; Gao et al., 2017b; Gao M. et al., 2015; Ghude et al., 2016; Hong et
885 al., 2019; Wang et al., 2017; Xing et al., 2016; Zhong et al., 2019). By applying WRF-Chem with

删除的内容: With the process analysis methodology in WRF-Chem, Gao J. et al. (2018) indicated that comparing to simulations without BC, the BC and PBL interaction slowed the O₃ growth from late morning to early afternoon somewhat before reaching its maximum value in afternoon due to less vertical mixing in PBL, even though more O₃ precursors were trapped in PBL that promoted photochemical reaction of O₃.

ARI and ACI, M. Gao et al. (2015) estimated the health and financial impacts induced by an intense air pollution event happened in the NCP area during January, 2013 and concluded that the mortality, morbidity, and financial loss over Beijing area were 690, 69070, and 253.8 million US\$, respectively. Targeting the same case, Gao M. et al. (2017b) pointed out that turning on the data assimilation of surface PM_{2.5} observations in WRF-Chem not only improved model simulations but also made the premature death numbers increased by 2 % in the NCP area, comparing to simulations without the PM_{2.5} data assimilation. In India, WRF-Chem simulations with aerosol feedbacks and updated population data revealed that the premature (COPD related) deaths caused by PM_{2.5} (O₃) were 570,000 (12,000), resulting in shortened life expectancy (3.4±1.1 years) and financial expenses (640 million US\$) during 2011 (Ghude et al., 2016). Based on WRF-CMAQ simulations with ARI for 21 years (1990-2010), Xing et al. (2016) pointed out that in EA the population-weighted PM_{2.5} induced mortality had an upward trend from 1990 (+3187) to 2010 (+3548) and the mean mortality caused by ARI-enhanced PM_{2.5} was 3.68 times more than that decreased by ARI-reduced temperature. The same 21 year simulations also showed that from 1990 to 2010, the PM_{2.5} related mortalities in EA and SA rose by 21 % and 85 %, respectively, while they declined in Europe and high-income North America by 67 % and 58 %, respectively (Wang et al., 2017). Conibear et al. (2018a) applied WRF-Chem with ARI to study how different emission sectors affected human health in India and demonstrated that the residential energy use sector played the most critical role among other sectors and could cause 511,000 premature deaths in 2014. Furthermore, Conibear et al. (2018b) investigated future PM_{2.5} pollution levels as well as health impacts in India under different emission scenarios (business as usual and two emission control pathways) and deduced that the burden of disease driven by PM_{2.5} and population factors (growth and aging) in 2050 increased by 75 % under the business as usual scenario but decreased by 9 % and 91 % under the International Energy Agencies New Policy Scenario and Clean Air Scenario, respectively, comparing with that in 2015. The sensitivity study using WRF-Chem with ARI under a variety of emission scenarios, population projections, and concentration-response functions (CRFs) for the years of 2008 and 2050 demonstrated that CRFs (future emission projections) were the main sources of uncertainty in the total mortality estimations related to PM_{2.5} (O₃) in China (Zhong et al., 2019). Applying a suite of models, including WRF-CMAQ with ARI, climate and epidemiology, Hong et al. (2019) inferred that under Representative Concentration Pathway 4.5, the future mortalities could be 12100 and 8900 per year in China led by PM_{2.5} and O₃, respectively, and the climate-driven weather extremes could add 39 % and 6 % to future mortalities due to stable atmosphere and heat waves, respectively. Ten Hoeve and Jacobson (2012) applied GATOR-GCMOM and a human exposure model to estimate the local and worldwide health effects induced by the 2011 Fukushima nuclear accident and a hypothetical one in California of US.

带格式的: 字体颜色: 文字 1

5 Effects of aerosol feedbacks on model performance

Even though there are a certain number of research papers using two-way coupled models to quantify the effects of aerosol feedbacks on regional meteorology and air quality in Asia, model performances impacted by considering aerosol effects varied to some extent. This section provides a summary of model performance by presenting the SI of meteorology and air quality variables as shown in Table S2. These SI were collected from the selected papers that supplying these indices and being defined as papers with SI (PSI) (listed in Tables B2-B3 of Appendix B). As aforementioned in Section 3, investigations of ACI effects were very limited and no former studies simultaneously exploring aerosol feedbacks with and without both ARI and ACI turned on. Here, we only compared the SI for simulations with and without ARI in the same study, as summarized in Appendix Tables B4-B5. It should be pointed out that all the reported evaluation results either from individual model or inter-model comparison studies were extracted and put into the Table S2.

5.1 Model performance for meteorology variables

With certain emissions, accurate simulations of meteorological elements are critical to air quality modeling and prediction (Appel et al., 2017; Bauer et al., 2015; Saylor et al., 2019; Seaman, 2000). Targeting meteorological variables, we summarized their SI and further analyzed the variations of SI on different simulated time scales and among multiple models.

948 5.1.1 Overall performance

949 Figure 3 shows the compiled statistical indicators (correlation coefficient (R) is in black, and
950 mean bias (MB) and root mean square error (RMSE) are in blue) of T2 (°C), RH2(%) and specific
951 humidity (SH2, g·kg⁻¹) at 2 meters, and WS10 (m·s⁻¹) from PSI (a-d), and simulations with and
952 without ARI (marked as ARI and NO-ARI in e-h). In this figure and following figures, NP and NS
953 are number of publications and samples with SI, respectively and summed up in Appendix Table
954 B2. In these two tables, we also listed the NS of positive (red upward arrow) and negative (blue
955 downward arrow) biases for the meteorological and air quality variables in parentheses in the MB
956 column. Note that NS in Fig. 3e-h and Appendix Table B4 counted the samples of SI provided by
957 the simulations simultaneously with and without ARI. Also, the 5th, 25th, 75th and 95th percentiles
958 of SI are illustrated in box-and-whisker plots, and the dashed line in the box is the mean value (not
959 median) and the circles are outliers.

960 The evaluations for T2 (Fig. 3a) from PSI revealed that in Asia coupled models performed
961 rather well for temperature (mean R = 0.90) with RMSE ranging from 0.64 to 5.90 °C, but 60 % of
962 samples showed the tendency towards temperature underestimations (mean value of MB = -0.20 °C)
963 with the largest average MB (-0.31 °C) occurring during winter months (70 samples). The
964 underestimations of temperature had been reported not only from modeling studies by using WRF
965 or coupled models, but also in Asia, Europe and North America (Brunner et al., 2015; Gao et al.,
966 2019; García-Díez et al., 2013; Makar et al., 2015a; Yahya et al., 2015). The WRF simulations in
967 China (Gao et al., 2019) and US (EPA, 2018) also showed wintertime cold biases of T2 but in Europe
968 warm biases were reported (García-Díez et al., 2013). This temperature bias was probably related
969 to the impacts of model resolutions (Kuik et al., 2016), urban canopies (Liao et al., 2014) and PBL
970 schemes (Hu et al., 2013). With the ARI turned on in the coupled models, modeled temperatures
971 (limited papers with 12 samples) were improved somewhat and the mean correlation coefficient
972 increased from 0.93 to 0.95 and RMSE decreased slightly (Fig. 3e), but average MB of temperature
973 was decreased from -0.98 to -1.24 °C. In short, temperatures from PSI or simulations with/without
974 ARI turned on agreed well with observations but were mostly underestimated, and the negative bias
975 of T2 simulated by models with ARI turned on got worse and reasons behind it will be explained in
976 Section 6.

977 Figures 3b-c illustrate that RH2 was simulated reasonably well (mean R = 0.73) and the
978 modeled SH2 was also well correlated with observations (R varied between 0.85 and 1.00). RH2
979 and SH2 from more than half of samples had slightly positive and negative mean biases with average
980 MB values of 0.4 % and -0.01 g·kg⁻¹, respectively. The overestimations of RH2 could be caused by
981 the negative bias of T2 (Cuchiara et al., 2014). Compared with results without ARI effects, statistics
982 of RH2 and SH2 from simulations with ARI showed better R and RMSE. However, the increased
983 positive mean biases (average MBs of RH2 and SH2 were from 6.4 % to 7.6 % and from 0.07 g·kg⁻¹
984 to 0.11 g·kg⁻¹, respectively) indicated that turning on ARI could cause further overprediction of
985 humidity variables. Overall, the modeled RH2 and SH2 were in good agreement with observations
986 with slight over- and under-estimations, respectively, and the limited studies showed that RH2 and
987 SH2 simulated by models with ARI turned on had marginally larger positive biases relative to the
988 results without ARI.

989 Compared with the correlation coefficients of T2, RH2 and SH2, mean R (0.59) of WS10 was
990 smallest with a large fluctuation ranging from 0.14 to 0.98 (Fig. 3d). The meta-analysis also
991 indicated that most modeled WS10 tended to be overestimated (81 % of the samples) with the
992 average MB value of 0.79 m·s⁻¹, and the mean RMSE value was 2.76 m·s⁻¹. The general
993 overpredictions of WS10 by WRF (Mass and Ovens, 2011) and coupled models (Gao M. et al.,
994 2018a; Gao Y. et al., 2015) had been explained with possible reasons such as out-of-date
995 geographical data, coarse model resolutions and lacking of better representations of urban canopy
996 physics. The PSI with ARI effects suggested that the correlation of wind speed was slightly
997 improved (mean R from 0.56 to 0.57) and the average RMSE and positive MB decreased by 0.003
998 m·s⁻¹ and 0.051 m·s⁻¹, respectively (Fig. 3h). The collected SI indicated relatively poor performance
999 of modeled WS10 (most wind speeds were overestimated) compared to T2 and humidity, but turning
1000 on ARI in coupled models could improve WS10 simulations somewhat.

1001 Besides the SI discussed above, very limited papers reported the normalized mean error (NME)
1002 (%) of surface meteorological variables (T2, SH2, RH2 and WS10) simulated by two-way coupled
1003 models (WRF-Chem and WRF-CMAQ) in Asia, which is summarized in Appendix Table B7. The
1004 evaluations with two-way coupled models in Asia showed that the overall mean percent errors of

删除的内容: It should be noted that only 2 or 1 PSI
supplying statistical analysis of modeled RH2 and SH2
with/without ARI effects may not be enough to make these
comparisons statistically significant and further investigations
are much needed.

删除的内容: very

T2, SH2, RH2 and WS10 were 22.71%, 10.32%, 13.94%, and 51.28%, respectively. The ranges of NME (%) values were quite wide for T2 (from -0.48 to 270.20%) and WS10 (from 0.33 to 112.28%) reported by the limited studies. Note that no NME of surface meteorological variables simulated by two-way coupled models simultaneously with and without enabling the ARI effects was mentioned in these studies.

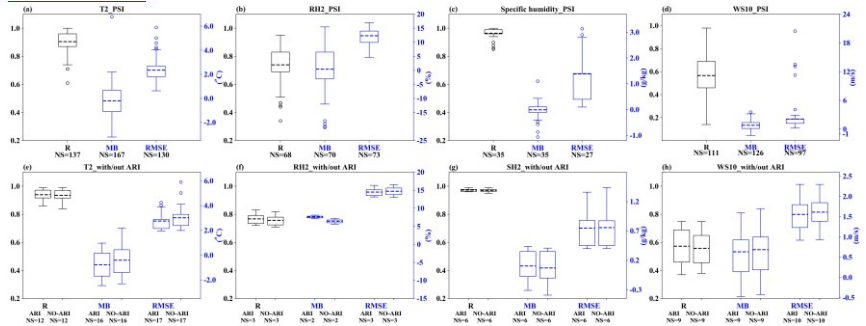


Figure 3. Quantile distributions of R, MB and RMSE for simulated surface meteorological variables by the five coupled models (WRF-Chem, WRF-CMAQ, GRAPES-CUACE, WRF-NAQPMS and GATOR-GCMOM) (a-d) and comparisons of statistical indices with/out ARI (e-h) in Asia.

5.1.2 Comparisons of SI for meteorology using different coupled models

Also, to examine how different coupled models (i.e., WRF-Chem, WRF-CMAQ, WRF-NAQPMS, GRAPES-CUACE and GATOR-GCMOM) performed in Asia with respect to meteorological variables, the SI were extracted from PSI in term of these five coupled models and displayed in Fig. 4. The SI for T2, RH2, SH2, and WS10 from WRF-NAQPMS, GRAPES-CUACE and GATOR-GCMOM simulations were missing or with rather limited samples so that the discussions here only focused on the WRF-Chem and WRF-CMAQ simulations. Moreover, the SI sample size from studies involving WRF-Chem was generally larger than that involving WRF-CMAQ, except for SH2.

As seen in Fig. 4a, the modeled T2 by both WRF-CMAQ and WRF-Chem was well correlated with observations but WRF-CMAQ (mean R = 0.95) outperformed WRF-Chem (mean R = 0.90) to some extent. On the other hand, WRF-CMAQ underestimated T2 (mean MB = -1.39 °C) but WRF-Chem slightly overestimated it (mean MB = 0.09 °C) (Fig. 4e). The RMSE of modeled T2 by both models was at the similar level with mean RMSE values of 2.51 °C and 2.31 °C by WRF-CMAQ and WRF-Chem simulations, respectively (Fig. 4i).

Both WRF-Chem and WRF-CMAQ performed better for SH2 (mean R = 0.96 and 0.97, respectively) than RH2 (mean R = 0.75 and 0.73, respectively) (Figures 4b and 4c), which might be due to the influence of temperature on RH2 (Bei et al., 2017). Also the modeled RH2 (SH2) by WRF-Chem correlated better (worsen) with observations than those by WRF-CMAQ. The mean RMSE of modeled RH2 (Fig. 4j) by WRF-Chem (11.1 %) was lower than that by WRF-CMAQ (14.3%) but the mean RMSE of modeled SH2 (Fig. 4k) by WRF-Chem (2.25 g·kg⁻¹) higher than that by WRF-CMAQ (0.71 g·kg⁻¹). It was seen in Figures 4f and 4d that WRF-CMAQ overestimated RH2 and SH2 (average MB were 5.30 % and 0.07 g·kg⁻¹, respectively), and WRF-Chem underpredicted RH2 (average MB = -0.32 %) and SH2 (average MB = -0.06 g·kg⁻¹). Generally, the modeled RH2 and SH2 were reproduced more reasonably by WRF-Chem than those by WRF-CMAQ.

The modeled WS10 by both WRF-Chem and WRF-CMAQ (Fig. 4d) correlated with observations on the same level with the mean R of 0.56. The mean RMSE of modeled WS10 by WRF-Chem and WRF-CMAQ were 1.54 m·s⁻¹ and 2.28 m·s⁻¹, respectively, as depicted in Fig. 4l. Both models overpredicted WS10 to some extent with average MBs of 0.55 m·s⁻¹ (WRF-CMAQ) and 0.84 m·s⁻¹ (WRF-Chem), respectively. These results demonstrated that overall WRF-CMAQ and WRF-Chem had similar model performance of WS10.

In general, WRF-CMAQ performed better than WRF-Chem for T2 but worse for humidity (RH2 and SH2), and both models' performance for WS10 was very similar. WRF-Chem overestimated T2, RH2 and WS10 and underestimated SH2 slightly, while WRF-CMAQ

删除的内容: Figure 3. The quantile distributions of R, MB and RMSE for different meteorological variables from coupled models performance data (a-d) and comparisons of the statistical indices with/out ARI (e-h).

5.1.2 Comparisons of SI at different temporal scales for meteorology

To probe the model performance of simulated T2, RH2, SH2 and WS2 at different temporal scales, the SI of these meteorological variables from PSI were grouped according to the simulation time (yearly, seasonal, monthly and daily) and plotted in Fig. 4. Note that the seasonal results contained SI values from simulations lasting more than one month and less than or equal to 3 months. Here in Fig. 4, NP and NS were the number of PSI and samples with SI at different time scales, respectively, and also their total values were the same as the ones listed in Appendix Table S2. The correlation between simulated and observed T2 (Fig. 4a) at the seasonal (mean R = 0.97 with the smallest sample size), yearly (0.91) and monthly (0.90) scales were stronger than that at the daily scale (0.87), indicating that long-term simulations of T2 were well reproduced by coupled models. As shown in Fig. 4e, T2 underestimation mentioned above (Fig. 3a) appeared also in the seasonal, monthly and yearly simulations (average MB = -0.87 °C, -0.15 °C and -0.34 °C, respectively), but the daily T2 were overestimated (average MB = 0.07 °C). It should be noted that T2 at the monthly scale was underpredicted mainly during winter months (16 samples). Regarding the mean RMSE, its value (Fig. 4i) at the daily scale was the largest (0.97 °C) in comparison with that at the other temporal scales. Given that no SI was available for RH2 at the seasonal scale, results at other time scales were discussed here. Figure 4b presented that simulated RH2 at the daily scale had the best correlation coefficient (mean R = 0.74), followed by those at the monthly (0.73) and yearly (0.71) scales. Except overestimation (average MB = 3.6 %) at the yearly scale (Fig. 4f), modeled RH2 were underestimated at the monthly (average MB = -1.1 %) and daily (average MB = -0.2 %) scales, respectively. Therefore, coupled models calculated RH2 reasonably well in short-term simulations. However, at the daily scale, RMSE of modeled RH2 (Fig. 4j) was relatively large fluctuation ranging from 6.2 % to 21.3 %. Lacking of SI for SH2 at the daily scale, only those at other time scales were compared. Even though NP and NS were very limited, the modeled SH2 (Fig. 4c) exhibited especially good correlation with observations with the mean R values exceeding 0.95 at the yearly, seasonal and monthly scales (0.99, 0.97 and 0.96, respectively) but had the largest mean RMSE (2.09 g·kg⁻¹) at the yearly scale (Fig. 4k). Also, both over- and under-estimations of modeled SH2 (Fig. 4g) were reported at different time scales with average MB values as 0.15 g·kg⁻¹, -0.02 g·kg⁻¹, and -0.14 g·kg⁻¹ for yearly, seasonal and monthly simulations, respectively. Generally, the long-term simulations of SH2 agreed better with observations than the short-term ones.

As seen in Fig. 4d, the modeled WS10 at the monthly scale (mean R = 0.68) correlated with observations better than that at the daily, yearly and seasonal scales (mean R = 0.62, 0.48 and 0.46, respectively). The simulations at all temporal scales tended to overestimate WS10 comparing against observations (Fig. 4h) and their average MB were 0.80 m·s⁻¹ (seasonal), 0.86 m·s⁻¹ (monthly), 0.64 m·s⁻¹ (yearly) and 0.62 m·s⁻¹ (daily).

删除的内容: 3

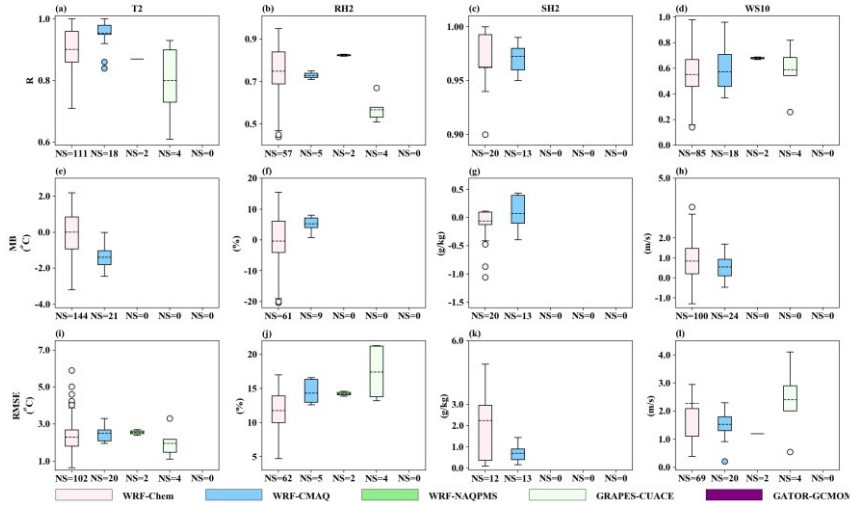
删除的内容: 5e

删除的内容: 5i

删除的内容: 5d

1186 overpredicted humidity and WS10 but underpredicted T2. Compared to WRF-Chem and WRF-
 1187 CMAQ, the very few SI samples indicated that for the meteorological variables excluding SH2,
 1188 WRF-NAQPMS simulations matched with observations better than GRAPES-CUACE simulations
 1189 but more applications and statistical analysis of these two models are needed to make this kind of
 1190 comparison conclusive.

1191



1193

1194 **Figure 4.** Quantile distributions of the statistical indices for simulated surface meteorological variables by WRF-
 1195 Chem, WRF-CMAQ, GRAPES-CUACE, WRF-NAQPMS and GATOR-GCMOM in Asia.

1196

1197 5.2 Model performance for air quality variables

1198

5.2.1 Overall performance

1199

1200 The results of the overall statistical evaluation for the online air quality simulations are
 1201 presented in Figure 5, and all labels and colors indicating SI were the same as those for
 1202 meteorological variables. In this figure and following figures, NP and NS are number of publications
 1203 and samples with SI, respectively and summed up in Appendix Table B3. In Fig. 5a, the correlation
 1204 between the simulated and observed $PM_{2.5}$ concentrations from PSI showed that in Asia coupled
 1205 models performed relatively well for $PM_{2.5}$ (mean $R = 0.63$), but RMSE was between -87.60 and
 1206 80.90 and more than half of samples of simulated $PM_{2.5}$ were underestimated (mean $MB = -2.08$
 1207 $\mu g \cdot m^{-3}$). Note that NS in Fig. 5c-d and Appendix Table B5 counted the samples of SI provided by
 1208 the simulations simultaneously with and without ARI. With the ARI turned on in the coupled models,
 1209 modeled $PM_{2.5}$ concentrations (limited papers with 15 samples) were improved somewhat and the
 1210 mean R slightly increased from 0.71 to 0.72 and mean absolute MB decreased from 4.10 to 1.33
 1211 $\mu g \cdot m^{-3}$ (Fig. 5c), but RMSE of $PM_{2.5}$ concentrations slightly increased from 35.40 to 36.20 $\mu g \cdot m^{-3}$.
 1212 In short, $PM_{2.5}$ with/without ARI agreed well with observations but were mostly underestimated,
 1213 and $PM_{2.5}$ bias simulated by models became overpredicted.

1214

1215 Compared with $PM_{2.5}$, mean R (0.59) of O_3 was relatively smaller (Fig. 5b). The statistical
 1216 analysis also showed the most modeled O_3 concentrations tended to be overestimated (76% of the
 1217 samples) with the average MB value of 8.05 $\mu g \cdot m^{-3}$, and the mean RMSE value was 32.65 $\mu g \cdot m^{-3}$.
 1218 The 14 PSI with ARI effects suggested that the correlation of O_3 was slightly improved (mean R
 1219 from 0.58 to 0.64) and the average RMSE and MB were decreased by 15.93 $\mu g \cdot m^{-3}$ and 1.55 $\mu g \cdot m^{-3}$,
 1220 respectively (Fig. 5d). The collected studies indicated relatively poor performance of modeled O_3
 1221 compared to $PM_{2.5}$, but turning on ARI in coupled models improved O_3 simulations somewhat.

1222

1223 In addition to the SI analyzed above and similar to the surface meteorological variables, the
 1224 NME (%) of $PM_{2.5}$ and O_3 is listed in Table B7. The limited studies with WRF-Chem and WRF-
 CMAQ indicated that the overall mean percent errors of $PM_{2.5}$ and O_3 were 47.63% (from 29.55 to
 104.70%) and 43.03% (from 21.10 to 127.00%), respectively. With the ARI effects enabled in
 WRF-Chem in different seasons over the China domain, the NME (%) of $PM_{2.5}$ increased slightly

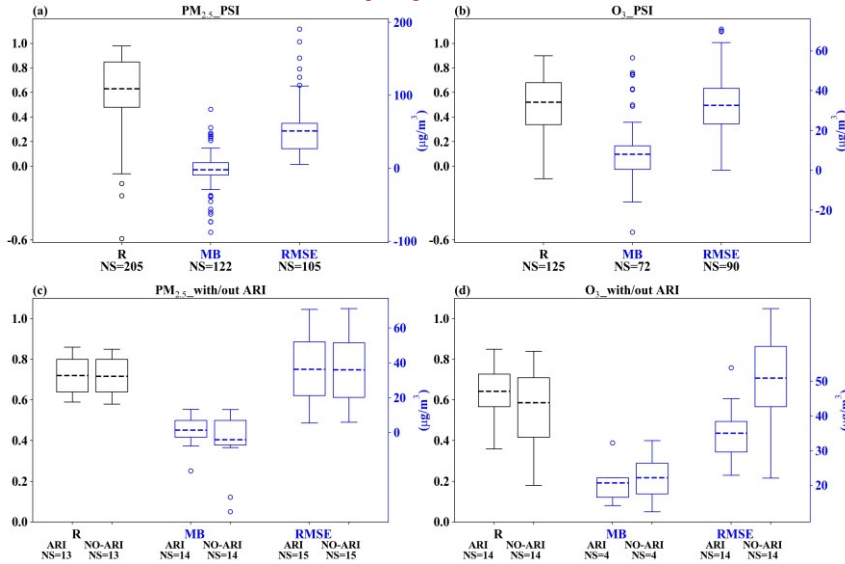
1225

删除的内容: 6c

删除的内容: 6d

1227
1228
1229

during most seasons, except during a spring month with little change (Zhang et al., 2018). Another study by Nguyen et al. (2019b) revealed that the NME (%) of $PM_{2.5}$ and O_3 simulated by WRF-CMAQ became a little worse in SEA comparing to the simulations without ARI.



1230
1231
1232
1233
1234
1235

Figure 5. Quantile distributions of statistical indices for simulated $PM_{2.5}$ and O_3 (a-b) by the five two-way coupled models (WRF-Chem, WRF-CMAQ, GRAPES-CUACE, WRF-NAQPMS and GATOR-GCMOM) and comparisons of statistical indices with/out ARI (c-d) in Asia.

5.2.2 Comparisons of SI for air quality using different coupled models

1236
1237
1238
1239
1240
1241
1242
1243
1244
1245
1246
1247
1248
1249

Figure 6 showed the SI for $PM_{2.5}$ and O_3 from different coupled models, and only WRF-Chem and WRF-CMAQ simulations were discussed for the same reason as in Section 5.1.2. The modeled $PM_{2.5}$ by WRF-CMAQ (mean $R = 0.69$) outperformed WRF-Chem (mean $R = 0.62$) to some extent (Fig. 6a) and the RMSE of modeled $PM_{2.5}$ by WRF-CMAQ ($33.24 \mu\text{g}\cdot\text{m}^{-3}$) was smaller than that by WRF-Chem ($56.16 \mu\text{g}\cdot\text{m}^{-3}$). With respect to MB, WRF-CMAQ overestimated $PM_{2.5}$ (mean $MB = +1.60 \mu\text{g}\cdot\text{m}^{-3}$) but WRF-Chem slightly underestimated it (mean $R = -3.12 \mu\text{g}\cdot\text{m}^{-3}$) (Fig. 6c). Figure 6b showed that the modeled O_3 by WRF-CMAQ (0.60) correlated better with observations than those by WRF-Chem (0.47), but the mean RMSE of modeled O_3 (Fig. 6f) by WRF-Chem ($27.13 \mu\text{g}\cdot\text{m}^{-3}$) was lower than that by WRF-CMAQ ($35.19 \mu\text{g}\cdot\text{m}^{-3}$). It was seen in Figures 6d that both WRF-CMAQ and WRF-Chem overestimated O_3 , with mean MBs as 11.98 and $7.21 \mu\text{g}\cdot\text{m}^{-3}$, respectively. Generally, the modeled $PM_{2.5}$ and O_3 were reproduced more reasonably by WRF-CMAQ than by WRF-Chem, even though there were much more samples available from WRF-Chem simulations than WRF-CMAQ simulations.

删除的内容: 3

删除的内容: 8b

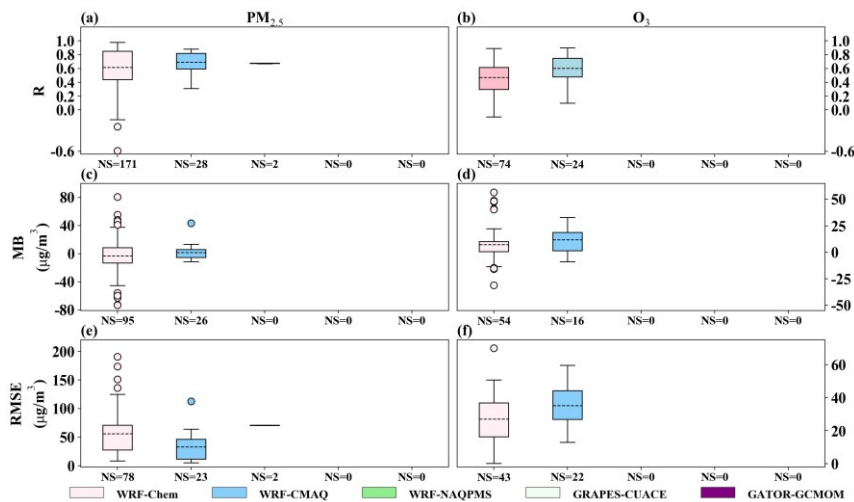


Figure 6. Quantile distributions of R, MB and RMSE of $PM_{2.5}$ and O_3 simulated by WRF-Chem, WRF-CMAQ, GRAPES-CUACE, WRF-NAQPMS and GATOR-GCMOM in Asia.

6 Impacts of aerosol feedbacks in Asia

Aerosol feedbacks not only impact the performances of two-way coupled models but also the simulated meteorological and air quality variables to a certain extent. In this section, we collected and quantified the variations (Table S3) of these variables induced by ARI or/and ACI from the modeling studies in Asia. Due to limited sample sizes in the collected papers, the target variables only include radiative forcing, surface meteorological parameters (T2, RH2, SH2 and WS10), PBLH, cloud, precipitation, and $PM_{2.5}$ and gaseous pollutants.

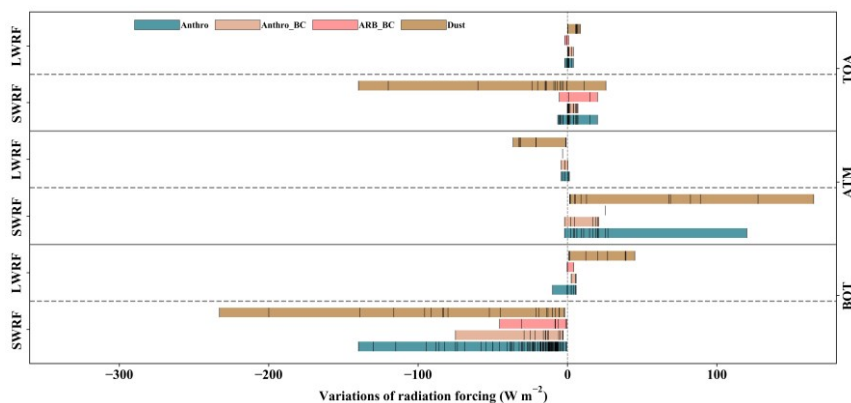
6.1 Impacts of aerosol feedbacks on meteorology

6.1.1 Radiative forcing

With regard to radiative forcing, most studies with two-way coupled models in Asia had focused on the effects of dust aerosols (Dust), BC emitted from ARB (ARB_BC) and anthropogenic sources (Anthro_BC), and total anthropogenic aerosols (Anthro). Figure 7 presents the variations of simulated SWRF and LWRF at the bottom (BOT) and TOA and in the ATM due to aerosol feedbacks, and detailed information of these variations are compiled in Table S5. In this figure, the color bars show the range of radiative forcing variations and the black tick marks inside the color bars represent these variations extracted from all the collected papers. It should be noted that in this figure all the radiative forcing variations were plotted regardless of temporal resolutions of data reporting and simulation durations. Apparently in Asia, most studies targeted the SWRF variations induced by anthropogenic aerosols at the BOT that exhibited the largest differences ranging from -140.00 to $-0.45 \text{ W}\cdot\text{m}^{-2}$, with the most variations (88 % of samples) concentrated in the range of -50.00 to $-0.45 \text{ W}\cdot\text{m}^{-2}$. The SWRF variations due to anthropogenic aerosols in the ATM and at the TOA were -2.00 to $+120.00 \text{ W}\cdot\text{m}^{-2}$ and -6.50 to $20.00 \text{ W}\cdot\text{m}^{-2}$, respectively. There were much less studies reported LWRF variations caused by anthropogenic aerosols, which ranged from -10.00 to $+5.78 \text{ W}\cdot\text{m}^{-2}$, -1.91 to $+3.94 \text{ W}\cdot\text{m}^{-2}$, and -4.26 to $+1.21 \text{ W}\cdot\text{m}^{-2}$ at the BOT and TOA, and in the ATM, respectively.

Considering BC from anthropogenic sources and ARB, they both led to positive SWRF at the TOA (with mean values of 2.69 and $7.55 \text{ W}\cdot\text{m}^{-2}$, respectively) and in the ATM (with mean values of 11.70 and $25.45 \text{ W}\cdot\text{m}^{-2}$, respectively) but negative SWRF at the BOT (with mean values of -18.43 and $-14.39 \text{ W}\cdot\text{m}^{-2}$, respectively). The responses of LWRF to Anthro_BC and ARB_BC at the BOT (in the ATM) on average were 4.01 and $0.72 \text{ W}\cdot\text{m}^{-2}$ (-1.89 and $-3.24 \text{ W}\cdot\text{m}^{-2}$), respectively, and weak at the TOA ($+0.92$ and $-0.53 \text{ W}\cdot\text{m}^{-2}$, respectively). The SWRF variations induced by dust were in the range of -233.00 to $-1.94 \text{ W}\cdot\text{m}^{-2}$ and -140.00 to $+25.70 \text{ W}\cdot\text{m}^{-2}$, and $+1.44$ to $+164.80 \text{ W}\cdot\text{m}^{-2}$ at the BOT and TOA, and in the ATM, respectively. The LWRF variations caused by dust were the

1291 largest (with mean values of $22.83 \text{ W}\cdot\text{m}^{-2}$ and $+5.20 \text{ W}\cdot\text{m}^{-2}$, and $-22.12 \text{ W}\cdot\text{m}^{-2}$ at the BOT and TOA,
 1292 and in the ATM, respectively), comparing to the ones caused by anthropogenic aerosols and BC
 1293 aerosols from anthropogenic sources and ARB.
 1294



1295 [Figure 7. Variations of shortwave and longwave radiative forcing \(SWRF and LWRF\) simulated by two-way](#)
 1296 [coupled models \(WRF-Chem, WRF-CMAQ, GRAPES-CUACE, WRF-NAQPMS and GATOR-GCMOM\) with](#)
 1297 [aerosol feedbacks at the bottom and top of atmosphere \(BOT and TOA\), and in the atmosphere \(ATM\) in Asia.](#)
 1298
 1299

1300 As shown in Fig. 7, SWRF variations at the BOT caused by total aerosols (sum of Anthro,
 1301 Anthro_BC, ARB_BC and Dust) had been widely assessed in Asia. Therefore, we further analyzed
 1302 their spatiotemporal distributions and inter-regional differences, which are displayed in Fig. 8.
 1303 Figure 8a presents the SWRF variations over different areas of Asia (the acronyms used in Fig. 8
 1304 are listed in Appendix Table B1) at different time scales. In Asia, almost 41 % of the selected papers
 1305 investigated SWRF towards its monthly variations, 36 % towards its hourly and daily variations,
 1306 and 23 % towards its seasonal and yearly variations. Most studies reported aerosol-induced SWRF
 1307 variations were primarily conducted in NCP, EA, China, and India. At the hourly scale, the range of
 1308 SWRF decreases was from -350.00 to $-5.90 \text{ W}\cdot\text{m}^{-2}$ (mean value of $-106.92 \text{ W}\cdot\text{m}^{-2}$) during typical
 1309 pollution episodes, and significant variations occurred in EA. The daily and monthly mean SWRF
 1310 reductions varied from -73.71 to $-5.58 \text{ W}\cdot\text{m}^{-2}$ and -82.20 to $-0.45 \text{ W}\cdot\text{m}^{-2}$, respectively, with relative
 1311 large perturbations in NCP. At the seasonal and yearly scales, the SWRF changes ranged from $-$
 1312 22.54 to $-3.30 \text{ W}\cdot\text{m}^{-2}$ and -30.00 to $-2.90 \text{ W}\cdot\text{m}^{-2}$ with mean value of -11.28 and $-11.82 \text{ W}\cdot\text{m}^{-2}$,
 1313 respectively, with EA as the most researched area.

1314 To identify the differences of aerosol-induced SWRF variations between high- (Asia) and low-
 1315 polluted regions (Europe and North America), their inter-regional comparisons are depicted in Fig.
 1316 8b. This figure does not include information about temporal resolutions of data reporting and
 1317 durations of model simulations with ARI or/and ACI, but intends to delineate the range of SWRF
 1318 changes due to aerosol feedbacks. The SWRF variations fluctuated from -233.00 to $-0.45 \text{ W}\cdot\text{m}^{-2}$, $-$
 1319 100.00 to $-1.00 \text{ W}\cdot\text{m}^{-2}$, and -600.00 to $-1.00 \text{ W}\cdot\text{m}^{-2}$ in Asia, Europe, and North America, respectively.
 1320 It should be pointed out that the two extreme values were caused by dust ($-233.00 \text{ W}\cdot\text{m}^{-2}$) in Asia
 1321 and wildfire ($-600.00 \text{ W}\cdot\text{m}^{-2}$) in North America. Overall, the median value of SWRF reductions due
 1322 to ARI or/and ACI in Asia ($-15.92 \text{ W}\cdot\text{m}^{-2}$) was larger than those in North America ($-10.50 \text{ W}\cdot\text{m}^{-2}$)
 1323 and Europe ($-7.00 \text{ W}\cdot\text{m}^{-2}$).
 1324

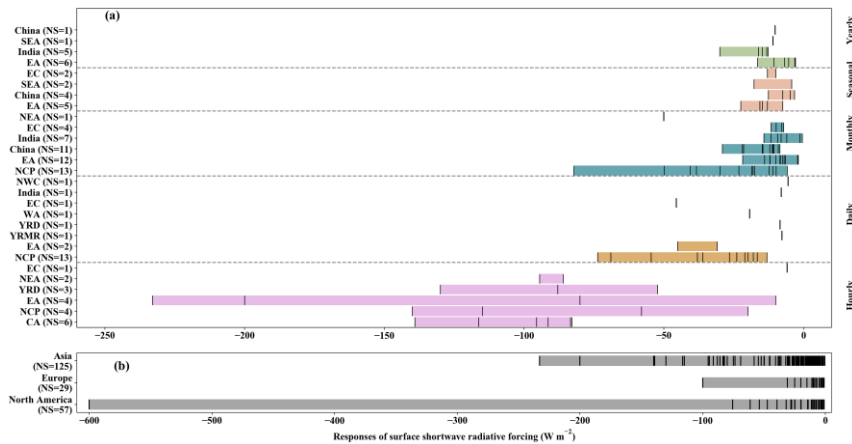


Figure 8. Responses of shortwave radiation forcing to aerosol feedbacks in different areas/periods in Asia (a) and the inter-regional comparisons of its variations in Asia, Europe and North America (b).

6.1.2 Temperature, wind speed, humidity and PBLH

The impact of aerosols on radiation can influence energy balance, which eventually alter other meteorological variables. The summary of aerosol-induced variations of T2, WS10, RH2, SH2 and PBLH in different regions of Asia as well as at different temporal scales are provided in Table 6. In this table, the minimum and maximum values were collected from the corresponding papers and the mean values were calculated with adding all the variations from these papers and then divided by the number of samples.

Overall, aerosol effects led to decreases of T2, WS10 and PBLH with average changes of -0.65 °C, -0.13 m s⁻¹ and -60.70 m, respectively, and increases of humidity (mean Δ RH2 = 2.56 %) in most regions of Asia. On average, the hourly aerosol-induced changes of surface meteorological variables (T2, WS10 and RH2) and PBLH were the largest among the different time scales. At the hourly time scale, the mean variations of T2, WS10, RH2 and PBLH due to ARI or/and ACI were -1.85 °C, -0.32 m s⁻¹, 4.60 % and -165.84 m, respectively, and their absolute maximum values in EC, YRD, NCP and NCP, respectively. Compared to variations at the hourly time scale, smaller daily variations of T2, WS10, RH2 and PBLH were caused by aerosol effects, and their mean values were -0.63 °C, -0.15 m s⁻¹, +2.89 % and -34.61 m, respectively. The largest daily variations of T2, WS10, RH2 and PBLH occurred in NCP, EC, EC and SEC, respectively. For other time scales (monthly, seasonal and yearly), the respective mean variations of T2, RH2 and PBLH induced by aerosol effects were comparable. However, the WS10 perturbations at the monthly time scale were about two to three times higher than those at the seasonal and yearly time scales. High variations at the monthly, seasonal and yearly time scales were reported in NCP (T2, RH2 and PBLH), EA (T2, WS10 and PBLH) and PRD (T2 and PBLH), respectively. In addition, comparing to T2 and PBLH, the aerosol-induced variations of WS10 and humidity were less revealed.

Table 6. Summary of variations of surface meteorological variables and planetary boundary layer height (PBLH) caused by aerosol feedbacks simulated by two-way coupled models (WRF-Chem, WRF-CMAQ, GRAPES-CUACE, WRF-NAQPMS and GATOR-GCMOM) in different regions of Asia and at different temporal scales.

Region	Time scale	Δ T2 [mean] (°C)	Δ WS10 [mean] (m s ⁻¹)	Δ RH2/SH2 [mean]	Δ PBLH [mean] (m)
EC	hours	-8.00 to -0.20 [-2.68]			-300.00 to -50.00 [-175.00]
EA	hours	-3.00 to -2.00 [-2.50]			
YRD	hours	-1.40 to -1.00 [-1.15]	-0.80 to -0.10 [-0.41]		-276.00 to -29.90 [-105.42]
NCP	hours	-2.80 to -0.20 [-1.05]	-0.30 to -0.10 [-0.23]	1.00 % to 12.00 % [4.60 %]	-287.20 to -147.00 [-217.10]
Hourly mean		-1.85	-0.32	4.60%	-165.84
NCP	days	-2.00 to -0.10 [-0.88]	-0.4 to -0.01 [-0.17]	0.51 % to 4.10 % [2.52 %]	-111.40 to -10.00 [-49.07]

EC	days	-0.94 to -0.65 [-0.79]	-0.52 to -0.37 [-0.45]	1.92 % to 9.75 % [5.84 %]	
India	days	-1.60 to 0.10 [-0.75]			
SEC	days	-1.38 to -0.18 [-0.70]	-0.07 to 0.05 [-0.023]	-0.37 % to 6.57 % [2.63 %]	-84.1 to -27.55 [-53.62]
NEA	days	-0.52	-0.08		-46.39
MRYSR	days	-0.16	-0.01	0.56 %	-16.46
India	days				-6.90
Daily mean		-0.63	-0.15	2.89 %	-34.61
India	months	-0.45			
NCP	months	-1.30 to -0.06 [-0.43]		1.30 % to 4.70 % [2.53 %]	-109.00 to -5.48 [-36.01]
NEA	months	-0.30	-0.10		-50.00
PRD	months	-0.60 to 0.13 [-0.16]			
EA	months	-0.45 to -0.03 [-0.13]			-35.70 to -13.00 [-24.35]
China	months	-0.89 to 0.60 [-0.12]			-66.60 to -2.30 [-25.67]
EC	months	-0.30 to -0.05 [-0.11]			-13.10 to -6.20 [-9.65]
Monthly mean		-0.24	-0.10	2.53 %	-29.13
EA	seasons	-0.58 to -0.30 [-0.40]	-0.05 to -0.02 [-0.035]		-64.62 to -30.70 [-43.27]
SEA	seasons	-0.39 to -0.03 [-0.21]	-0.06 to -0.01 [-0.035]		-48.33 to -6.71 [-27.52]
Seasonal mean		-0.31	-0.035		-34.61
PRD	years	-0.27			-45.00
TP	years	-0.24			
SEA	years	-0.21	-0.03		-27.25
EA	years		-0.03	0.13 g·kg ⁻¹	-46.47 to -45.00 [-45.74]
EC	years		-0.014	0.21 %	
Yearly mean		-0.24	-0.025	0.21 %	-39.33

1357

1358 6.1.3 Cloud and precipitation

1359 In the included publications, only a few papers focusing on the effects of aerosol feedbacks on
1360 cloud properties (cloud fraction, LWP, ice water path (IWP), CDNC and cloud effective radius) and
1361 precipitation characteristics (amount, spatial distribution, peak occurrence and onset time) using
1362 two-way coupled models in Asia, as shown in Table 7. In this table, the abbreviations representing
1363 aerosol emission sources (Dust, ARB_BC, Anthro_BC, and Anthro) and regions in Asia are defined
1364 in Appendix Table B1. The plus and minus signs indicate increase and decrease, respectively.

1365 The variations of cloud properties and precipitation characteristics induced by ARI or/and ACI
1366 are rather complex and not uniform in different parts of Asia and time periods. BC from both ARB
1367 and anthropogenic sources reduced cloud fraction through ARI and both ARI and ACI in several
1368 areas in China. ARI or/and ACI induced by anthropogenic aerosols could increase or decrease cloud
1369 fraction and affect cloud fraction differently in various atmospheric layers and time periods.
1370 Considering EA and subareas in China, anthropogenic aerosols tended to increase LWP through ARI
1371 and ACI as well as ACI alone but decrease LWP in some areas of SC (ARI and ACI) at noon and in
1372 afternoon during summertime and NC (ACI) in winter. ARI and ACI induced by anthropogenic BC
1373 aerosols had negative effects on LWP except at daytime in CC. Dust aerosols increased both LWP
1374 and IWP through ACI in EA, which was reported only by one study. The increase (decrease) of
1375 CDNC caused by the ARI and ACI effects of anthropogenic (anthropogenic BC) aerosols in EC
1376 during summertime was reported. Through ACI, anthropogenic aerosols affected CDNC positively
1377 in EA and China. Compared to anthropogenic aerosols, dust aerosols could have much larger
1378 positive impacts on CDNC via ACI in springtime over EA. The ACI effects of anthropogenic
1379 aerosols reduced cloud effective radius over China (January) and EA (July).

1380 Among all the variables describing cloud properties and precipitation characteristics, the
1381 variations of precipitation amount were studied the most using two-way coupled models in Asia.
1382 How turning on ARI or/and ACI in coupled models can change precipitation amount is not
1383 unidirectional and depends on many factors, including different aerosol sources, areas, emission
1384 levels, atmospheric humidity, precipitation types, seasons, and time of a day. [Under the high](#)

1385 [emission levels as well as at slightly different humidity levels of RH > 85 % with increasing](#)
1386 [emissions, the ACI effects of anthropogenic aerosols induced precipitation increase in the MRYR](#)
1387 [area of China. Over the same area, precipitation decreased due to the ACI effects of anthropogenic](#)
1388 [aerosols with the low emission levels and RH < 80 %. In PRD, wintertime precipitation was](#)
1389 [enhanced by the ACI effects of anthropogenic aerosols but inhibited by ARI. In SK, summertime](#)
1390 [precipitation was both enhanced and inhibited by the ACI and ARI effects of anthropogenic aerosols.](#)
1391 In locations upwind (downwind) of Beijing, rainfall amount was raised (lowered) by the ARI effects
1392 of anthropogenic aerosols but lowered (raised) by ACI. Both ARI and ACI induced by anthropogenic
1393 aerosols had positive impacts on total, convective, and stratiform rain in India during the summer
1394 season and the increase of convective rain was larger than those of stratiform. Summertime
1395 precipitation amounts could be enhanced or inhibited at various subareas inside simulation domains
1396 over India, China, and Korea and during day- or night-time due to ARI and ACI of anthropogenic
1397 aerosols. Over China, dust-induced ACI decreased (increased) springtime precipitation in CC
1398 (western part of NC), and over India, dust aerosols from local sources and ME had positive impacts
1399 on total, convective, and stratiform rain through ARI and ACI. Simulations in India also revealed
1400 that precipitation could be increased in some subareas but decreased in another and absorptive (non-
1401 absorptive) dust enhanced (inhibited) summertime precipitation via ARI and ACI. The ARI (ACI)
1402 effects of BC from ARB caused precipitation reduction (increase) in SEC but CAs emitted from
1403 ARB (ARB_CAs) caused rainfall enhancement in Myanmar. During pre-monsoon (monsoon)
1404 season, ARI induced by anthropogenic BC could lead to +42 % (-5 to -8 %) variations of
1405 precipitation in NEI (SI). Considering both ARI and ACI effects, BC from ARB and sea salt aerosols
1406 enhanced or inhibited precipitation in different parts of India and BC from anthropogenic sources
1407 enhanced (inhibited) nighttime (daytime) rainfall in CC (NC and SC) at the rate of +1 to +4 mm·day⁻¹
1408 (-2 to -6 mm·day⁻¹) during summer season. With respect to spatial variations, 6.5 % larger rainfall
1409 area in PRD was caused by ARI and ACI effects under 50 % reduced anthropogenic emissions. ACI
1410 induced by anthropogenic aerosols tended to delay the peak occurrence time and onset time of
1411 precipitation by one to nine hours in China and South Korea.
1412

1413 [Table 7. Summary of changes of cloud properties and precipitation characteristics due to aerosol feedbacks](#)
1414 [simulated by two-way coupled models \(WRF-Chem, WRF-CMAQ, GRAPES-CUACE, WRF-NAQPMS and](#)
1415 [GATOR-GCMOM\) in Asia.](#)

Variables	Variations (aerosol effects)	Simulation time period	Regions	References
	-7 % low-level cloud (ARB_BC ARI)	Apr., 2013	SEC	Huang et al., 2019
	+0.03 to +0.08 below 850 hPa and at 750 hPa (Anthro ARI & ACI), esp. at early morning and nighttime	Aug., 2008	EC	Gao and Zhang, 2018
	Max -0.06 between 750 hPa and 850 hPa (Anthro ARI & ACI), esp. in afternoon and evening	Aug., 2008	CC	Gao and Zhang, 2018
	-0.02 to -0.06 below 750 hPa (Anthro_BC ARI & ACI), esp. in afternoon	Aug., 2008	SC & NC	Gao and Zhang, 2018
Cloud fraction	-0.04 to -0.06 between 750 hPa and 850 hPa (Anthro_BC ARI & ACI), esp. in afternoon	Aug., 2008	CC	Gao and Zhang, 2018
	-6.7 % to +3.8 % (Anthro ARI)	Jun. 6-9 & Jun. 11-14, 2015	SK	Park et al., 2018
	+22.7 % (Anthro ACI)	Jun. 6-9 & Jun. 11-14, 2015	SK	Park et al., 2018
	-0.03 % low-, -0.54 % middle- and -0.58 % high-level cloud (Anthro ACI)	2008 to 2012	PRD	Liu Z. et al., 2018
Cloud properties	+5 to +50 g·m ⁻² (Anthro ARI & ACI)	Aug., 2008	EC	Gao and Zhang, 2018
	+10 to +20 g·m ⁻² (Anthro_BC ARI & ACI) at daytime	Aug., 2008	CC	Gao and Zhang, 2018
	-5 to -40 g·m ⁻² (Anthro ARI & ACI) at noon and in afternoon	Aug., 2008	Part of SC	Gao and Zhang, 2018
	-2 to -20 g·m ⁻² (Anthro_BC ARI & ACI)	Aug., 2008	SC	Gao and Zhang, 2018
	-2 to -30 g·m ⁻² (Anthro_BC ARI & ACI)	Aug., 2008	NC	Gao and Zhang, 2018
LWP	Max+18 g·m ⁻² (Dust ACI)	Mar.-May., 2010	EA	Wang et al., 2018
	+40 to +60 g·m ⁻² (Anthro ACI)	Jan., 2008	SC	Gao et al., 2012
	+40 g·m ⁻² (Anthro ACI)	Jan., 2008	CC	Gao et al., 2012
	Less than +5 g·m ⁻² or -5 g·m ⁻² (Anthro ACI)	Jan., 2008	NC	Gao et al., 2012
	+30 to +50 g·m ⁻² (Anthro ACI)	Jul., 2008	EA	Gao et al., 2012
IWP	+5 to +10 g·m ⁻² (Dust ACI)	Mar. 17-Apr. 30, 2012	EA	Su and Fung, 2018a
CDNC	+20 to +160 cm ⁻³ (Anthro ARI & ACI)	Aug., 2008	EC	Gao and Zhang, 2018

Cloud effective radius		-5 to -60 cm ⁻³ (Anthro_BC ARI & ACI)	Aug., 2008	EC	Gao and Zhang, 2018		
		Max +10500 cm ⁻³ (Dust ACI)	Mar.-May., 2010	EA	Wang et al., 2018		
		+650 cm ⁻³ (Anthro ACI)	Jan., 2008	EC	Gao et al., 2012		
		+400 cm ⁻³ (Anthro ACI)	Jan., 2008	CC & SWC	Gao et al., 2012		
		Less than +200 cm ⁻³ (Anthro ACI)	Jan., 2008	NC	Gao et al., 2012		
		+250 to +400 cm ⁻³ (Anthro ACI)	Jul., 2008	EA	Gao et al., 2012		
		More than -4 μm (Anthro ACI)	Jan., 2008	SWC, CC & SEC	Gao et al., 2012		
		More than -2 μm (Anthro ACI)	Jan., 2008	NC	Gao et al., 2012		
		-3 μm (Anthro ACI)	Jul., 2008	EA	Gao et al., 2012		
	Precipitation (precip.)	Amount	Enhancement/inhibition of precip. due to high/low Anthro emission. ACI inhibited (enhanced) precip. at RH < 80 % (> 85 %) with increasing Anthro emissions	Jun. 18-19, 2018	MRYS	Bai et al., 2020	
-4.72 mm (Anthro ARI) and +33.7 mm (Anthro ACI)			Dec. 14-16, 2013	PRD	Liu Z. et al., 2020		
+2 to +5 % (ARB CAs ARI)			Mar.-Apr., 2013	Myanmar	Singh et al., 2020		
-1.09 mm·day ⁻¹ (ARB_BC ARI)			Apr., 2013	SEC	Huang et al., 2019		
+0.49 mm·day ⁻¹ (ARB_BC ACI)			Apr., 2013	SEC	Huang et al., 2019		
-0 to -4 mm·day ⁻¹ (Anthro ARI & ACI)			Jun.-Sep., 2010	Indus basin & eastern IGP	Kedia et al., 2019b		
+1 to +3 mm·day ⁻¹ non-convective rain (Anthro ARI & ACI)			Jun.-Sep., 2010	WG of India	Kedia et al., 2019b		
+5 mm·day ⁻¹ non-convective rain (Anthro ARI & ACI)			Jun.-Sep., 2010	NEI	Kedia et al., 2019b		
Increase of total rain (Dust ARI & ACI)			Jun.-Sep., 2010	NI, CI, WG, NEI & central IGP	Kedia et al., 2019b		
Decrease of total rain (Dust ARI & ACI)			Jun.-Sep., 2010	NWI & SPI	Kedia et al., 2019b		
Decrease of total rain (ARB_BC ARI & ACI)			Jun.-Sep., 2010	WG, SPI, NWI, EI & NEI	Kedia et al., 2019b		
Increase of total rain (ARB_BC ARI & ACI)			Jun.-Sep., 2010	CI, Central IGP & EPI	Kedia et al., 2019b		
Decrease of total rain (Sea salt ARI & ACI)			Jun.-Sep., 2010	EPI, WPI, CPI & SPI	Kedia et al., 2019b		
Increase of total rain (Sea salt ARI & ACI)			Jun.-Sep., 2010	NCI & central IGP	Kedia et al., 2019b		
				-20 to -200mm (Anthro ARI & ACI)	Aug., 2008	SC & NC	Gao and Zhang, 2018
				+20 to +100 mm (Anthro_BC ARI & ACI)	Aug., 2008	CC	Gao and Zhang, 2018
				+1 to +4 mm·day ⁻¹ nighttime precip. (ARI & ACI of Anthro or Anthro_BC)	Aug., 2008	CC	Gao and Zhang, 2018
				-2 to -6 mm·day ⁻¹ daytime precip. (ARI & ACI of Anthro or Anthro_BC)	Aug., 2008	NC	Gao and Zhang, 2018
				-2 to -4 mm·day ⁻¹ daytime precip. (Anthro ARI & ACI)	Aug., 2008	SC	Gao and Zhang, 2018
				-2 to -6 mm·day ⁻¹ daytime precip. (Anthro_BC ARI & ACI)	Aug., 2008	SC	Gao and Zhang, 2018
				-54.6 to +24.1 mm (Anthro ARI)	Jun. 6-9, 2015	SK	Park et al., 2018
				-23.8 to +24.0 mm (Anthro ACI)	Jun. 6-9, 2015	SK	Park et al., 2018
				-63.2 to +27.1 mm (Anthro ARI & ACI)	Jun. 6-9, 2015	SK	Park et al., 2018
				Min -7.0 mm (Anthro ARI)	Jun. 11-14, 2015	SK	Park et al., 2018
				Min -36.6 mm (Anthro ACI)	Jun. 11-14, 2015	SK	Park et al., 2018
				+42 % (Anthro_BC ARI) during pre-monsoon season	Mar.-May., 2010	NEI	Soni et al., 2018
				-5 to -8 % (Anthro_BC ARI) during monsoon season	Jun.-Sep., 2010	SI	Soni et al., 2018
		+1 mm·day ⁻¹ precip. (Dust ACI)	Mar. 17-Apr. 30, 2012	Western part of NC	Su and Fung, 2018b		
		-1 mm·day ⁻¹ precip. (Dust ACI)	Mar. 17-Apr. 30, 2012	CC	Su and Fung, 2018b		
		+0.95 mm·day ⁻¹ precip. (absorptive Dust ARI & ACI)	Jun.-Aug., 2008	India	Jin et al., 2016a		
		-0.4 mm·day ⁻¹ precip. (non-absorptive Dust ARI & ACI)	Jun.-Aug., 2008	India	Jin et al., 2016a		
		+0.44 mm·day ⁻¹ total precip. (Dust ARI & ACI over whole study domain)	Jun.-Aug., 2008	India	Jin et al., 2016b		

删除的内容: (ACI)

	+0.34 mm·day ⁻¹ total precip. (Dust ARI & ACI from ME)	Jun.-Aug., 2008	India	Jin et al., 2016b
	+0.31 mm·day ⁻¹ total precip. (Anthro ARI & ACI over whole study domain)	Jun.-Aug., 2008	India	Jin et al., 2016b
	+0.32 mm·day ⁻¹ convective precip. (Dust ARI & ACI over whole study domain)	Jun.-Aug., 2008	India	Jin et al., 2016b
	+0.24 mm·day ⁻¹ convective precip. (ARI & ACI of Dust from ME)	Jun.-Aug., 2008	India	Jin et al., 2016b
	+0.20 mm·day ⁻¹ convective precip. (Anthro ARI & ACI over whole study domain)	Jun.-Aug., 2008	India	Jin et al., 2016b
	+0.12 mm·day ⁻¹ stratiform precip. (Dust ARI & ACI over whole study domain)	Jun.-Aug., 2008	India	Jin et al., 2016b
	+0.10 mm·day ⁻¹ stratiform precip. (ARI & ACI of Dust from ME)	Jun.-Aug., 2008	India	Jin et al., 2016b
	+0.11 mm·day ⁻¹ stratiform precip. (Anthro ARI & ACI over whole study domain)	Jun.-Aug., 2008	India	Jin et al., 2016b
	-48.29 %/+24.87 % precip. in downwind/upwind regions (Anthro ARI)	Jun. 27-28, 2008	Beijing	Zhong et al. 2015
	+33.26 % /-4.64 % precip. in downwind/upwind regions (Anthro ACI)	Jun. 27-28, 2008	Beijing	Zhong et al. 2015
	+0.44 mm·day ⁻¹ precip. (Dust ARI & ACI)	Jun. 1-Aug. 31, 2008	India	Jin et al., 2015
Spatial variation	+6.5 % precip. area (ARI & ACI) with 50% Anthro emissions	Jun. 9-12, 2017	YRD	Liu C. et al., 2019
	1 to 2h delay (Anthro ACI)	Jun. 18-19, 2018	MRYS	Bai et al., 2020
Peak occurrence time	1h delay (ARI & ACI) with 50% Anthro emissions	Jun. 9-12, 2017	YRD	Liu C. et al., 2019
	9h delay (Anthro ACI)	Jun. 7, 2015	Gosan, SK	Park et al., 2018
	4h delay (Anthro ACI)	Jun. 7, 2015	Jinju, SK	Park et al., 2018
Onset time	9h delay (Anthro ACI)	Jun. 7, 2015	Gosan, SK	Park et al., 2018
	2h delay (Anthro ACI)	Jun. 7, 2015	Jinju, SK	Park et al., 2018

1417
1418

6.2 Impacts of aerosol feedbacks on air quality

1419
1420
1421
1422
1423
1424

Aerosol effects not only gave rise to changes in meteorological variables but also air quality. Table 8 (the minimum, maximum and mean values were defined in the same way as in Table 6) summarizes the variations of atmospheric pollutant concentrations induced by aerosol effects in different regions of Asia and at different time scales. In Asia, most modeling studies with coupled models targeted the impacts of aerosol feedbacks on surface PM_{2.5} and O₃ concentrations, with only few focusing on other gaseous pollutants.

1425
1426
1427
1428
1429
1430
1431
1432
1433
1434
1435

Simulation results showed that turning on aerosol feedbacks in coupled models generally made PM_{2.5} concentrations increased in different regions of Asia at various time scales, which stemmed from decrease of shortwave radiation, T₂, WS10 and PBLH and increase of RH₂. Some studies did show negative impacts of aerosol effects on hourly, daily, and seasonal PM_{2.5} at some areas that could be attributed to ACI effects, changes in transport and dispersion patterns, reductions in humidity levels and secondary aerosol formations (Zhang B. et al., 2015; Zhan et al., 2017; Yang et al., 2017; Wang K. et al., 2018). Similar to the perturbations of surface meteorological variables due to aerosol effects, the hourly PM_{2.5} variations and the range were the largest compared to those at other time scales. The largest PM_{2.5} increases were reported in NCP, SEC, EA, SEA and PRD at the hourly, daily, monthly, seasonal and yearly time scales with average values of 23.48 μg·m⁻³, 14.73 μg·m⁻³, 16.50 μg·m⁻³, 1.12 μg·m⁻³ and 2.90 μg·m⁻³, respectively.

1436
1437
1438
1439
1440
1441
1442
1443
1444
1445
1446
1447
1448

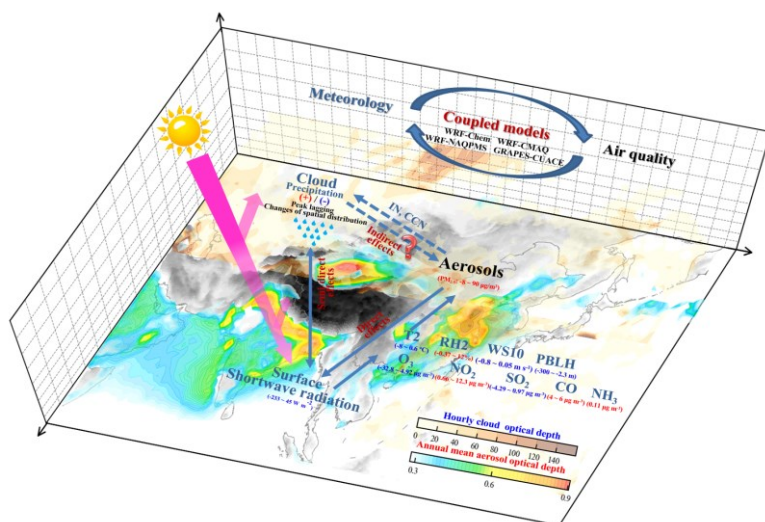
In addition to PM_{2.5}, gaseous pollutants (O₃, NO₂, SO₂, CO and NH₃) are impacted by ARI or/and ACI effects as well. As shown in Table 8, general reductions of ozone concentrations were reported in Asia across all the modeling domains and time scales based on coupled models' simulations. However, the influences of aerosol feedbacks on atmospheric dynamics and stability, and photochemistry (photolysis rate and ozone formation regimes) could make ozone concentrations increase somewhat in summer months or during wet season (Jung et al., 2019; Nguyen et al., 2019b; Xing et al., 2017). The largest hourly, daily, monthly, seasonal, and annual variations of O₃ occurred in YRD (-32.80 μg·m⁻³), EC (-5.97 μg·m⁻³), China (-23.90 μg·m⁻³), EA (-4.48 μg·m⁻³) and EA (-2.76 μg·m⁻³), respectively. Along with reduced O₃ due to ARI or/and ACI, NO₂ concentrations were enhanced with average changes of +12.30 μg·m⁻³ (YRD) at the hourly scale and +0.66 μg·m⁻³ (EA) at both the seasonal and yearly scales, which could be attributed to slower photochemical reactions, strengthened atmospheric stability and O₃ titration (Nguyen et al., 2019b). Regarding other gaseous pollutants, limited studies pointed out daily and annual SO₂ concentrations increased in NEA and

1449 EA due to lower PBLH induced by the ARI effects of anthropogenic aerosols (Jung et al.,2019;
 1450 Nguyen et al., 2019b). The seasonal SO₂ reduction was rather large, which related to higher PBLH
 1451 induced by the ACI effects of dust aerosols in the NCP area of EA (Wang K. et al., 2018). The slight
 1452 increase of seasonal SO₂ was reported in the whole domain of EA due to lower PBLH caused by
 1453 ARI effects of anthropogenic aerosols (Nguyen et al., 2019b). There was only one study depicted
 1454 increased CO (NH₃) concentration in EC (NEA) due to both the ARI and ACI (ARI) effects of
 1455 anthropogenic aerosols but these results may not be conclusive.

1456
 1457 Table 8. Compilation of aerosol-induced variations of PM_{2.5} and gaseous pollutants simulated by two-way
 1458 coupled models (WRF-Chem, WRF-CMAQ, GRAPES-CUACE, WRF-NAQPMS and GATOR-GCMOM) in
 1459 different regions of Asia and at different temporal scales.

Region	Time scale	ΔPM _{2.5} [mean] (μg·m ⁻³)	ΔO ₃ [mean] (μg·m ⁻³)	ΔNO ₂ [mean] (μg·m ⁻³)	ΔSO ₂ [mean] (μg·m ⁻³)	ΔCO [mean] (μg·m ⁻³)	ΔNH ₃ [mean] (μg·m ⁻³)
NCP	hours	-3.50 to 90.00 [23.48]					
YRD	hours	7.00 to 30.50 [15.17]	-32.80 to -0.20 [-11.25]	12.30			
Hourly mean		19.32	-11.25	12.30			
SEC	days	-1.91 to 32.49 [14.73]					
NCP	days	-5.00 to 56.00 [14.51]					
EC	days	2.87 to 18.60 [10.74]	-5.97 to -1.45 [-3.71]				
NEA	days	1.75			0.97		0.11
Daily mean		10.43	-3.71		0.97		0.11
India	months	3.00 to 30.00 [16.50]					
EC	months	1.00 to 40.00 [16.33]	-2.40 to -1.00 [-1.70]			4.00 to 6.00 [5.00]	
China	months	1.60 to 33.20 [14.38]	-23.90 to 4.92 [-3.42]				
EA	months	3.60 to 10.20 [5.79]					
Monthly mean		13.25	-2.56			5.00	
SEA	seasons	0.15 to 2.09 [1.12]	-1.92 to 0.26 [-0.83]				
EA	seasons	-8.00 to 2.70 [-0.14]	-4.48 to -1.00 [-2.99]	0.43 to 0.88 [0.66]	-4.29 to 0.72 [-0.42]		
Seasonal mean		0.49	-1.91	0.66	-0.42		
PRD	years	2.90					
EA	years	1.82	-2.76	0.66	0.54		
NCP	years	0.10 to 5.10 [1.70]					
SEA	years	1.21	-0.80				
Yearly mean		1.91	-1.78	0.66	0.54		

1460



1462 Figure 9. A schematic diagram depicting aerosol-radiation-cloud interactions and quantitative effects of aerosol
 1463 feedbacks on meteorological and air quality variables simulated by two-way coupled models in Asia.
 1464

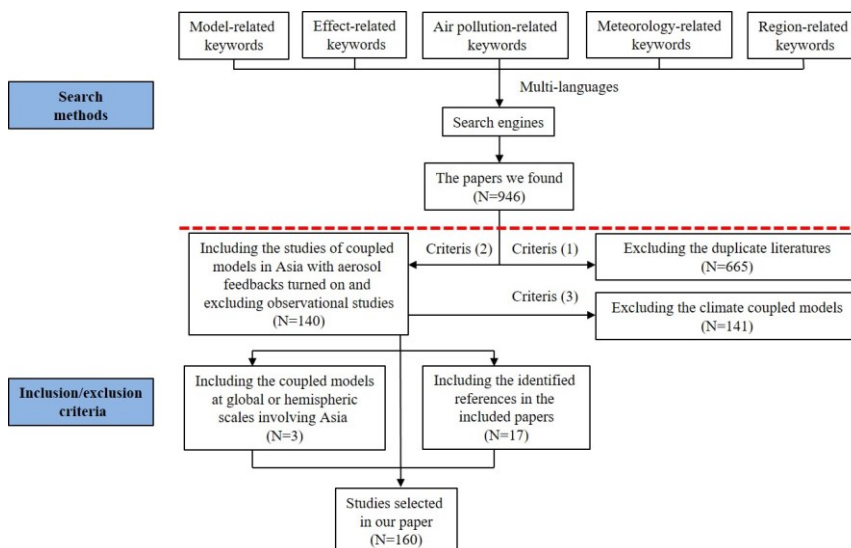
1465
 1466 Two-way coupled models have been applied in US and Europe extensively and then in Asia
 1467 due to frequent occurrences of severe air pollution events accompanied with rapid economic growth
 1468 in the region. Until now, no comprehensive study is conducted to elucidate the recent advances in
 1469 two-way coupled models' applications in Asia. This paper provides a critical overview of current
 1470 status and research focuses of related modeling studies using two-way coupled models in Asia
 1471 between 2010 and 2019, and summarizes the effects of aerosol feedbacks on meteorological and air
 1472 quality variables from these studies.

1473 Through systematically searching peer-reviewed publications with several scientific-based
 1474 search engines and a variety of key word combinations and applying certain selection criteria, 160
 1475 relevant papers were identified. Our bibliometric analysis results (as schematically illustrated in Fig.
 1476 9) showed that in Asia, the research activities with two-way coupled models had increased gradually
 1477 in the past decade and the five two-way coupled models (WRF-Chem, WRF-CMAQ, WRF-
 1478 NAQPMS, GRAPES-CUACE and GATOR-GCMOM) were extensively utilized to explore the ARI
 1479 or/and ACI effects in Asia with focusing on several high aerosol loading areas (e.g., EA, India, China
 1480 and NCP) during wintertime or/and severe pollution events, with less investigations looking into
 1481 other areas and seasons with low pollution levels. Among the 160 papers, nearly 82 % of them
 1482 focused on ARI (72 papers) and both ARI and ACI effects (60 papers), but papers that only
 1483 considering ACI effects were relatively limited. The ARI or/and ACI effects of natural mineral dust,
 1484 BC and BrC from anthropogenic sources and BC from ARB were mostly investigated, while a few
 1485 studies quantitatively assessed the health impacts induced by aerosol effects.

1486 Meta-analysis results revealed that enabling aerosol effects in two-way coupled models could
 1487 improve their simulation/forecast capabilities of meteorology and air quality in Asia, but a wide
 1488 range of differences occurred among the previous studies perhaps due to various model
 1489 configurations (selections of model versions and parameterization schemes) and largest
 1490 uncertainties related to ACI processes and their treatments in models. Compared to US and Europe,
 1491 the aerosol-induced decrease of the shortwave radiative forcing was larger because of higher air
 1492 pollution levels in Asia. The overall decrease (increase) of T2, WS10, PBLH and O₃ (RH2, PM_{2.5}
 1493 and other gaseous pollutant concentrations) caused by ARI or/and ACI effects were reported from
 1494 the modeling studies using two-way coupled models in Asia. The ranges of aerosol-induced
 1495 variations of T2, PBLH, PM_{2.5} and O₃ concentrations were larger than other meteorological and air
 1496 quality variables. For variables of CO, SO₂, NO₂, and NH₃, reliable estimates could not be obtained
 1497 due to insufficient numbers of samples in past studies.

1498 Even though noticeable progresses toward the application of two-way coupled meteorology
 1499 and air quality models have been made in Asia and the world during the last decade, several
 1500 limitations are still presented. Enabling aerosol feedbacks lead to higher computational cost
 1501 compared to offline models, but this shortcoming can be overcome with the new developments of
 1502 cluster computing technology (i.e., Graphics Processing Unit (GPU)-accelerated computing and
 1503 cloud computing). The latest advances in the measurements and research of cloud properties,
 1504 precipitation characteristics, and physiochemical characteristics of aerosols that play pivotal roles
 1505 in CCN or IN activation mechanisms can guide the improvements and enhancements in two-way
 1506 coupled models, especially to abate the uncertainties in simulating ACI effects. Special attention
 1507 needs to be paid to assess the accuracies of different methodologies in terms of ARI and ACI
 1508 calculations in two-way coupled models in Asia and other regions. Besides the five two-way coupled
 1509 models mentioned in this paper, more models capable of simulating aerosol feedbacks (such as
 1510 WRF-CHIMERE and WRF-GEOS-Chem) have become available and projects covering more
 1511 comprehensive intercomparisons of these coupled models should be conducted in Asia. Future
 1512 assessments of the ARI or/and ACI effects should pay extra attention to their impacts on dry and
 1513 wet depositions simulated by two-way coupled models. So far, the majority of two-way coupled
 1514 models' simulations and evaluations focuses on episodic air pollution events occurring in certain
 1515 areas, therefore their long-term applications and evaluations are necessary and their real-time
 1516 forecasting capabilities should be explored as well.
 1517

1518 Appendix A



1519 Figure A1. Flowchart of literature search and identification
 1520
 1521
 1522

1523 Appendix B

1524 Table B1. Lists of abbreviations and acronyms

ACI	Aerosol-cloud interactions
AOD	Aerosol optical depth
AQCHEM	the CMAQ's standard aqueous chemistry module
ARB	Agriculture residue burning
ARB_BC	BC emitted from agriculture residue burning
ARB_CAs	Carbonaceous aerosols emitted from agriculture residue burning
ARI	Aerosol-radiation interactions
ATM	In the atmosphere
BB	Biomass burning
BC	Black carbon
BCs	Boundary conditions
BOT	At the bottom

BrC	Brown carbon
CA	Central Asia
CAMx	Comprehensive Air quality Model with extensions
CAs	Carbonaceous aerosols
CC	Central China
CCN	Cloud condensation nuclei
CDNC	Cloud droplet number concentration
CHIMERE	A multi-scale chemistry-transport model for atmospheric composition analysis and forecast
CMAQ	Community Multiscale Air Quality model
CO	Carbon monoxide
CRFs	Concentration-response functions
DRF	Direct radiative forcing
EA	East Asia
EC	East China
EQUISOLV II	the EQUilibrium SOLVer version 2
GATOR-GCMOM	Gas, aerosol, transport, radiation, general circulation, mesoscale, and ocean Model
GOCART	The Global Ozone Chemistry Aerosol Radiation and Transport
GPRAPES-CUACE	Global-regional assimilation and prediction system coupled with the Chinese Unified Atmospheric Chemistry Environment forecasting system
GSI	Gridpoint Statistical Interpolation
H ₂ O ₂	Hydrogen peroxide
HNO ₃	Nitric acid
HO ₂	Hydroperoxyl
ICs	Initial conditions
IN	Ice nuclei
INPs	Ice nucleation parameterizations
IPCC	Intergovernmental Panel on Climate Change
IPR	Ice particle radius
IWP	Ice water path
LWP	Liquid water path
LWRF	Longwave radiative forcing
MARS-A	the Model for an Aerosol Reacting System-version A
MB	Mean bias
ME	Middle East
MESA-MTEM	the Multicomponent Equilibrium Solver for Aerosols with the Multicomponent Taylor Expansion Method
MICS-Asia	Model Inter-Comparison Study for Asia
MOZART	Model for Ozone and Related Chemical Tracer
MRYR	Middle reaches of the Yangtze River
N	Nitrate
N ₂ O ₅	Nitrogen pentoxide
NAQPMS	Nested Air Quality Prediction Modeling System
NC	North China
NCP	North China Plain
NEA	Northeast Asia
NME	Normalized mean error
NO ₂	Nitrogen dioxide
NU-WRF	National aeronautics and space administration Unified Weather Research and Forecasting model
NWC	Northwest China
O ₃	Ozone
OA	Organic aerosols
OC	Organic carbon
-OH	Hydroxyl radical
OPAC	Optical Properties of Aerosols and Clouds
PBL	Planetary boundary layer
PBLH	Planetary boundary layer height
PM _{2.5}	Fine particulate matter
PRD	Pearl River Delta
PSI	Papers with statistical indices
R	Correlation coefficient
RADM	the Regional Acid Deposition Mode
RH2	Relative humidity at 2 meters above the surface
RMSE	Root mean square error
RRTM	The Rapid Radiative Transfer Model
RRTMG	The Rapid Radiative Transfer Model for General Circulation Models
S	Sulfate
SA	South Asia
SC	South China
SEA	Southeast Asia
SEC	Southeast China
SH2	Specific humidity at 2 meters above the surface
SI	Statistical indices
SO ₂	Sulfur dioxide
SOA	Secondary organic aerosol
SWC	Southwest China
SWRF	Shortwave radiative forcing
T2	Air temperature at 2 meters above the surface
TOA	At the top of atmosphere
TP	Tibetan Plateau
US	the United States
VBS	Volatility basis set

WA	West Asia
WRF	Weather Research and Forecasting model
WRF-Chem	Weather Research and Forecasting model coupled with Chemistry
WRF-CHIMERE	Weather Research and Forecasting model coupled with a multi-scale Chemistry-Transport Model (CTM) for air quality forecasting and simulation
WRF-CMAQ	Weather Research and Forecasting model coupled with Community Multiscale Air Quality model
WRF-NAQPMS	Weather Research and Forecasting model coupled with the Nested Air Quality Prediction Modeling System
WS10	Wind speed at 10 meters above the surface
YRD	Yangtze River Delta

1525
1527
1528
1529

Table B2. The compiled number of publications (NP) and number of samples (NS) for papers that providing statistical indices (SI) of meteorological variables.

No.*	Meteorological variables															
	T2				RH2				SH2				WS10			
	NS		NS		NS		NS		NS		NS		NS			
NP	R	MB	RMSE	NP	R	MB	RMSE	NP	R	MB	RMSE	NP	R	MB	RMSE	
4	1	5	5 (4†, 1)	5	1	5	5 (1†, 4)	5								
5					1		3 (2†, 1)	3								
7	1	4	4 (3†, 1)													
13	1		1 (1)		1		1 (1†)									
15	1	1			1	1						1	2			
16	1	1												1 (1†)	1	
20	1	2	2 (1†, 1)	2	1	2	2 (1†, 1)	2				1	1	2 (1†, 1)	2	
21	1	0	2 (2)	2								1	1	1 (1)	1	
22	1	1	1 (1)	1	1	1	1 (1†)	1				1	1	1 (1)		
23	1	1	1 (1†)		1	1	1 (1)					1	1	1 (1†)		
24	1	1	1 (1†)		1	1	1 (1)					1	1	1 (1†)		
25	1	1	1 (1)													
28	1	1	1 (1†)	1	1		1 (1)	1				1		1 (1†)	1	
29	1	9	9 (6†, 3)	9	1	8		9				1	9	9 (9†)	9	
33	1	6	6 (4†, 2)	6												
34	1	2	2 (2†)	2								1	2	2 (2)	2	
35	1	2	2 (2)	2	1	1		1				1	1		1	
38	1	4	4 (4)	4	1	4	4 (3†, 1)	4								
50	1		8 (8)	8												
56	1	1	1 (1)	1	1	1	1 (1)	1				1	1	1 (1†)	1	
57	1	1			1	1						1	1			
61	1	4	4 (4)	4	1	4	4 (4†)	4				1	4	4 (4†)	4	
62	1		5 (5)	5								1		5 (4†, 1)	5	
63	1	1														
71	1	1														
72	1	4	4 (3†, 1)	4	1	4	4 (3†, 1)	4								
73	1	1	1 (1)	1					1	1	1 (1†)	1	1	1 (1†)	1	
75	1	4	4 (4†)		1	4	4 (4†)					0	1	4 (1†, 3)		
77	1	4	4 (2†, 2)						1	4	3 (3†)	4	1	4 (4†)	4	
79	1		8 (6†, 2)	8												
80	1	8	8 (8†)	8	1	8	8 (8)	8				1	8	8 (6†, 2)	8	
85	1		4 (1†, 3)	4	1		4 (2†, 2)	4				1		4 (4†)	4	
87	1		3 (2†, 1)	3								1		3 (2†, 1)	3	
88	1	3	3 (1†, 2)	3	1	3	3 (2†, 1)	3				1	3	3 (2†, 1)	3	
90	1	4	4 (1†, 3)									1	4	4 (4†)		
91	1	1	1 (1)	1					1	4	4 (4†)	1	1	1 (1†)	1	
94	1	6	6 (4†, 2)	6	1	6	6 (2†, 4)	6				1	6	6 (6†)	6	
96	1	16	16 (11†, 5)									1	16	16 (11†, 5)		
97	1	1	1 (1)	1	1	1	1 (1†)	1				1	1	1 (1†)	1	
106	1	6	6 (6)						1	6	5 (2†, 3)		1	6 (6†)		
109	1	2	2 (2)	2	1	3	3 (3†)	3				1	2	2 (2†)	2	
112	1		2 (2)	2					1		2 (2)	2	1	2 (2†)	2	
116	1	2	2 (1†, 1)	0	1	2	2 (1†, 1)									
121	1	1	1 (1)	1								1	1	1 (1†)	1	
122	1	2	2 (2)	2	1		2 (2†)	2				1		2 (2†)	2	
125	1	4	4 (4)	4	1	4	4 (4†)	4				1	4	4 (4)	4	
126	1	4	4 (4)	4					1	4	4 (2†, 2)	4	1	4 (4†)	4	
127	1		2 (2)	2								1		2 (2†)	2	
128	1	8	8 (8)	8					1	8	8 (5†, 3)	8	1	8 (8†)	8	
129	1	1	1 (1)	1	1	1	1 (1†)	1				1	1	1 (1†)	1	
133	1		1 (1)	0	1		4 (4†)					1				
143	1	4	4 (4)	4	1	4		4				1	4	4 (3†, 1)	4	
147	1	2		2	1	2		2				1	2		2	
151	1	7	7 (7)	7					1	7	7 (3†, 4)	7	1	7 (7†)	7	
Total	53	137	167 (67†, 100)	130	30	68	70 (42†, 28)	73	9	35	35 (21†, 14)	27	40	111	126 (104†, 22)	97

Note that the No.* is consistent with the No. in Table 1, and † and ‡ mark over- and underestimations of variables, respectively, along with their number of samples.

1530
1531
1532
1533
1534

Table B3. The compiled number of publications (NP) and number of samples (NS) for papers that providing statistical indices (SI) of air quality variables.

No.*	Air quality variables							
	PM _{2.5}				O ₃			
	NP	R	MB	RMSE	NP	R	MB	RMSE
4	1	5	5 (5)	5				
5	1		1 (1)		1		1 (1)	1
11	1	60						
15	1	1						
21	1		2 (1†, 1)					
22	1	1	1 (1†)	1				
23	1	1	1 (1)		1	1	1 (1)	
24	1	1	1 (1)		1		1 (1)	
25	1	1	1 (1)		1	1	1 (1)	
29	1	9	9 (6†, 3)	9				

33	1	4	4 (4)	4	1	4	4 (3↑, 1↓)	4
34	1	2	2 (1↑, 1↓)	2				
35					1	1		1
50	1		4 (1↑, 3↓)	4				
56	1	1	1 (1↑)	1				
57	1	1						
59	1	6	6 (6↓)	6	1	6	6 (6↓)	6
61	1	12	12 (12↑)	12				
67	1	10	2 (2↓)	10				
71	1	1						
73	1	2	2 (1↑, 1↓)		1	4	4 (4↑)	
77	1	4						
85	1	3	3 (3↓)					
86	1	4	4 (2↑, 2↓)	4				
88	1	3	3 (1↑, 2↓)	3				
90	1	8	8 (2↑, 6↓)					
91	1	4	4 (1↑, 3↓)	4	1	14	14 (14↑)	6
94	1	4	4 (3↑, 1↓)	4	1	6	6 (4↑, 2↓)	
97	1	1	1 (1↓)	1				
100	1	1			1	1		
106	1	6	6 (2↑, 4↓)		1	8	8 (4↑, 4↓)	
112	1				1			
121					1			5
122	1	4	4 (1↑, 3↓)					
125	1	4	4 (2↑, 2↓)	4	1	4	4 (4↑)	4
126	1	4	4 (2↑, 2↓)	4	1	4	4 (4↑)	4
127	1		1 (1↑)	1				
128	1	8	8 (3↑, 5↓)	8				
129	1	3	3 (2↑, 1↓)	3	1	2	2 (1↑, 1↓)	2
133					1	4	4 (3↑, 1↓)	4
136	1	5	5 (5↓)					
146	1	1			1	20		20
147	1	2		2				
149	1	6		6				
150					1	21		21
151	1	12	6 (6↑)	6	1	24	12 (7↑, 5↓)	12
Total	42	205	122 (55↑, 67↓)	105	21	125	72 (55↑, 17↓)	90

1535 Note that the No.* is consistent with the No. in Table 1, and ↑ and ↓ mark over- and underestimations of variables, respectively, along with
 1536 their number of samples.

1537
 1538 **Table B4. The compiled number of publications (NP) and number of samples (NS) for papers that simultaneously**
 1539 **providing the statistical indices (SI) of meteorological variables simulated by coupled models (WRF-Chem, WRF-**
 1540 **CMAQ, GRAPES-CUACE, WRF-NAQPMS and GATOR-GCMOM) with/out ARI.**

No.*	Meteorological variables															
	T2			RH2				SH2			WS10					
	NP	NS		NP	NS			NP	NS		NP	NS				
	R	MB	RMSE	R	MB	RMSE	R	MB	RMSE	R	MB	RMSE				
32	1	3	3 (2↑, 1↓)	3												
78	1		4 (3↑, 1↓)	4												
124	1	2	2 (2↓)	2	1	2	2 (2↑)	2		1	2	2 (2↓)	2			
125	1	2	2 (2↓)	2				1	2	2 (1↑, 1↓)	2	1	2	2 (2↑)	2	
126	1		1 (1↓)	1								1		1 (1↑)	1	
127	1	4	4 (4↓)	4				1	4	4 (3↑, 1↓)	4	1	4	4 (4↑)	4	
146	1	1		1	1	1		1				1	1		1	
Total	7	12	16 (5↑, 11↓)	17	2	3	2 (2↑)	3	2	6	6 (4↑, 2↓)	6	5	9	9 (7↑, 2↓)	10

1541 Note that the No.* is consistent with the No. in Table 1, and ↑ and ↓ mark over- and underestimations of variables, respectively, along with
 1542 their number of samples.

1543
 1544 **Table B5. The compiled number of publications (NP) and number of samples (NS) for papers that simultaneously**
 1545 **providing the statistical indices (SI) of air quality variables simulated by coupled models (WRF-Chem, WRF-CMAQ,**
 1546 **GRAPES-CUACE, WRF-NAQPMS and GATOR-GCMOM) with/out ARI.**

No.*	Air quality variables									
	PM _{2.5}				O ₃					
	NP	NS			NP	NS				
	R	MB	RMSE	R	MB	RMSE	R	MB	RMSE	
49	1		2 (1↑, 1↓)	2	1		10		10	
60	1		4 (4↑)	4						
124	1	2	2 (1↑, 1↓)	2	1		2		2 (2↑)	2
125	1	2	2 (1↑, 1↓)	2	1		2		2 (2↑)	2
127	1		4 (2↑, 2↓)	4						
146	1		1	1						
Total	5	13	14 (9↑, 5↓)	15	3		14		4 (4↑)	14

1547 Note that the No.* is consistent with the No. in Table 1, and ↑ and ↓ mark over- and underestimations of variables, respectively, along with
 1548 their number of samples.

1549
 1550 **Table B6. Description of refractive indices and radiation schemes used in the WRF-Chem and WRF-CMAQ in Asia.**

Model	Refractive indices of aerosol species groups		Radiation scheme	
	SW	LW	SW scheme (Spectral intervals)	LW scheme (Spectral intervals)
WRF-Chem	1, Water (1.35+1.524 ^λ),	1, Water (1.532+0.336 ^λ),	GODDARD (0.175-0.225, 0.225-0.245, 0.245-	BRTMG (10-350, 350-500, 500-630, 630-700)

带格式的: 字体: 非倾斜, 字体颜色: 文字 1

带格式的: 字体: 非倾斜, 字体颜色: 文字 1

T2 were overestimated (average MB = 0.07 °C). It should be noted that T2 at the monthly scale was underpredicted mainly during winter months (16 samples). Regarding the mean RMSE, its value (Figure C1i) at the daily scale was the largest (0.97 °C) in comparison with that at the other temporal scales.

Given that no SI was available for RH2 at the seasonal scale, results at other time scales were discussed here. Figure C1b presented that simulated RH2 at the daily scale had the best correlation coefficient (mean R = 0.74), followed by those at the monthly (0.73) and yearly (0.71) scales. Except overestimation (average MB = 3.6 %) at the yearly scale (Figure C1f), modeled RH2 were underestimated at the monthly (average MB = -1.1 %) and daily (average MB = -0.2 %) scales, respectively. Therefore, coupled models calculated RH2 reasonably well in short-term simulations. However, at the daily scale, RMSE of modeled RH2 (Figure C1j) was relatively large fluctuation ranging from 6.2 % to 21.3 %.

Lacking of SI for SH2 at the daily scale, only those at other time scales were compared. Even though NP and NS were very limited, the modeled SH2 (Figure C1e) exhibited especially good correlation with observations with the mean R values exceeding 0.95 at the yearly, seasonal and monthly scales (0.99, 0.97 and 0.96, respectively) but had the largest mean RMSE (2.09 g·kg⁻¹) at the yearly scale (Figure C1k). Also, both over- and under-estimations of modeled SH2 (Fig. C1g) were reported at different time scales with average MB values as 0.15 g·kg⁻¹, -0.02 g·kg⁻¹, and -0.14 g·kg⁻¹ for yearly, seasonal and monthly simulations, respectively. Generally, the long-term simulations of SH2 agreed better with observations than the short-term ones.

As seen in Figure C1d, the modeled WS10 at the monthly scale (mean R = 0.68) correlated with observations better than that at the daily, yearly and seasonal scales (mean R = 0.62, 0.48 and 0.46, respectively). The simulations at all temporal scales tended to overestimate WS10 comparing against observations (Figure C1h) and their average MB were 0.80 m·s⁻¹ (seasonal), 0.86 m·s⁻¹ (monthly), 0.64 m·s⁻¹ (yearly) and 0.62 m·s⁻¹ (daily), respectively. The short-term simulations of WS10 better matched with observations compared to the long-term ones. At the same time, the largest mean RMSE (1.79 m·s⁻¹) of simulated WS10 (Figure C1l) appeared at the seasonal scale.

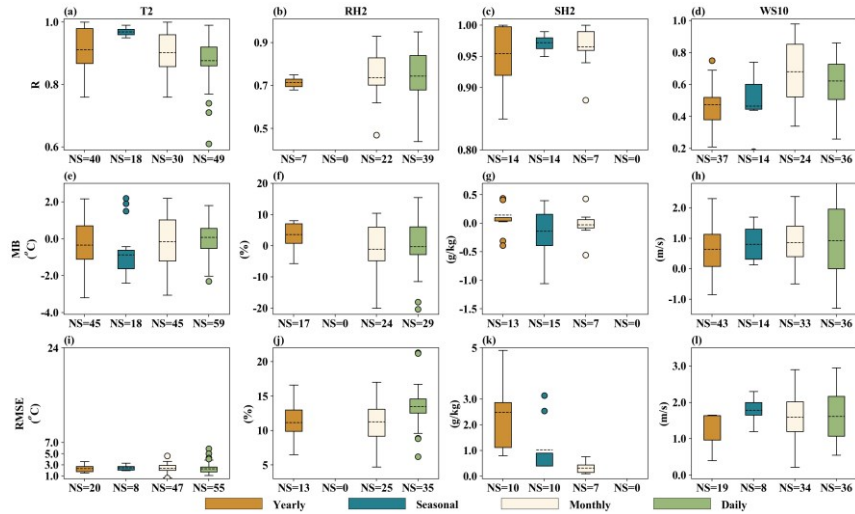


Figure C1. The statistical indices of modeled meteorological variables at different temporal scales (Yearly, Seasonal, Monthly and Daily) from past studies in Asia.

C2 Comparisons of SI at different temporal scales for air quality

Figure C2 depicted the SI of simulated PM_{2.5} and O₃ at yearly, seasonal, monthly and daily scales. The correlation between simulated and observed PM_{2.5} (Figure C2a) at the monthly scale (mean R = 0.68) was largest compared to those at the yearly (0.64), seasonal (0.59), daily (0.57) scales. All the simulated PM_{2.5} were underestimated, with the average daily, monthly, seasonal, and

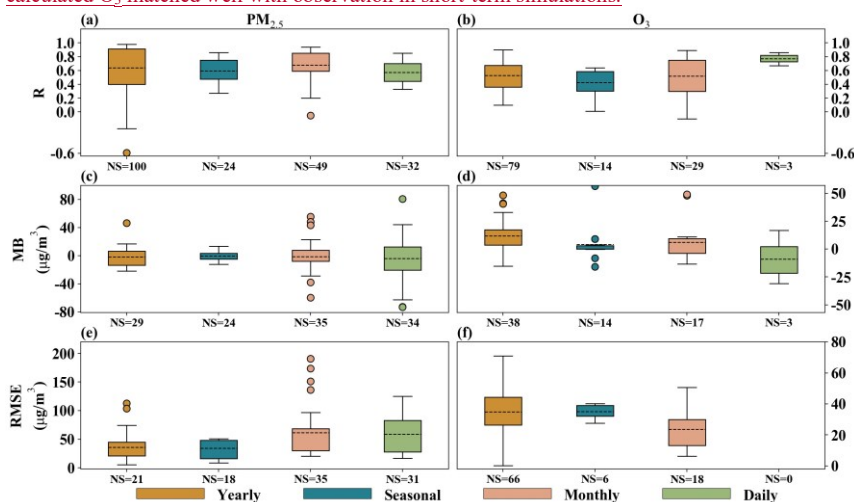
带格式的：字体：(中文)+中文正文(宋体)，五号，加粗

带格式的：2级，孤行控制，与下段同页，段中不分页

带格式的：字体：(中文)+中文正文(宋体)，五号，加粗

1607 [yearly MB as -4.13, -1.46, -0.28, and -1.89 \$\mu\text{g}\cdot\text{m}^{-3}\$, respectively \(Figure C2c\). As displayed in Figure](#)
 1608 [C2e, the mean RMSE at the monthly scale was the largest \(61.57 \$\mu\text{g}\cdot\text{m}^{-3}\$ \).](#)

1609 [Regarding to correlation between simulated and observed \$\text{O}_3\$ \(Figure C2b\), it was the best at](#)
 1610 [the daily scale \(mean \$R=0.77\$ \). Modeled \$\text{O}_3\$ were overestimated at the seasonal \(average MB =](#)
 1611 [+4.12 \$\mu\text{g}\cdot\text{m}^{-3}\$ \), monthly \(average MB = +6.11 \$\mu\text{g}\cdot\text{m}^{-3}\$ \) and yearly \(average MB = +11.71 \$\mu\text{g}\cdot\text{m}^{-3}\$ \)](#)
 1612 [scales, but underestimated at the daily scale \(average MB = -8.89 \$\mu\text{g}\cdot\text{m}^{-3}\$ \) \(Figure C2d\). Note that no](#)
 1613 [RMSE for \$\text{O}_3\$ simulation was available at the daily scale, and the RMSE at the yearly scale \(Figure](#)
 1614 [C2f\) had relatively large fluctuation ranging from 0.21 to 71 \$\mu\text{g}\cdot\text{m}^{-3}\$. Therefore, coupled models](#)
 1615 [calculated \$\text{O}_3\$ matched well with observation in short-term simulations.](#)



1616 [Figure C2. The quantile distributions of simulated \$\text{PM}_{2.5}\$ and \$\text{O}_3\$ performance metrics at different temporal scales](#)
 1617 [from past studies in Asia.](#)

1620 **Data availability**

1621 The related dataset can be downloaded from <https://doi.org/10.5281/zenodo.5571076> (Gao et al., 2021), and this dataset includes basic information (Table S1), performance metrics (Table S2), quantitative effects of aerosol feedbacks on meteorological and air quality variables (Table S3), [model configuration and setup \(Table S4\) and aerosol-induced variations of simulated shortwave and longwave radiative forcing \(Table S5\)](#) extracted from collected studies of applications of two-way coupled meteorology and air quality models in Asia.

1627

1628 **Author contribution**

1629 Chao Gao, Aijun Xiu, Xuelei Zhang and Qingqing Tong carried out the data collection, related analysis, figure plotting, and manuscript writing; Hongmei Zhao, Shichun Zhang, Guangyi Yang and Mengduo Zhang involved with the original research plan and made suggestions to the manuscript writing.

1633

1634 **Competing interest**

1635 The authors declare that they have no conflict of interest.

1636

1637 **Acknowledgement**

1638 [This study was financially sponsored by National Key Research and Development Program of](#)

1639 [China \(No. 2017YFC0212304\), Talent Program of Chinese Academy of Sciences, and National](#)
1640 [Natural Science Foundation of China \(No. 41571063 and No. 41771071\). The authors are very](#)
1641 [grateful to many researchers who provided detailed information on the two-way coupled models](#)
1642 [and related research work. The list includes but is not limited to Xueshun Chen, Zifa Wang, Yi Gao,](#)
1643 [Meigen Zhang and Baozhu Ge \(Institute of Atmospheric Physics, Chinese Academy of Sciences\),](#)
1644 [Chunhong Zhou \(Chinese Academy of Meteorological Sciences\), Yang Zhang \(Northeastern](#)
1645 [University\), Mark Zachary Jacobson \(Stanford University\), Tianliang Zhao \(Nanjing University of](#)
1646 [Information Science & Technology\), Xin Huang \(Nanjing University\), Chun Zhao \(University of](#)
1647 [Science and Technology of China\), Junhua Yang and Shichang Kang \(Northwest Institute of Eco-](#)
1648 [Environment and Resources, Chinese Academy of Sciences\), Sachin Ghude \(Ministry of Earth](#)
1649 [Sciences Government of India\) and Luke Conibear \(University of Leeds\). We would also like to](#)
1650 [express our deepest appreciation to the editor James Allan and two anonymous reviewers for their](#)
1651 [constructive comments and suggestions, which helped to improve the quality and readability of this](#)
1652 [article.](#)

1654 Reference

- 1655 [Albrecht, B.A., 1989. Aerosols, cloud microphysics, and fractional cloudiness. *Science* \(80-. \). 245,](#)
1656 [1227-1230. <https://doi.org/10.1126/science.245.4923.1227>.](#)
- 1657 [Ahmadov, R., McKeen, S.A., Robinson, A.L., Bahreini, R., Middlebrook, A.M., De Gouw, J.A.,](#)
1658 [Meagher, J., Hsie, E., Edgerton, E., Shaw, S., 2012. A volatility basis set model for summertime](#)
1659 [secondary organic aerosols over the eastern United States in 2006. *J. Geophys. Res. Atmos.*](#)
1660 [117. <https://doi.org/10.1029/2011JD016831>.](#)
- 1661 [An, Z., Huang, R.-J., Zhang, R., Tie, X., Li, G., Cao, J., Zhou, W., Shi, Z., Han, Y., Gu, Z., 2019.](#)
1662 [Severe haze in northern China: A synergy of anthropogenic emissions and atmospheric](#)
1663 [processes. *Proc. Natl. Acad. Sci.* 116, 8657-8666. <https://doi.org/10.1073/pnas.1900125116>.](#)
- 1664 [Andreae, M.O., Rosenfeld, D., 2008. Aerosol-cloud-precipitation interactions. Part I. The nature](#)
1665 [and sources of cloud-active aerosols. *Earth-Science Rev.* 89, 13-41.](#)
1666 [<https://doi.org/10.1016/j.earscirev.2008.03.001>.](#)
- 1667 [Appel, K.W., Bash, J.O., Fahey, K.M., Foley, K.M., Gilliam, R.C., Hogrefe, C., Hutzell, W.T., Kang,](#)
1668 [D., Mathur, R., Murphy, B.N., 2021. The Community Multiscale Air Quality \(CMAQ\) model](#)
1669 [versions 5.3 and 5.3.1: system updates and evaluation. *Geosci. Model Dev.* 14, 2867–2897.](#)
1670 [<https://doi.org/10.5194/gmd-14-2867-2021>.](#)
- 1671 [Appel, K.W., Napelenok, S.L., Foley, K.M., Pye, H.O.T., Hogrefe, C., Luecken, D.J., Bash, J.O.,](#)
1672 [Roselle, S.J., Pleim, J.E., Foroutan, H., Hutzell, W.T., Pouliot, G.A., Sarwar, G., Fahey, K.M.,](#)
1673 [Gantt, B., Gilliam, R.C., Heath, N.K., Kang, D., Mathur, R., Schwede, D.B., Spero, T.L., Wong,](#)
1674 [D.C., Young, J.O., 2017. Description and evaluation of the Community Multiscale Air Quality](#)
1675 [\(CMAQ\) modeling system version 5.1. *Geosci. Model Dev.* 10, 1703-1732.](#)
1676 [<https://doi.org/10.5194/gmd-10-1703-2017>.](#)
- 1677 [Appel, K.W., Pouliot, G.A., Simon, H., Sarwar, G., Pye, H.O.T., Napelenok, S.L., Akhtar, F., Roselle,](#)
1678 [S.J., 2013. Evaluation of dust and trace metal estimates from the Community Multiscale Air](#)
1679 [Quality \(CMAQ\) model version 5.0. *Geosci. Model Dev.* 6, 883–899.](#)
1680 [<https://doi.org/10.5194/gmd-6-883-2013>.](#)
- 1681 [Archer - Nicholls, S., Lowe, D., Lacey, F., Kumar, R., Xiao, Q., Liu, Y., Carter, E., Baumgartner, J.,](#)
1682 [Wiedinmyer, C., 2019. Radiative Effects of Residential Sector Emissions in China: Sensitivity](#)
1683 [to Uncertainty in Black Carbon Emissions. *J. Geophys. Res. Atmos.* 124, 5029-5044.](#)
1684 [<https://doi.org/10.1029/2018JD030120>.](#)
- 1685 [Ashrafi, K., Motlagh, M.S., Neyestani, S.E., 2017. Dust storms modeling and their impacts on air](#)
1686 [quality and radiation budget over Iran using WRF-Chem. *Air Qual. Atmos. Heal.* 10, 1059-](#)
1687 [1076. <https://doi.org/10.1007/s11869-017-0494-8>.](#)
- 1688 [Bai, Y., Qi, H., Zhao, T., Zhou, Y., Liu, L., Xiong, J., Zhou, Z., Cui, C., 2020. Simulation of the](#)
1689 [responses of rainstorm in the Yangtze River Middle Reaches to changes in anthropogenic](#)
1690 [aerosol emissions. *Atmos. Environ.* 220, 117081.](#)
1691 [<https://doi.org/10.1016/j.atmosenv.2019.117081>.](#)
- 1692 [Baklanov, A., Schlünzen, K., Suppan, P., Baldasano, J., Brunner, D., Aksoyoglu, S., Carmichael, G.,](#)
1693 [Douros, J., Flemming, J., Forkel, R., 2014. Online coupled regional meteorology chemistry](#)
1694 [models in Europe: current status and prospects. *Atmos. Chem. Phys.* 14, 317-398.](#)
1695 [<https://doi.org/10.5194/acp-14-317-2014>.](#)

1696 [Baró, R., Jiménez-Guerrero, P., Balzarini, A., Curci, G., Forkel, R., Grell, G., Hirtl, M., Honzak, L.,](#)
1697 [Langer, M., Pérez, J.L., 2015. Sensitivity analysis of the microphysics scheme in WRF-Chem](#)
1698 [contributions to AQMEII phase 2. Atmos. Environ. 115, 620-629.](#)
1699 [https://doi.org/10.1016/j.atmosenv.2015.01.047.](https://doi.org/10.1016/j.atmosenv.2015.01.047)

1700 [Barth, M.C., Rasch, P.J., Kiehl, J.T., Benkovitz, C.M., Schwartz, S.E., 2000. Sulfur chemistry in the](#)
1701 [NCAR CCM: Description, evaluation, features and sensitivity to aqueous chemistry. J.](#)
1702 [Geophys. Res 105, 1387–1415. https://doi.org/10.1029/1999JD900773.](#)

1703 [Bauer, P., Thorpe, A., Brunet, G., 2015. The quiet revolution of numerical weather prediction.](#)
1704 [Nature 525, 47-55. https://doi.org/10.1038/nature14956.](#)

1705 [Bei, N., Wu, J., Elser, M., Tian, F., Cao, J., El-Haddad, I., Li, X., Huang, R., Li, Z., Long, X., 2017.](#)
1706 [Impacts of meteorological uncertainties on the haze formation in Beijing-Tianjin-Hebei \(BTH\)](#)
1707 [during wintertime: a case study. Atmos. Chem. Phys. 17, 14579. https://doi.org/10.5194/acp-](#)
1708 [17-14579-2017.](#)

1709 [Beig, G., Chate, D.M., Ghude, S.D., Mahajan, A.S., Srinivas, R., Ali, K., Sahu, S.K., Parkhi, N.,](#)
1710 [Surendran, D., Trimbake, H.R., 2013. Quantifying the effect of air quality control measures](#)
1711 [during the 2010 Commonwealth Games at Delhi, India. Atmos. Environ. 80, 455-463.](#)
1712 [https://doi.org/10.1016/j.atmosenv.2013.08.012.](https://doi.org/10.1016/j.atmosenv.2013.08.012)

1713 [Bellouin, N., Jones, A., Haywood, J., Christopher, S.A., 2008. Updated estimate of aerosol direct](#)
1714 [radiative forcing from satellite observations and comparison against the Hadley Centre climate](#)
1715 [model. J. Geophys. Res. Atmos. 113. https://doi.org/10.1029/2007JD009385.](#)

1716 [Benas, N., Meirink, J.F., Karlsson, K.-G., Stengel, M., Stammes, P., 2020. Satellite observations of](#)
1717 [aerosols and clouds over southern China from 2006 to 2015: analysis of changes and possible](#)
1718 [interaction mechanisms. Atmos. Chem. Phys. 20, 457-474. https://doi.org/10.5194/acp-20-](#)
1719 [457-2020.](#)

1720 [Bennartz, R., Fan, J., Rausch, J., Leung, L.R., Heidinger, A.K., 2011. Pollution from China increases](#)
1721 [cloud droplet number, suppresses rain over the East China Sea. Geophys. Res. Lett. 38,](#)
1722 [https://doi.org/10.1029/2011GL047235.](https://doi.org/10.1029/2011GL047235)

1723 [Bharali, C., Nair, V.S., Chutia, L., Babu, S.S., 2019. Modeling of the effects of wintertime aerosols](#)
1724 [on boundary layer properties over the Indo Gangetic Plain. J. Geophys. Res. Atmos. 124, 4141-](#)
1725 [4157. https://doi.org/10.1029/2018JD029758.](#)

1726 [Bhattacharya, A., Chakraborty, A., Venugopal, V., 2017. Role of aerosols in modulating cloud](#)
1727 [properties during active-break cycle of Indian summer monsoon. Clim. Dyn. 49, 2131-2145.](#)
1728 [https://doi.org/10.1007/s00382-016-3437-4.](https://doi.org/10.1007/s00382-016-3437-4)

1729 [Binkowski, F.S., Roselle, S.J., 2003. Models - 3 Community Multiscale Air Quality \(CMAQ\) model](#)
1730 [aerosol component 1. Model description. J. Geophys. Res. Atmos. 108,](#)
1731 [https://doi.org/10.1029/2001JD001409.](https://doi.org/10.1029/2001JD001409)

1732 [Binkowski, F.S., Shankar, U., 1995. The regional particulate matter model: 1. Model description](#)
1733 [and preliminary results. J. Geophys. Res. Atmos. 100, 26191–26209.](#)
1734 [https://doi.org/10.1029/95JD02093.](https://doi.org/10.1029/95JD02093)

1735 [Bollasina, M.A., Ming, Y., Ramaswamy, V., 2011. Anthropogenic aerosols and the weakening of the](#)
1736 [South Asian summer monsoon. Science \(80-. \). 334, 502-505.](#)
1737 [https://doi.org/10.1126/science.1204994.](https://doi.org/10.1126/science.1204994)

1738 [Boucher, O., Randall, D., Artaxo, P., Bretherton, C., Feingold, G., Forster, P., Kerminen, V.M.,](#)
1739 [Kondo, Y., Liao, H., Lohmann, U., 2013. Clouds and aerosols. Climate change 2013: The](#)
1740 [physical science basis. Contribution of working group I to the fifth assessment report of the](#)
1741 [intergovernmental panel on climate change. Cambridge Univ. Press. Cambridge, United](#)
1742 [Kingdom New York, NY, USA 571-657. https://doi.org/10.13140/2.1.1081.8883.](#)

1743 [Bran, S.H., Jose, S., Srivastava, R., 2018. Investigation of optical and radiative properties of aerosols](#)
1744 [during an intense dust storm: A regional climate modeling approach. J. Atmos. Solar-Terrestrial](#)
1745 [Phys. 168, 21-31. https://doi.org/10.1016/j.jastp.2018.01.003.](#)

1746 [Briant, R., Tuccella, P., Deroubaix, A., Khvorostyanov, D., Menut, L., Mailler, S., Turquety, S., 2017.](#)
1747 [Aerosol-radiation interaction modelling using online coupling between the WRF 3.7.1](#)
1748 [meteorological model and the CHIMERE 2016 chemistry-transport model, through the](#)
1749 [OASIS3-MCT coupler. Geosci. Model Dev. 10, 927-944. https://doi.org/10.5194/gmd-10-927-](#)
1750 [2017.](#)

1751 [Brunekreef, B., Holgate, S.T., 2002. Air pollution and health. Lancet 360, 1233-1242.](#)
1752 [https://doi.org/10.1016/S0140-6736\(02\)11274-8.](https://doi.org/10.1016/S0140-6736(02)11274-8)

1753 [Brunner, D., Savage, N., Jorba, O., Eder, B., Giordano, L., Badia, A., Balzarini, A., Baro, R.,](#)
1754 [Bianconi, R., Chemel, C., 2015. Comparative analysis of meteorological performance of](#)
1755 [coupled chemistry-meteorology models in the context of AQMEII phase 2. Atmos. Environ.](#)
1756 [115, 470-498. <https://doi.org/10.1016/j.atmosenv.2014.12.032>.](#)

1757 [Byun, D., Schere, K.L., 2006. Review of the governing equations, computational algorithms, and](#)
1758 [other components of the Models-3 Community Multiscale Air Quality \(CMAQ\) modeling](#)
1759 [system. Appl. Mech. Rev. 59, 51-77. <https://doi.org/10.1115/1.2128636>.](#)

1760 [Campbell, P., Zhang, Y., Wang, K., Leung, R., Fan, J., Zheng, B., Zhang, Q., He, K., 2017.](#)
1761 [Evaluation of a multi-scale WRF-CAM5 simulation during the 2010 East Asian Summer](#)
1762 [Monsoon. Atmos. Environ. 169, 204-217. <https://doi.org/10.1016/j.atmosenv.2017.09.008>.](#)

1763 [Campbell, P., Zhang, Y., Yahya, K., Wang, K., Hogrefe, C., Pouliot, G., Knote, C., Hodzic, A., San](#)
1764 [Jose, R., Perez, J.L., 2015. A multi-model assessment for the 2006 and 2010 simulations under](#)
1765 [the Air Quality Model Evaluation International Initiative \(AQMEII\) phase 2 over North](#)
1766 [America: Part I. Indicators of the sensitivity of O₃ and PM_{2.5} formation regimes. Atmos.](#)
1767 [Environ. 115, 569-586. <https://doi.org/10.1016/j.atmosenv.2014.12.026>.](#)

1768 [Carlton, A.G., Bhave, P.V., Napelenok, S.L., Edney, E.O., Sarwar, G., Pinder, R.W., Pouliot, G.A.,](#)
1769 [Houyoux, M., 2010. Model representation of secondary organic aerosol in CMAQv4.7.](#)
1770 [Environ. Sci. Technol. 44, 8553-8560. <https://doi.org/10.1021/es100636q>.](#)

1771 [Casazza, M., Lega, M., Liu, G., Ulgiati, S., Endreny, T.A., 2018. Aerosol pollution, including eroded](#)
1772 [soils, intensifies cloud growth, precipitation, and soil erosion: A review. J. Clean. Prod. 189,](#)
1773 [135-144. <https://doi.org/10.1016/j.jclepro.2018.04.004>.](#)

1774 [Chang, S., 2018. Characteristics of aerosols and cloud condensation nuclei \(CCN\) over China](#)
1775 [investigated by the two-way coupled WRF-CMAQ air quality model.](#)

1776 [Chapman, E.G., Jr, W.I.G., Easter, R.C., Barnard, J.C., Ghan, S.J., Pekour, M.S., Fast, J.D., 2009.](#)
1777 [and Physics Coupling aerosol-cloud-radiative processes in the WRF-Chem model?:](#)
1778 [Investigating the radiative impact of elevated point sources 945-964.](#)
1779 [https://doi.org/10.5194/acp-9-945-2009.](#)

1780 [Chen, D.-S., Ma, X., Xie, X., Wei, P., Wen, W., Xu, T., Yang, N., Gao, Q., Shi, H., Guo, X., 2015.](#)
1781 [Modelling the effect of aerosol feedbacks on the regional meteorology factors over China.](#)
1782 [Aerosol. Air. Qual. Res. 15, 1559-1579. <https://doi.org/10.4209/aaqr.2014.11.0272>.](#)

1783 [Chen, J., Li, C., Ristovski, Z., Milic, A., Gu, Y., Islam, M.S., Wang, S., Hao, J., Zhang, H., He, C.,](#)
1784 [2017. A review of biomass burning: Emissions and impacts on air quality, health and climate](#)
1785 [in China. Sci. Total Environ. 579, 1000-1034. <https://doi.org/10.1016/j.scitotenv.2016.11.025>.](#)

1786 [Chen, L., Gao, Y., Zhang, M., Fu, J.S., Zhu, J., Liao, H., Li, J., Huang, K., Ge, B., Wang, X., 2019a.](#)
1787 [MICS-Asia III: Multi-model comparison and evaluation of aerosol over East Asia. Atmos.](#)
1788 [Chem. Phys. 19, 11911-11937. <https://doi.org/10.5194/acp-19-11911-2019>.](#)

1789 [Chen, L., Zhu, J., Liao, H., Gao, Y., Qiu, Y., Zhang, M., Liu, Z., Li, N., Wang, Y., 2019b. Assessing](#)
1790 [the formation and evolution mechanisms of severe haze pollution in the Beijing-Tianjin-Hebei](#)
1791 [region using process analysis. Atmos. Chem. Phys. 19, 10845-10864.](#)
1792 [https://doi.org/10.5194/acp-19-10845-2019.](#)

1793 [Chen, S., Huang, J., Kang, L., Wang, H., Ma, X., He, Y., Yuan, T., Yang, B., Huang, Z., Zhang, G.,](#)
1794 [2017a. Emission, transport, and radiative effects of mineral dust from the Taklimakan and Gobi](#)
1795 [deserts: comparison of measurements and model results. Atmos. Chem. Phys. 17,](#)
1796 [https://doi.org/10.5194/acp-17-2401-2017.](#)

1797 [Chen, S., Huang, J., Qian, Y., Zhao, C., Kang, L., Yang, B., Wang, Y., Liu, Y., Yuan, T., Wang, T.,](#)
1798 [2017b. An overview of mineral dust modeling over East Asia. J. Meteorol. Res. 31, 633-653.](#)
1799 [https://doi.org/10.1007/s13351-017-6142-2.](#)

1800 [Chen, S., Huang, J., Zhao, C., Qian, Y., Leung, L.R., Yang, B., 2013. Modeling the transport and](#)
1801 [radiative forcing of Taklimakan dust over the Tibetan Plateau: A case study in the summer of](#)
1802 [2006. J. Geophys. Res. Atmos. 118, 797-812. <https://doi.org/10.1002/jgrd.50122>.](#)

1803 [Chen, S., Zhao, C., Qian, Y., Leung, L.R., Huang, J., Huang, Z., Bi, J., Zhang, W., Shi, J., Yang, L.,](#)
1804 [2014. Regional modeling of dust mass balance and radiative forcing over East Asia using](#)
1805 [WRF-Chem. Aeolian Res. 15, 15-30. <https://doi.org/10.1016/j.aeolia.2014.02.001>.](#)

1806 [Chen, X., Wang, Zifa, Yu, F., Pan, X., Li, J., Ge, B., Wang, Zhe, Hu, M., Yang, W., Chen, H., 2017.](#)
1807 [Estimation of atmospheric aging time of black carbon particles in the polluted atmosphere over](#)
1808 [central-eastern China using microphysical process analysis in regional chemical transport](#)
1809 [model. Atmos. Environ. 163, 44-56. <https://doi.org/j.atmosenv.2017.05.016>.](#)

1810 [Chen, X., Yang, W., Wang, Zifa, Li, J., Hu, M., An, J., Wu, Q., Wang, Zhe, Chen, H., Wei, Y., 2019. Improving new particle formation simulation by coupling a volatility-basis set \(VBS\) organic aerosol module in NAQPMS+APM. *Atmos. Environ.* 204, 1–11. <https://doi.org/j.atmosenv.2019.01.053>.](#)

1811

1812 [Chen, X., Yu, F., Yang, W., Sun, Y., Chen, H., Du, W., Zhao, J., Wei, Y., Wei, L., Du, H., 2021. Global–regional nested simulation of particle number concentration by combing microphysical processes with an evolving organic aerosol module. *Atmos. Chem. Phys.* 21, 9343–9366.](#)

1813

1814 [Chen, Y., Zhang, Y., Fan, J., Leung, L.-Y.R., Zhang, Q., He, K., 2015. Application of an online-coupled regional climate model, WRF-CAM5, over East Asia for examination of ice nucleation schemes: Part I. Comprehensive model evaluation and trend analysis for 2006 and 2011. *Climate* 3, 627-667. <https://doi.org/10.3390/cli3030627>.](#)

1815

1816 [Choobari, O.A., Zawar-Reza, P., Sturman, A., 2014. The global distribution of mineral dust and its impacts on the climate system: A review. *Atmos. Res.* 138, 152-165. <https://doi.org/10.1016/j.atmosres.2013.11.007>.](#)

1817

1818 [Chung, C.E., 2012. Aerosol direct radiative forcing: a review. *Atmospheric Aerosols-Regional Characteristics-Chemistry and Physics*; Abdul-Razzak, H., Ed. <https://doi.org/10.5772/50248>.](#)

1819

1820 [Conibear, L., Butt, E.W., Knote, C., Arnold, S.R., Spracklen, D. V., 2018b. Residential energy use emissions dominate health impacts from exposure to ambient particulate matter in India. *Nat. Commun.* 9, 1-9. <https://doi.org/10.1038/s41467-018-02986-7>.](#)

1821

1822 [Conibear, L., Butt, E.W., Knote, C., Arnold, S.R., Spracklen, D. V., 2018a. Stringent Emission Control Policies Can Provide Large Improvements in Air Quality and Public Health in India. *GeoHealth* 2, 196-211. <https://doi.org/10.1029/2018gh000139>.](#)

1823

1824 [Conti, G.O., Heibati, B., Kloog, I., Fiore, M., Ferrante, M., 2017. A review of AirQ Models and their applications for forecasting the air pollution health outcomes. *Environ. Sci. Pollut. Res.* 24, 6426-6445. <https://doi.org/10.1007/s11356-016-8180-1>.](#)

1825

1826 [Corbin, J.C., Gysel-Beer, M., 2019. Detection of tar brown carbon with a single particle soot photometer \(SP2\). *Atmos. Chem. Phys.* 19, 15673–15690.](#)

1827

1828 [Craig, A., Valcke, S., Coquart, L., 2017. Development and performance of a new version of the OASIS coupler, OASIS3-MCT 3. 0. *Geosci. Model Dev.* 10, 3297. <https://doi.org/10.5194/gmd-10-3297-2017>.](#)

1829

1830 [Cuchiara, G.C., Li, X., Carvalho, J., Rappenglück, B., 2014. Intercomparison of planetary boundary layer parameterization and its impacts on surface ozone concentration in the WRF/Chem model for a case study in Houston/Texas. *Atmos. Environ.* 96, 175-185. <https://doi.org/10.1016/j.atmosenv.2014.07.013>.](#)

1831

1832 [Dahutia, P., Pathak, B., Bhuyan, P.K., 2019. Vertical distribution of aerosols and clouds over north-eastern South Asia: Aerosol-cloud interactions. *Atmos. Environ.* 215, 116882. <https://doi.org/10.1016/j.atmosenv.2019.116882>.](#)

1833

1834 [Ding, A.J., Huang, X., Nie, W., Sun, J.N., Kerminen, V., Pet?j?, T., Su, H., Cheng, Y.F., Yang, X., Wang, M.H., 2016. Enhanced haze pollution by black carbon in megacities in China. *Geophys. Res. Lett.* 43, 2873-2879. <https://doi.org/10.1002/2016GL067745>.](#)

1835

1836 [Ding, Q.J., Sun, J., Huang, X., Ding, A., Zou, J., Yang, X., Fu, C., 2019. Impacts of black carbon on the formation of advection-radiation fog during a haze pollution episode in eastern China. *Atmos. Chem. Phys.* 19, 7759-7774. <https://doi.org/10.5194/acp-19-7759-2019>.](#)

1837

1838 [Dipu, S., Prabha, T. V, Pandithurai, G., Dudhia, J., Pfister, G., Rajesh, K., Goswami, B.N., 2013. Impact of elevated aerosol layer on the cloud macrophysical properties prior to monsoon onset. *Atmos. Environ.* 70, 454-467. <https://doi.org/10.1016/j.atmosenv.2012.12.036>.](#)

1839

1840 [Donat, M.G., Lowry, A.L., Alexander, L. V, O’Gorman, P.A., Maher, N., 2016. More extreme precipitation in the world’s dry and wet regions. *Nat. Clim. Chang.* 6, 508-513. <https://doi.org/10.1038/nclimate2941>.](#)

1841

1842 [Dong, X., Fu, J.S., Huang, K., Zhu, Q., Tipton, M., 2019. Regional Climate Effects of Biomass Burning and Dust in East Asia: Evidence From Modeling and Observation. *Geophys. Res. Lett.* 46, 11490-11499. <https://doi.org/10.1029/2019GL083894>.](#)

1843

1844 [Easter, R.C., Ghan, S.J., Zhang, Y., Saylor, R.D., Chapman, E.G., Laulainen, N.S., Abdul - Razzak, H., Leung, L.R., Bian, X., Zaveri, R.A., 2004. MIRAGE: Model description and evaluation of aerosols and trace gases. *J. Geophys. Res. Atmos.* 109. <https://doi.org/10.1029/2004JD004571>.](#)

1845

1846 [Eck, T.F., Holben, B.N., Reid, J.S., Xian, P., Giles, D.M., Sinyuk, A., Smirnov, A., Schafer, J.S., Slutsker, I., Kim, J., 2018. Observations of the interaction and transport of fine mode aerosols](#)

1867 [with cloud and/or fog in Northeast Asia from Aerosol Robotic Network and satellite remote](#)
1868 [sensing. J. Geophys. Res. Atmos. 123, 5560-5587. <https://doi.org/10.1029/2018JD028313>.](#)

1869 [El-Harbawi, M., 2013. Air quality modelling, simulation, and computational methods: a review.](#)
1870 [Environ. Rev. 21, 149-179. <https://doi.org/10.1139/er-2012-0056>.](#)

1871 [ENVIRON, U.G., 2008. Comprehensive Air Quality Model with Extensions \(CAMx\). Version 4.50.](#)
1872 [Env. Int. Corp. Novato.](#)

1873 [EPA, 2018. Meteorological Model Performance for Annual 2016 Simulation WRF v3.8. United](#)
1874 [States Environ. Prot. Agency.](#)

1875 [Fahey, K.M., Carlton, A.G., Pye, H.O.T., Baek, J., Hutzell, W.T., Stanier, C.O., Baker, K.R., Appel,](#)
1876 [K.W., Jaoui, M., Offenberg, J.H., 2017. A framework for expanding aqueous chemistry in the](#)
1877 [Community Multiscale Air Quality \(CMAQ\) model version 5.1. Geosci. Model Dev. 10, 1587–](#)
1878 [1605. <https://doi.org/10.5194/gmd-10-1587-2017>.](#)

1879 [Fan, J., Rosenfeld, D., Yang, Y., Zhao, C., Leung, L.R., Li, Z., 2015. Substantial contribution of](#)
1880 [anthropogenic air pollution to catastrophic floods in Southwest China. Geophys. Res. Lett. 42,](#)
1881 [6066-6075. <https://doi.org/10.1002/2015GL064479>.](#)

1882 [Fan, J., Rosenfeld, D., Zhang, Y., Giangrande, S.E., Li, Z., Machado, L.A.T., Martin, S.T., Yang, Y.,](#)
1883 [Wang, J., Artaxo, P., 2018. Substantial convection and precipitation enhancements by ultrafine](#)
1884 [aerosol particles. Science \(80-. \). 359, 411-418. <https://doi.org/10.1126/science.aan8461>.](#)

1885 [Fan, J., Wang, Y., Rosenfeld, D., Liu, X., 2016. Review of aerosol-cloud interactions: Mechanisms,](#)
1886 [significance, and challenges. J. Atmos. Sci. 73, 4221-4252. \[0037.1.\]\(https://doi.org/10.1175/JAS-D-16-

1887 <a href=\)](#)

1888 [Fast, J.D., Gustafson Jr, W.I., Easter, R.C., Zaveri, R.A., Barnard, J.C., Chapman, E.G., Grell, G.A.,](#)
1889 [Peckham, S.E., 2006. Evolution of ozone, particulates, and aerosol direct radiative forcing in](#)
1890 [the vicinity of Houston using a fully coupled meteorology - chemistry - aerosol model. J.](#)
1891 [Geophys. Res. Atmos. 111. <https://doi.org/10.1029/2005JD006721>.](#)

1892 [Feingold, G., Eberhard, W.L., Veron, D.E., Previdi, M., 2003. First measurements of the Twomey](#)
1893 [indirect effect using ground - based remote sensors. Geophys. Res. Lett. 30,](#)
1894 [https://doi.org/10.1029/2002GL016633.](#)

1895 [Feng, Y., Kotamarthi, V.R., Coulter, R., Zhao, C., Cadetdu, M., 2016. Radiative and thermodynamic](#)
1896 [responses to aerosol extinction profiles during the pre-monsoon month over South Asia. Atmos.](#)
1897 [Chem. Phys. 16. <https://doi.org/10.5194/acp-16-247-2016>.](#)

1898 [Foley, K.M., Roselle, S.J., Appel, K.W., Bhave, P.V., Pleim, J.E., Otte, T.L., Mathur, R., Sarwar, G.,](#)
1899 [Young, J.O., Gilliam, R.C., 2010. Incremental testing of the Community Multiscale Air Quality](#)
1900 [\(CMAQ\) modeling system version 4.7. Geosci. Model Dev. 3, 205–226.](#)
1901 [https://doi.org/10.5194/gmd-3-205-2010.](#)

1902 [Forkel, R., Brunner, D., Baklanov, A., Balzarini, A., Hirtl, M., Honzak, L., Jiménez-Guerrero, P.,](#)
1903 [Jorba, O., Pérez, J.L., San José, R., 2016. A multi-model case study on aerosol feedbacks in](#)
1904 [online coupled chemistry-meteorology models within the cost action ES1004 EuMetChem. in:](#)
1905 [Air Pollution Modeling and Its Application XXIV. Springer, pp. 23-28.](#)
1906 [https://doi.org/10.1007/978-3-319-24478-5_4.](#)

1907 [Fu, P., Aggarwal, S.G., Chen, J., Li, J., Sun, Y., Wang, Z., Chen, H., Liao, H., Ding, A., Umarji, G.S.,](#)
1908 [2016. Molecular markers of secondary organic aerosol in Mumbai, India. Environ. Sci. Technol.](#)
1909 [50, 4659–4667. <https://doi.org/10.1021/acs.est.6b00372>.](#)

1910 [Gao, C., Zhang, X., Xiu, A., Huang, L., Zhao, H., Wang, K., Tong, Q., 2019. Spatiotemporal](#)
1911 [distribution of biogenic volatile organic compounds emissions in China. Acta Sci.](#)
1912 [Circumstantiae 39, 4140-4151. <https://doi.org/10.13671/j.hjkxxb.2019.0243>.](#)

1913 [Gao, J., Zhu, B., Xiao, H., Kang, H., Pan, C., Wang, D., Wang, H., 2018. Effects of black carbon](#)
1914 [and boundary layer interaction on surface ozone in Nanjing, China. Atmos. Chem. Phys. 18,](#)
1915 [https://doi.org/10.5194/acp-18-7081-2018.](#)

1916 [Gao, M., Carmichael, G.R., Saide, P.E., Lu, Z., Yu, M., Streets, D.G., Wang, Z., 2016a. Response of](#)
1917 [winter fine particulate matter concentrations to emission and meteorology changes in North](#)
1918 [China. Atmos. Chem. Phys. 16, 11837. <https://doi.org/10.5194/acp-16-11837-2016>.](#)

1919 [Gao, M., Carmichael, G.R., Wang, Y., Saide, P.E., Liu, Z., Xin, J., Shan, Y., Wang, Z., 2017a.](#)
1920 [Chemical and Meteorological Feedbacks in the Formation of Intense Haze Events, in: Air](#)
1921 [Pollution in Eastern Asia: An Integrated Perspective. Springer, pp. 437-452.](#)
1922 [https://doi.org/10.1007/978-3-319-59489-7_21.](#)

1923 [Gao, M., Carmichael, G.R., Wang, Y., Saide, P.E., Yu, M., Xin, J., Liu, Z., Wang, Z., 2016b.](#)

1924 [Modeling study of the 2010 regional haze event in the North China Plain. Atmos. Chem. Phys.](#)
1925 [16, 1673. https://doi.org/10.5194/acp-16-1673-2016.](#)

1926 [Gao, M., Guttikunda, S.K., Carmichael, G.R., Wang, Y., Liu, Z., Stanier, C.O., Saide, P.E., Yu, M.,](#)
1927 [2015. Health impacts and economic losses assessment of the 2013 severe haze event in Beijing](#)
1928 [area. Sci. Total Environ. 511, 553-561. https://doi.org/10.1016/j.scitotenv.2015.01.005.](#)

1929 [Gao, M., Han, Z., Liu, Z., Li, M., Xin, J., Tao, Z., Li, J., Kang, J.E., Huang, K., Dong, X., Zhuang,](#)
1930 [B., Li, S., Ge, B., Wu, Q., Cheng, Y., Wang, Y., Lee, H.J., Kim, C.H., Fu, J.S., Wang, T., Chin,](#)
1931 [M., Woo, J.H., Zhang, Q., Wang, Z., Carmichael, G.R., 2018a. Air quality and climate change,](#)
1932 [Topic 3 of the Model Inter-Comparison Study for Asia Phase III \(MICS-Asia III\)- Part 1:](#)
1933 [Overview and model evaluation. Atmos. Chem. Phys. 18, 4859-4884.](#)
1934 [https://doi.org/10.5194/acp-18-4859-2018.](#)

1935 [Gao, M., Ji, D., Liang, F., Liu, Y., 2018b. Attribution of aerosol direct radiative forcing in China and](#)
1936 [India to emitting sectors. Atmos. Environ. 190, 35-42.](#)
1937 [https://doi.org/10.1016/j.atmosenv.2018.07.011.](#)

1938 [Gao, M., Liu, Z., Wang, Y., Lu, X., Ji, D., Wang, L., Li, M., Wang, Z., Zhang, Q., Carmichael, G.R.,](#)
1939 [2017b. Distinguishing the roles of meteorology, emission control measures, regional transport,](#)
1940 [and co-benefits of reduced aerosol feedbacks in “APEC Blue.” Atmos. Environ. 167, 476-486.](#)
1941 [https://doi.org/10.1016/j.atmosenv.2017.08.054.](#)

1942 [Gao, M., Saide, P.E., Xin, J., Wang, Yuesi, Liu, Z., Wang, Yuxuan, Wang, Z., Pagowski, M.,](#)
1943 [Guttikunda, S.K., Carmichael, G.R., 2017c. Estimates of health impacts and radiative forcing](#)
1944 [in winter haze in eastern China through constraints of surface PM_{2.5} predictions. Environ. Sci.](#)
1945 [Technol. 51, 2178-2185. https://doi.org/10.1021/acs.est.6b03745.](#)

1946 [Gao, Y., Zhang, M., 2018. Changes in the diurnal variations of clouds and precipitation induced by](#)
1947 [anthropogenic aerosols over East China in August 2008. Atmos. Pollut. Res. 9, 513-525.](#)
1948 [https://doi.org/10.1016/j.apr.2017.11.013.](#)

1949 [Gao, Y., Zhang, M., Liu, X., Wang, L., 2016. Change in diurnal variations of meteorological](#)
1950 [variables induced by anthropogenic aerosols over the North China Plain in summer 2008. Theor.](#)
1951 [Appl. Climatol. 124, 103-118. https://doi.org/10.1007/s00704-015-1403-4.](#)

1952 [Gao, Y., Zhang, M., Liu, X., Zhao, C., 2012. Model Analysis of the Anthropogenic Aerosol Effect](#)
1953 [on Clouds over East Asia. Atmos. Ocean. Sci. Lett. 5, 1-7.](#)
1954 [https://doi.org/10.1080/16742834.2012.11446968.](#)

1955 [Gao, Y., Zhang, M., Liu, Z., Wang, L., Wang, P., Xia, X., Tao, M., Zhu, L., 2015. Modeling the](#)
1956 [feedback between aerosol and meteorological variables in the atmospheric boundary layer](#)
1957 [during a severe fog-haze event over the North China Plain. Atmos. Chem. Phys. 15,](#)
1958 [https://doi.org/10.5194/acp-15-4279-2015.](#)

1959 [Gao, Y., Zhao, C., Liu, X., Zhang, M., Leung, L.R., 2014. WRF-Chem simulations of aerosols and](#)
1960 [anthropogenic aerosol radiative forcing in East Asia. Atmos. Environ. 92, 250-266.](#)
1961 [https://doi.org/10.1016/j.atmosenv.2014.04.038.](#)

1962 [García - Díez, M., Fernández, J., Fita, L., Yagüe, C., 2013. Seasonal dependence of WRF model](#)
1963 [biases and sensitivity to PBL schemes over Europe. Q. J. R. Meteorol. Soc. 139, 501-514.](#)
1964 [https://doi.org/10.1002/qj.1976.](#)

1965 [Ge, C., Wang, J., Reid, J.S., 2014. Mesoscale modeling of smoke transport over the Southeast Asian](#)
1966 [Maritime Continent: coupling of smoke direct radiative effect below and above the low-level](#)
1967 [clouds. Atmos. Chem. Phys. 14, 159. https://doi.org/10.5194/acp-14-159-2014.](#)

1968 [Gery, M.W., Whitten, G.Z., Killus, J.P., Dodge, M.C., 1989. A photochemical kinetics mechanism](#)
1969 [for urban and regional scale computer modeling. J. Geophys. Res. Atmos. 94, 12925–12956.](#)
1970 [https://doi.org/10.1029/JD094iD10p12925.](#)

1971 [Ghan, S.J., Zaveri, R.A., 2007. Parameterization of optical properties for hydrated internally mixed](#)
1972 [aerosol. J. Geophys. Res. Atmos. 112, 1–10. https://doi.org/10.1029/2006JD007927.](#)

1973 [Ghude, S.D., Chate, D.M., Jena, C., Beig, G., Kumar, R., Barth, M.C., Pfister, G.G., Fadnavis, S.,](#)
1974 [Pithani, P., 2016. Premature mortality in India due to PM_{2.5} and ozone exposure. Geophys. Res.](#)
1975 [Lett. 43, 4650-4658. https://doi.org/10.1002/2016GL068949.](#)

1976 [Giorgi, F., Chameides, W.L., 1986. Rainout lifetimes of highly soluble aerosols and gases as inferred](#)
1977 [from simulations with a general circulation model. J. Geophys. Res. Atmos. 91, 14367–14376.](#)
1978 [https://doi.org/10.1029/JD091iD13p14367.](#)

1979 [Gong, S.L., Barrie, L.A., Blanchet, J., 1997. Modeling sea-salt aerosols in the atmosphere: 1. Model](#)
1980 [development. J. Geophys. Res. Atmos. 102, 3805–3818. https://doi.org/10.1029/96JD02953.](#)

1981 [Gong, S.L., Barrie, L.A., Blanchet, J., Von Salzen, K., Lohmann, U., Lesins, G., Spacek, L., Zhang,](#)
1982 [L.M., Girard, E., Lin, H., 2003. Canadian Aerosol Module: A size-segregated simulation of](#)
1983 [atmospheric aerosol processes for climate and air quality models 1. Module development. J.](#)
1984 [Geophys. Res. Atmos. 108, AAC-3. <https://doi.org/10.1029/2001JD002002>](#)
1985 [Gong, S.L., Zhang, X.Y., Zhao, T.L., McKendry, I.G., Jaffe, D.A., Lu, N.M., 2003. Characterization](#)
1986 [of soil dust aerosol in China and its transport and distribution during 2001 ACE-Asia: 2. Model](#)
1987 [simulation and validation. J. Geophys. Res. Atmos. 108,](#)
1988 [https://doi.org/10.1029/2002JD002633.](#)
1989 [Goren, T., Rosenfeld, D., 2014. Decomposing aerosol cloud radiative effects into cloud cover, liquid](#)
1990 [water path and Twomey components in marine stratocumulus. Atmos. Res. 138, 378-393.](#)
1991 [https://doi.org/10.1016/j.atmosres.2013.12.008.](#)
1992 [Govardhan, G., Nanjundiah, R.S., Satheesh, S.K., Krishnamoorthy, K., Kotamarthi, V.R., 2015.](#)
1993 [Performance of WRF-Chem over Indian region: Comparison with measurements. J. Earth Syst.](#)
1994 [Sci. 124, 875-896. <https://doi.org/10.1007/s12040-015-0576-7>.](#)
1995 [Govardhan, G.R., Nanjundiah, R.S., Satheesh, S.K., Moorthy, K.K., Takemura, T., 2016. Inter-](#)
1996 [comparison and performance evaluation of chemistry transport models over Indian region.](#)
1997 [Atmos. Environ. 125, 486-504. <https://doi.org/10.1016/j.atmosenv.2015.10.065>.](#)
1998 [Gray, L.J., Beer, J., Geller, M., Haigh, J.D., Lockwood, M., Matthes, K., Cubasch, U., Fleitmann,](#)
1999 [D., Harrison, G., Hood, L., 2010. Solar influences on climate. Rev. Geophys. 48,](#)
2000 [https://doi.org/10.1029/2009RG000282.](#)
2001 [Grell, G., Freitas, S.R., Stuefer, M., Fast, J., 2011. Inclusion of biomass burning in WRF-Chem:](#)
2002 [impact of wildfires on weather forecasts. Atmos. Chem. Phys 11, 5289-5303.](#)
2003 [https://doi.org/10.5194/acp-11-5289-2011.](#)
2004 [Grell, G.A., Peckham, S.E., Schmitz, R., McKeen, S.A., Frost, G., Skamarock, W.C., Eder, B., 2005.](#)
2005 [Fully coupled "online" chemistry within the WRF model. Atmos. Environ. 39, 6957-6975.](#)
2006 [https://doi.org/10.1016/j.atmosenv.2005.04.027.](#)
2007 [Groß, S., Esselborn, M., Weinzierl, B., Wirth, M., Fix, A., Petzold, A., 2013. Aerosol classification](#)
2008 [by airborne high spectral resolution lidar observations. Atmos. Chem. Phys. 13, 2487.](#)
2009 [https://doi.org/10.5194/acp-13-2487-2013.](#)
2010 [Guo, J., Deng, M., Fan, J., Li, Z., Chen, Q., Zhai, P., Dai, Z., Li, X., 2014. Precipitation and air](#)
2011 [pollution at mountain and plain stations in northern China: Insights gained from observations](#)
2012 [and modeling. J. Geophys. Res. Atmos. 119, 4793-4807.](#)
2013 [https://doi.org/10.1002/2013JD021161.](#)
2014 [Guo, J., Liu, H., Li, Z., Rosenfeld, D., Jiang, M., Xu, W., Jiang, J.H., 2018. Aerosol-induced changes](#)
2015 [in the vertical structure of precipitation?: a perspective of TRMM precipitation radar 13329-](#)
2016 [13343. <https://doi.org/10.5194/acp-18-13329-2018>.](#)
2017 [Gurjar, B.R., Ravindra, K., Nagpure, A.S., 2016. Air pollution trends over Indian megacities and](#)
2018 [their local-to-global implications. Atmos. Environ. 142, 475-495.](#)
2019 [https://doi.org/10.1016/j.atmosenv.2016.06.030.](#)
2020 [Haywood, J., Boucher, O., 2000. Estimates of the direct and indirect radiative forcing due to](#)
2021 [tropospheric aerosols: A review. Rev. Geophys. 38, 513-543.](#)
2022 [https://doi.org/10.1029/1999RG000078.](#)
2023 [He, J., Zhang, Y., 2014. Improvement and further development in CESM/CAM5: gas-phase](#)
2024 [chemistry and inorganic aerosol treatments. Atmos. Chem. Phys. 14, 9171-9200.](#)
2025 [https://doi.org/10.5194/acp-14-9171-2014.](#)
2026 [He, J., Zhang, Y., Wang, K., Chen, Y., Leung, L.R., Fan, J., Li, M., Zheng, B., Zhang, Q., Duan, F.,](#)
2027 [2017. Multi-year application of WRF-CAM5 over East Asia-Part I: Comprehensive evaluation](#)
2028 [and formation regimes of O₃ and PM_{2.5}. Atmos. Environ. 165, 122-142.](#)
2029 [https://doi.org/10.1016/j.atmosenv.2017.06.015.](#)
2030 [Hodshire, A.L., Akherati, A., Alvarado, M.J., Brown-Steiner, B., Jathar, S.H., Jimenez, J.L.,](#)
2031 [Kreidenweis, S.M., Lonsdale, C.R., Onasch, T.B., Ortega, A.M., 2019. Aging effects on](#)
2032 [biomass burning aerosol mass and composition: A critical review of field and laboratory studies.](#)
2033 [Environ. Sci. Technol. 53, 10007-10022. <https://doi.org/10.1021/acs.est.9b02588>.](#)
2034 [Hodzic, A., Jimenez, J.L., 2011. Modeling anthropogenically controlled secondary organic aerosols](#)
2035 [in a megacity: A simplified framework for global and climate models. Geosci. Model Dev. 4,](#)
2036 [901-917. <https://doi.org/10.5194/gmd-4-901-2011>.](#)
2037 [Hong, C., Zhang, Q., Zhang, Y., Davis, S.J., Tong, D., Zheng, Y., Liu, Z., Guan, D., He, K.,](#)

2038 [Schellnhuber, H.J., 2019. Impacts of climate change on future air quality and human health in](#)
2039 [China. Proc. Natl. Acad. Sci. 116, 17193-17200. <https://doi.org/10.1073/pnas.1812881116>.](#)

2040 [Hong, C., Zhang, Q., Zhang, Y., Tang, Y., Tong, D., He, K., 2017. Multi-year downscaling](#)
2041 [application of two-way coupled WRF v3.4 and CMAQ v5.0.2 over east Asia for regional](#)
2042 [climate and air quality modeling: model evaluation and aerosol direct effects. Geosci. Model](#)
2043 [Dev. 10. <https://doi.org/10.5194/gmd-10-2447-2017>.](#)

2044 [Hu, X., Klein, P.M., Xue, M., 2013. Evaluation of the updated YSU planetary boundary layer](#)
2045 [scheme within WRF for wind resource and air quality assessments. J. Geophys. Res. Atmos.](#)
2046 [118, 10-490. <https://doi.org/10.1002/jgrd.50823>.](#)

2047 [Huang, J., Wang, T., Wang, W., Li, Z., Yan, H., 2014. Climate effects of dust aerosols over East](#)
2048 [Asian arid and semiarid regions. J. Geophys. Res. Atmos. 119, 11-398.](#)
2049 [https://doi.org/10.1002/2014JD021796.](#)

2050 [Huang, L., Lin, W., Li, F., Wang, Y., Jiang, B., 2019. Climate impacts of the biomass burning in](#)
2051 [Indochina on atmospheric conditions over southern China. Aerosol Air Qual. Res. 19, 2707-](#)
2052 [2720. <https://doi.org/10.4209/aaqr.2019.01.0028>.](#)

2053 [Huang, X., Ding, A., Liu, L., Liu, Q., Ding, K., Niu, X., Nie, W., Xu, Z., Chi, X., Wang, M., 2016.](#)
2054 [Effects of aerosol-radiation interaction on precipitation during biomass-burning season in East](#)
2055 [China. Atmos. Chem. Phys. 16. <https://doi.org/10.5194/acp-16-10063-2016>.](#)

2056 [Huang, X., Song, Y., Zhao, C., Cai, X., Zhang, H., Zhu, T., 2015. Direct radiative effect by](#)
2057 [multicomponent aerosol over China. J. Clim. 28, 3472-3495. \[14-00365.1.\]\(https://doi.org/10.1175/JCLI-D-

2058 <a href=\)](#)

2059 [Illingworth, A.J., Barker, H.W., Beljaars, A., Ceccaldi, M., Chepfer, H., Clerbaux, N., Cole, J.,](#)
2060 [Delano?, J., Domenech, C., Donovan, D.P., 2015. The EarthCARE satellite: The next step](#)
2061 [forward in global measurements of clouds, aerosols, precipitation, and radiation. Bull. Am.](#)
2062 [Meteorol. Soc. 96, 1311-1332. <https://doi.org/10.1175/BAMS-D-12-00227.1>.](#)

2063 [Im, U., Bianconi, R., Solazzo, E., Kioutsioukis, I., Badia, A., Balzarini, A., Baró, R., Bellasio, R.,](#)
2064 [Brunner, D., Chemel, C., 2015a. Evaluation of operational online-coupled regional air quality](#)
2065 [models over Europe and North America in the context of AQMEII phase 2. Part II: Particulate](#)
2066 [matter. Atmos. Environ. 115, 421-441. <https://doi.org/10.1016/j.atmosenv.2014.08.072>.](#)

2067 [Im, U., Bianconi, R., Solazzo, E., Kioutsioukis, I., Badia, A., Balzarini, A., Baró, R., Bellasio, R.,](#)
2068 [Brunner, D., Chemel, C., 2015b. Evaluation of operational on-line-coupled regional air quality](#)
2069 [models over Europe and North America in the context of AQMEII phase 2. Part I: Ozone.](#)
2070 [Atmos. Environ. 115, 404-420. <https://doi.org/10.1016/j.atmosenv.2014.09.042>.](#)

2071 [IPCC, 2007. Climate change 2007: Synthesis Report. Contribution of Working Groups I, II and III](#)
2072 [to the Fifth Assessment Report of the Intergovernmental Panel on Climate Change.](#)

2073 [IPCC, 2014. Climate change 2014: Synthesis Report. Contribution of Working Groups I, II and III](#)
2074 [to the fifth assessment report of the Intergovernmental Panel on Climate Change.](#)

2075 [Jacobson, M.Z., 2001. Strong radiative heating due to the mixing state of black carbon in](#)
2076 [atmospheric aerosols 409, 695-697. <https://doi.org/10.1038/35055518>.](#)

2077 [Jacobson, M.Z., 2002. Analysis of aerosol interactions with numerical techniques for solving](#)
2078 [coagulation, nucleation, condensation, dissolution, and reversible chemistry among multiple](#)
2079 [size distributions. J. Geophys. Res. Atmos. 107, AAC-2.](#)
2080 [https://doi.org/10.1029/2001JD002044.](#)

2081 [Jacobson, M.Z., 2003. Development of mixed-phase clouds from multiple aerosol size distributions](#)
2082 [and the effect of the clouds on aerosol removal. J. Geophys. Res. Atmos. 108.](#)
2083 [https://doi.org/10.1029/2002JD002691.](#)

2084 [Jacobson, M.Z., 2012. Investigating cloud absorption effects: Global absorption properties of black](#)
2085 [carbon, tar balls, and soil dust in clouds and aerosols. J. Geophys. Res. Atmos. 117.](#)
2086 [https://doi.org/10.1029/2011JD017218.](#)

2087 [Jacobson, M.Z., Jacobson, M.Z., 1999. Fundamentals of atmospheric modeling. Cambridge](#)
2088 [university press.](#)

2089 [Jacobson, M.Z., Jadhav, V., 2018. World estimates of PV optimal tilt angles and ratios of sunlight](#)
2090 [incident upon tilted and tracked PV panels relative to horizontal panels. Sol. Energy 169, 55-](#)
2091 [66. <https://doi.org/10.1016/j.solener.2018.04.030>.](#)

2092 [Jacobson, M.Z., Kaufman, Y.J., Rudich, Y., 2007. Examining feedbacks of aerosols to urban climate](#)
2093 [with a model that treats 3-D clouds with aerosol inclusions. J. Geophys. Res. Atmos. 112.](#)
2094 [https://doi.org/10.1029/2007JD008922.](#)

2095 [Jacobson, M.Z., Nghiem, S. V, Sorichetta, A., 2019. Short-term impacts of the megaurbanizations](#)
2096 [of New Delhi and Los Angeles between 2000 and 2009. J. Geophys. Res. Atmos. 124, 35–56.](#)
2097 <https://doi.org/10.1029/2018JD029310>.

2098 [Jacobson, M.Z., Nghiem, S. V, Sorichetta, A., Whitney, N., 2015. Ring of impact from the mega -](#)
2099 [urbanization of Beijing between 2000 and 2009. J. Geophys. Res. Atmos. 120, 5740 – 5756.](#)
2100 <https://doi.org/10.1002/2014JD023008>.

2101 [Jacobson, M.Z., Turco, R.P., 1995. Simulating condensational growth, evaporation, and coagulation](#)
2102 [of aerosols using a combined moving and stationary size grid. Aerosol Sci. Technol. 22, 73–](#)
2103 [92. https://doi.org/10.1080/02786829408959729.](#)

2104 [Jacobson, M.Z., Turco, R.P., Jensen, E.J., Toon, O.B., 1994. Modeling coagulation among particles](#)
2105 [of different composition and size. Atmos. Environ. 28, 1327–1338.](#)
2106 [https://doi.org/10.1016/1352-2310\(94\)90280-1](https://doi.org/10.1016/1352-2310(94)90280-1).

2107 [Jena, C., Ghude, S.D., Pfister, G.G., Chate, D.M., Kumar, R., Beig, G., Surendran, D.E., Fadnavis,](#)
2108 [S., Lal, D.M., 2015. Influence of springtime biomass burning in South Asia on regional ozone](#)
2109 [\(O₃\): A model based case study. Atmos. Environ. 100, 37-47.](#)
2110 <https://doi.org/10.1016/j.atmosenv.2014.10.027>.

2111 [Jeong, J.I., Park, R.J., 2017. Winter monsoon variability and its impact on aerosol concentrations in](#)
2112 [East Asia. Environ. Pollut. 221, 285-292. https://doi.org/10.1016/j.envpol.2016.11.075.](#)

2113 [Jia, X., Guo, X., 2012. Impacts of Anthropogenic Atmospheric Pollutant on Formation and](#)
2114 [Development of a Winter Heavy Fog Event. Chinese J. Atmos. Sci. 36, 995-1008.](#)
2115 <https://doi.org/10.1007/s11783-011-0280-z>.

2116 [Jia, X., Quan, J., Zheng, Z., Liu, X., Liu, Q., He, H., Liu, Y., 2019. Impacts of Anthropogenic](#)
2117 [Aerosols on Fog in North China Plain. J. Geophys. Res. Atmos. 124, 252-265.](#)
2118 <https://doi.org/10.1029/2018JD029437>.

2119 [Jiang, B., Huang, B., Lin, W., Xu, S., 2016. Investigation of the effects of anthropogenic pollution](#)
2120 [on typhoon precipitation and microphysical processes using WRF-Chem. J. Atmos. Sci. 73,](#)
2121 [1593-1610. https://doi.org/10.1175/JAS-D-15-0202.1.](#)

2122 [Jiang, B., Lin, W., Li, F., Chen, B., 2019a. Simulation of the effects of sea-salt aerosols on cloud ice](#)
2123 [and precipitation of a tropical cyclone. Atmos. Sci. Lett. 20, e936.](#)
2124 <https://doi.org/10.1002/asl.936>.

2125 [Jiang, B., Lin, W., Li, F., Chen, J., 2019b. Sea-salt aerosol effects on the simulated microphysics](#)
2126 [and precipitation in a tropical cyclone. J. Meteorol. Res. 33, 115-125.](#)
2127 <https://doi.org/10.1007/s13351-019-8108-z>.

2128 [Jiang, X., Wiedinmyer, C., Carlton, A.G., 2012. Aerosols from fires: An examination of the effects](#)
2129 [on ozone photochemistry in the Western United States. Environ. Sci. Technol. 46, 11878–11886.](#)
2130 <https://doi.org/10.1021/es301541k>.

2131 [Jimenez, P.A., Hacker, J.P., Dudhia, J., Haupt, S.E., Ruiz-Arias, J.A., Gueymard, C.A., Thompson,](#)
2132 [G., Eidhammer, T., Deng, A., 2016. WRF-Solar: Description and clear-sky assessment of an](#)
2133 [augmented NWP model for solar power prediction. Bull. Am. Meteorol. Soc. 97, 1249-1264.](#)
2134 <https://doi.org/10.1175/BAMS-D-14-00279.1>.

2135 [Jin, Q., Wei, J., Yang, Z.-L., Pu, B., Huang, J., 2015. Consistent response of Indian summer monsoon](#)
2136 [to Middle East dust in observations and simulations. Atmos. Chem. Phys. 15, 9897-9915.](#)
2137 <https://doi.org/10.5194/acp-15-9897-2015>.

2138 [Jin, Q., Yang, Z.-L., Wei, J., 2016a. Seasonal responses of Indian summer monsoon to dust aerosols](#)
2139 [in the Middle East, India, and China. J. Clim. 29, 6329-6349. https://doi.org/10.1175/JCLI-D-](#)
2140 [15-0622.1.](#)

2141 [Jin, Q., Yang, Z.-L., Wei, J., 2016b. High sensitivity of Indian summer monsoon to Middle East dust](#)
2142 [absorptive properties. Sci. Rep. 6, 1-8. https://doi.org/10.1038/srep30690.](#)

2143 [Jung, J., Souri, A.H., Wong, D.C., Lee, S., Jeon, W., Kim, J., Choi, Y., 2019. The Impact of the](#)
2144 [Direct Effect of Aerosols on Meteorology and Air Quality Using Aerosol Optical Depth](#)
2145 [Assimilation During the KORUS - AQ Campaign. J. Geophys. Res. Atmos. 124, 8303-8319.](#)
2146 <https://doi.org/10.1029/2019JD030641>.

2147 [Kajino, M., Ueda, H., Han, Z., Kudo, R., Inomata, Y., Kaku, H., 2017. Synergy between air pollution](#)
2148 [and urban meteorological changes through aerosol-radiation-diffusion feedback—A case study](#)
2149 [of Beijing in January 2013. Atmos. Environ. 171, 98-110.](#)
2150 <https://doi.org/10.1016/j.atmosenv.2017.10.018>.

2151 [Kant, S., Panda, J., Gautam, R., 2019. A seasonal analysis of aerosol-cloud-radiation interaction](#)

2152 [over Indian region during 2000-2017. Atmos. Environ. 201, 212-222.](#)
 2153 <https://doi.org/10.1016/j.atmosenv.2018.12.044>.
 2154 [Kedia, S., Cherian, R., Islam, S., Das, S.K., Kaginalkar, A., 2016. Regional simulation of aerosol](#)
 2155 [radiative effects and their influence on rainfall over India using WRFChem model. Atmos. Res.](#)
 2156 [182, 232-242. https://doi.org/10.1016/j.atmosres.2016.07.008.](#)
 2157 [Kedia, S., Kumar, S., Islam, S., Hazra, A., Kumar, N., 2019a. Aerosols impact on the convective](#)
 2158 [and non-convective rain distribution over the Indian region?: Results from WRF-Chem](#)
 2159 [simulation. Atmos. Environ. 202, 64-74. https://doi.org/10.1016/j.atmosenv.2019.01.020.](#)
 2160 [Kedia, S., Vellore, R.K., Islam, S., Kaginalkar, A., 2019b. A study of Himalayan extreme rainfall](#)
 2161 [events using WRF-Chem. Meteorol. Atmos. Phys. 131, 1133-1143.](#)
 2162 <https://doi.org/10.1007/s00703-018-0626-1>.
 2163 [Keita, S.A., Girard, E., Raut, J.-C., Leriche, M., Blanchet, J.-P., Pelon, J., Onishi, T., Cirisan, A.,](#)
 2164 [2020. A new parameterization of ice heterogeneous nucleation coupled to aerosol chemistry in](#)
 2165 [WRF-Chem model version 3.5.1: evaluation through ISDAC measurements. Geosci. Model](#)
 2166 [Dev. 13, 5737–5755. https://doi.org/10.5194/gmd-13-5737-2020.](#)
 2167 [Kim, B., Schwartz, S.E., Miller, M.A., Min, Q., 2003. Effective radius of cloud droplets by ground-](#)
 2168 [based remote sensing: Relationship to aerosol. J. Geophys. Res. Atmos. 108.](#)
 2169 <https://doi.org/10.1029/2003JD003721>.
 2170 [Knote, C., Hodzic, A., Jimenez, J.L., Volkamer, R., Orlando, J.J., Baidar, S., Brioude, J., Fast, J.,](#)
 2171 [Gentner, D.R., Goldstein, A.H., 2014. Simulation of semi-explicit mechanisms of SOA](#)
 2172 [formation from glyoxal in aerosol in a 3-D model. Atmos. Chem. Phys. 14, 6213–6239.](#)
 2173 <https://doi.org/10.5194/acp-14-6213-2014>.
 2174 [Koch, D., Del Genio, A.D., 2010. Black carbon semi-direct effects on cloud cover: review and](#)
 2175 [synthesis. Atmos. Chem. Phys. 10, https://doi.org/10.5194/acp-10-7685-2010.](#)
 2176 [Kong, X., Forkel, R., Sokhi, R.S., Suppan, P., Baklanov, A., Gauss, M., Brunner, D., Barò, R.,](#)
 2177 [Balzarini, A., Chemel, C., Curci, G., Jiménez-Guerrero, P., Hirtl, M., Honzak, L., Im, U., Pérez,](#)
 2178 [J.L., Pirovano, G., San Jose, R., Schlünzen, K.H., Tsegas, G., Tuccella, P., Werhahn, J., ?abkar,](#)
 2179 [R., Galmarini, S., 2015. Analysis of meteorology-chemistry interactions during air pollution](#)
 2180 [episodes using online coupled models within AQMEII phase-2. Atmos. Environ. 115, 527-540.](#)
 2181 <https://doi.org/10.1016/j.atmosenv.2014.09.020>.
 2182 [Kuik, F., Lauer, A., Churkina, G., Denier van der Gon, H., Fenner, D., Mar, K., Butler, T., 2016. Air](#)
 2183 [quality modelling in the Berlin-Brandenburg region using WRF-Chem v3. 7.1: sensitivity to](#)
 2184 [resolution of model grid and input data. Geosci. Model Dev. 4339-4363.](#)
 2185 <https://doi.org/10.5194/gmd-9-4339-2016>.
 2186 [Kulmala, M., Laaksonen, A., Pirjola, L., 1998. Parameterizations for sulfuric acid/water nucleation](#)
 2187 [rates. J. Geophys. Res. Atmos. 103, 8301–8307. https://doi.org/10.1029/97JD03718.](#)
 2188 [Kumar, P., Sokolik, I.N., Nenes, A., 2009. Parameterization of cloud droplet formation for global](#)
 2189 [and regional models: including adsorption activation from insoluble CCN. Atmos. Chem. Phys.](#)
 2190 [9. https://doi.org/10.5194/acp-9-2517-2009.](#)
 2191 [Kumar, R., Barth, M.C., Pfister, G.G., Naja, M., Brasseur, G.P., 2014. WRF-Chem simulations of a](#)
 2192 [typical pre-monsoon dust storm in northern India: influences on aerosol optical properties and](#)
 2193 [radiation budget. Atmos. Chem. Phys. 14, 2431-2446. https://doi.org/10.5194/acp-14-2431-](#)
 2194 [2014.](#)
 2195 [Kumar, R., Naja, M., Pfister, G.G., Barth, M.C., Brasseur, G.P., 2012a. Simulations over South Asia](#)
 2196 [using the Weather Research and Forecasting model with Chemistry \(WRF-Chem\): set-up and](#)
 2197 [meteorological evaluation. Geosci. Model Dev. 5, 321-343. https://doi.org/10.5194/gmd-5-](#)
 2198 [321-2012.](#)
 2199 [Kumar, R., Naja, M., Pfister, G.G., Barth, M.C., Wiedinmyer, C., Brasseur, G.P., 2012b. Simulations](#)
 2200 [over South Asia using the Weather Research and Forecasting model with Chemistry \(WRF-](#)
 2201 [Chem\): chemistry evaluation and initial results. Geosci. Model Dev. 5, 619-648.](#)
 2202 <https://doi.org/10.5194/gmd-5-619-2012>.
 2203 [Kuniyal, J.C., Guleria, R.P., 2019. The current state of aerosol-radiation interactions: a mini review.](#)
 2204 [J. Aerosol Sci. 130, 45-54. https://doi.org/10.1016/j.jaerosci.2018.12.010.](#)
 2205 [Lau, W.K.M., Kim, K.-M., Shi, J.-J., Matsui, T., Chin, M., Tan, Q., Peters-Lidard, C., Tao, W.-K.,](#)
 2206 [2017. Impacts of aerosol-monsoon interaction on rainfall and circulation over Northern India](#)
 2207 [and the Himalaya Foothills. Clim. Dyn. 49, 1945-1960. https://doi.org/10.1007/s00382-016-](#)
 2208 [3430-y.](#)

2209 [Lee, H.-H., Chen, S.-H., Kumar, A., Zhang, H., Kleeman, M.J., 2020. Improvement of aerosol](#)
2210 [activation/ice nucleation in a source-oriented WRF-Chem model to study a winter Storm in](#)
2211 [California. Atmos. Res. 235, 104790. <https://doi.org/10.1016/j.atmosres.2019.104790>.](#)
2212 [Lee, Y.C., Yang, X., Wenig, M., 2010. Transport of dusts from East Asian and non-East Asian](#)
2213 [sources to Hong Kong during dust storm related events 1996-2007. Atmos. Environ. 44, 3728-](#)
2214 [3738. <https://doi.org/10.1016/j.atmosenv.2010.03.034>.](#)
2215 [Lelieveld, J., Bourtsoukidis, E., Brühl, C., Fischer, H., Fuchs, H., Harder, H., Hofzumahaus, A.,](#)
2216 [Holland, F., Marno, D., Neumaier, M., 2018. The South Asian monsoon-pollution pump and](#)
2217 [purifier. Science \(80-. \). 361, 270-273. <https://doi.org/10.1126/science.aar2501>.](#)
2218 [Lelieveld, J., Evans, J.S., Fnais, M., Giannadaki, D., Pozzer, A., 2015. The contribution of outdoor](#)
2219 [air pollution sources to premature mortality on a global scale. Nature 525, 367.](#)
2220 [https://doi.org/10.1038/nature15371.](#)
2221 [Li, J., Chen, X., Wang, Z., Du, H., Yang, W., Sun, Y., Hu, B., Li, Jianjun, Wang, W., Wang, T., 2018.](#)
2222 [Radiative and heterogeneous chemical effects of aerosols on ozone and inorganic aerosols over](#)
2223 [East Asia. Sci. Total Environ. 622, 1327-1342. <https://doi.org/10.1016/j.scitotenv.2017.12.041>.](#)
2224 [Li, J., Nagashima, T., Kong, L., Ge, B., Yamaji, K., Fu, J.S., Wang, X., Fan, Q., Itahashi, S., Hyo-](#)
2225 [Jung, L., 2019. Model evaluation and intercomparison of surface-level ozone and relevant](#)
2226 [species in East Asia in the context of MICS-Asia Phase III-Part 1: Overview. Atmos. Chem.](#)
2227 [Phys. 19, 12993-13015. <https://doi.org/10.5194/acp-19-12993-2019>.](#)
2228 [Li, J., Wang, Z., Wang, X., Yamaji, K., Takigawa, M., Kanaya, Y., Pochanart, P., Liu, Y., Irie, H.,](#)
2229 [Hu, B., 2011. Impacts of aerosols on summertime tropospheric photolysis frequencies and](#)
2230 [photochemistry over Central Eastern China. Atmos. Environ. 45, 1817-1829.](#)
2231 [https://doi.org/10.1016/j.atmosenv.2011.01.016.](#)
2232 [Li, Jie, Chen, X., Wang, Z., Du, H., Yang, W., Sun, Y., Hu, B., Li, Jianjun, Wang, W., Wang, T., 2018.](#)
2233 [Radiative and heterogeneous chemical effects of aerosols on ozone and inorganic aerosols over](#)
2234 [East Asia. Sci. Total Environ. 622, 1327-1342. <https://doi.org/10.1016/j.scitotenv.2017.12.041>.](#)
2235 [Li, L., Hong, L., 2014. Role of the Radiative Effect of Black Carbon in Simulated PM_{2.5}](#)
2236 [Concentrations during a Haze Event in China. Atmos. Ocean. Sci. Lett. 7, 434-440.](#)
2237 [https://doi.org/10.3878/j.issn.1674-2834.14.0023.](#)
2238 [Li, L., Sokolik, I.N., 2018. The Dust Direct Radiative Impact and Its Sensitivity to the Land Surface](#)
2239 [State and Key Minerals in the WRF - Chem - DuMo Model: A Case Study of Dust Storms in](#)
2240 [Central Asia. J. Geophys. Res. Atmos. 123, 4564-4582. <https://doi.org/10.1029/2017JD027667>.](#)
2241 [Li, L., Sokolik, I.N., 2018. The Dust Direct Radiative Impact and Its Sensitivity to the Land Surface](#)
2242 [State and Key Minerals in the WRF - Chem - DuMo Model: A Case Study of Dust Storms in](#)
2243 [Central Asia. J. Geophys. Res. Atmos. 123, 4564 - 4582.](#)
2244 [https://doi.org/10.1029/2017JD027667.](#)
2245 [Li, M., Wang, T., Xie, M., Li, S., Zhuang, B., Chen, P., Huang, X., Han, Y., 2018. Agricultural fire](#)
2246 [impacts on ozone photochemistry over the Yangtze River Delta region, East China. J. Geophys.](#)
2247 [Res. Atmos. <https://doi.org/10.1029/2018JD028582>.](#)
2248 [Li, M., Wang, T., Xie, M., Li, S., Zhuang, B., Huang, X., Chen, P., Zhao, M., Liu, J., 2019. Formation](#)
2249 [and evolution mechanisms for two extreme haze episodes in the Yangtze River Delta region of](#)
2250 [China during winter 2016. J. Geophys. Res. Atmos. 124, 3607-3623.](#)
2251 [https://doi.org/10.1029/2019JD030535.](#)
2252 [Li, M., Zhang, Q., Kurokawa, J., Woo, J.-H., 2017. MIX: a mosaic Asian anthropogenic emission](#)
2253 [inventory under the international collaboration framework of the MICS-Asia and HTAP. Atmos.](#)
2254 [Chem. Phys. 17, 935-963. <https://doi.org/10.5194/acp-17-935-2017>.](#)
2255 [Li, M.M., Wang, T., Han, Y., Xie, M., Li, S., Zhuang, B., Chen, P., 2017a. Modeling of a severe dust](#)
2256 [event and its impacts on ozone photochemistry over the downstream Nanjing megacity of](#)
2257 [eastern China. Atmos. Environ. 160, 107-123. <https://doi.org/10.1016/j.atmosenv.2017.04.010>.](#)
2258 [Li, M.M., Wang, T., Xie, M., Zhuang, B., Li, S., Han, Y., Chen, P., 2017b. Impacts of aerosol-](#)
2259 [radiation feedback on local air quality during a severe haze episode in Nanjing megacity](#)
2260 [eastern China. Tellus, Ser. B Chem. Phys. Meteorol. 69, 1-16.](#)
2261 [https://doi.org/10.1080/16000889.2017.1339548.](#)
2262 [Li, Z., Guo, J., Ding, A., Liao, H., Liu, J., Sun, Y., Wang, T., Xue, H., Zhang, H., Zhu, B., 2017.](#)
2263 [Aerosol and boundary-layer interactions and impact on air quality. Natl. Sci. Rev. 4, 810-833.](#)
2264 [https://doi.org/10.1093/nsr/nwx117.](#)
2265 [Li, Z., Lau, W.K.M., Ramanathan, V., Wu, G., Ding, Y., Manoj, M.G., Liu, J., Qian, Y., Li, J., Zhou,](#)

2266 [T., Fan, J., Rosenfeld, D., Ming, Y., Wang, Y., Huang, J., Wang, B., Xu, X., Lee, S.S., Cribb,](#)
2267 [M., Zhang, F., Yang, X., Zhao, C., Takemura, T., Wang, K., Xia, X., Yin, Y., Zhang, H., Guo,](#)
2268 [J., Zhai, P.M., Sugimoto, N., Babu, S.S., Brasseur, G.P., 2016. Aerosol and monsoon climate](#)
2269 [interactions over Asia. *Rev. Geophys.* 54, 866-929. <https://doi.org/10.1002/2015RG000500>.](#)
2270 [Li, Z., Niu, F., Fan, J., Liu, Y., Rosenfeld, D., Ding, Y., 2011. Long-term impacts of aerosols on the](#)
2271 [vertical development of clouds and precipitation. *Nat. Geosci.* 4, 888-894.](#)
2272 [https://doi.org/10.1038/ngeo1313.](#)
2273 [Li, Z., Wang, Y., Guo, J., Zhao, C., Cribb, M.C., Dong, X., Fan, J., Gong, D., Huang, J., Jiang, M.,](#)
2274 [2019. East Asian study of tropospheric aerosols and their impact on regional clouds,](#)
2275 [precipitation, and climate \(EAST - AIRCPC\). *J. Geophys. Res. Atmos.* 124, 13026-13054.](#)
2276 [https://doi.org/10.1029/2019JD030758.](#)
2277 [Liao, J., Wang, T., Wang, X., Xie, M., Jiang, Z., Huang, X., Zhu, J., 2014. Impacts of different urban](#)
2278 [canopy schemes in WRF/Chem on regional climate and air quality in Yangtze River Delta,](#)
2279 [China. *Atmos. Res.* 145, 226-243. <https://doi.org/10.1016/j.atmosres.2014.04.005>.](#)
2280 [Lin, C.-Y., Zhao, C., Liu, X., Lin, N.-H., Chen, W.-N., 2014. Modelling of long-range transport of](#)
2281 [Southeast Asia biomass-burning aerosols to Taiwan and their radiative forcings over East Asia.](#)
2282 [Tellus B Chem. Phys. Meteorol. 66, 23733. <https://doi.org/10.3402/tellusb.v66.23733>.](#)
2283 [Lin, N.-H., Sayer, A.M., Wang, S.-H., Loftus, A.M., Hsiao, T.-C., Sheu, G.-R., Hsu, N.C., Tsay, S.-](#)
2284 [C., Chantara, S., 2014. Interactions between biomass-burning aerosols and clouds over](#)
2285 [Southeast Asia: Current status, challenges, and perspectives. *Environ. Pollut.* 195, 292-307.](#)
2286 [https://doi.org/10.1016/j.envpol.2014.06.036.](#)
2287 [Liu, C., Wang, T., Chen, P., Li, M., Zhao, M., Zhao, K., Wang, M., Yang, X., 2019. Effects of](#)
2288 [Aerosols on the Precipitation of Convective Clouds: A Case Study in the Yangtze River Delta](#)
2289 [of China. *J. Geophys. Res. Atmos.* 124, 7868-7885. <https://doi.org/10.1029/2018JD029924>.](#)
2290 [Liu, G., Shao, H., Coakley Jr, J.A., Curry, J.A., Haggerty, J.A., Tschudi, M.A., 2003. Retrieval of](#)
2291 [cloud droplet size from visible and microwave radiometric measurements during INDOEX:](#)
2292 [Implication to aerosols' indirect radiative effect. *J. Geophys. Res. Atmos.* 108, AAC-2.](#)
2293 [https://doi.org/10.1029/2001JD001395.](#)
2294 [Liu, L., Bai, Y., Lin, C., Yang, H., 2018. Evaluation of Regional Air Quality Numerical Forecasting](#)
2295 [System in Central China and Its Application for Aerosol Radiative Effect. *Meteorol. Mon.* 44,](#)
2296 [1179-1190. <https://doi.org/10.7519/j.issn.1000-0526.2018.09.006>.](#)
2297 [Liu, L., Huang, X., Ding, A., Fu, C., 2016. Dust-induced radiative feedbacks in north China?: A dust](#)
2298 [storm episode modeling study using WRF-Chem. *Atmos. Environ.* 129, 43-54.](#)
2299 [https://doi.org/10.1016/j.atmosenv.2016.01.019.](#)
2300 [Liu, Q., Jia, X., Quan, J., Li, J., Li, X., Wu, Y., Chen, D., Wang, Z., Liu, Y., 2018. New positive](#)
2301 [feedback mechanism between boundary layer meteorology and secondary aerosol formation](#)
2302 [during severe haze events. *Sci. Rep.* 8, 1-8. <https://doi.org/10.1038/s41598-018-24366-3>.](#)
2303 [Liu, X., Easter, R.C., Ghan, S.J., Zaveri, R., Rasch, P., Shi, X., Lamarque, J.-F., Gettelman, A.,](#)
2304 [Morrison, H., Vitt, F., 2012. Toward a minimal representation of aerosols in climate models:](#)
2305 [Description and evaluation in the Community Atmosphere Model CAM5. *Geosci. Model Dev.*](#)
2306 [5, 709-739. <https://doi.org/10.5194/gmd-5-709-2012>.](#)
2307 [Liu, X., Zhang, Y., Zhang, Q., He, K., 2016. Application of online-coupled WRF/Chem-MADRID](#)
2308 [in East Asia?: Model evaluation and climatic effects of anthropogenic aerosols. *Atmos. Environ.*](#)
2309 [124, 321-336. <https://doi.org/10.1016/j.atmosenv.2015.03.052>.](#)
2310 [Liu, Z., Yi, M., Zhao, C., Lau, N.C., Guo, J., Bollasina, M., Yim, S.H.L., 2020. Contribution of local](#)
2311 [and remote anthropogenic aerosols to a record-breaking torrential rainfall event in Guangdong](#)
2312 [Province, China. *Atmos. Chem. Phys.* 20, 223-241. <https://doi.org/10.5194/acp-20-223-2020>.](#)
2313 [Liu, Z., Yim, S.H.L., Wang, C., Lau, N.C., 2018. The Impact of the Aerosol Direct Radiative Forcing](#)
2314 [on Deep Convection and Air Quality in the Pearl River Delta Region. *Geophys. Res. Lett.* 45,](#)
2315 [4410-4418. <https://doi.org/10.1029/2018GL077517>.](#)
2316 [Lohmann, U., Diehl, K., 2006. Sensitivity studies of the importance of dust ice nuclei for the indirect](#)
2317 [aerosol effect on stratiform mixed-phase clouds. *J. Atmos. Sci.* 63, 968-982.](#)
2318 [https://doi.org/10.1175/JAS3662.1.](#)
2319 [Lohmann, U., Feichter, J., 2005. Global indirect aerosol effects: a review. *Atmos. Chem. Phys.* 5,](#)
2320 [715-737. <https://doi.org/10.5194/acp-5-715-2005>.](#)
2321 [Ma, X., Chen, D., Wen, W., Sheng, L., Hu, J., Tong, H., Wei, P., 2016. Effect of Particle Pollution](#)
2322 [on Regional Meteorological Factors in China. *J. Beijing Univ. Technol.* 285-295.](#)

<https://doi.org/10.11936/bjutxb2015040075>.
 2324 Ma, X., Wen, W., 2017. Modelling the Effect of Black Carbon and Sulfate Aerosol on the Regional
 2325 Meteorology Factors, in: IOP Conf. Ser. Earth Environ. Sci. p. 12002.
 2326 <https://doi.org/10.1088/1755-1315/78/1/012002>.
 2327 Mailler, S., Menut, L., Khvorostyanov, D., Valari, M., Couvidat, F., Siour, G., Turquety, S., Briant,
 2328 R., Tuccella, P., Bessagnet, B., 2017. CHIMERE-2017: from urban to hemispheric chemistry-
 2329 transport modeling. *Geosci. Model Dev.* 10, 2397-2423. [https://doi.org/10.5194/gmd-10-2397-
 2330 2017](https://doi.org/10.5194/gmd-10-2397-2017).
 2331 Makar, P.A., Gong, W., Hogrefe, C., Zhang, Y., Curci, G., ?abkar, R., Milbrandt, J., Im, U., Balzarini,
 2332 A., Baró, R., Bianconi, R., Cheung, P., Forkel, R., Gravel, S., Hirtl, M., Honzak, L., Hou, A.,
 2333 Jiménez-Guerrero, P., Langer, M., Moran, M.D., Pabla, B., Pérez, J.L., Pirovano, G., San José,
 2334 R., Tuccella, P., Werhahn, J., Zhang, J., Galmarini, S., 2015a. Feedbacks between air pollution
 2335 and weather, part 2: Effects on chemistry. *Atmos. Environ.* 115, 499-526.
 2336 <https://doi.org/10.1016/j.atmosenv.2014.10.021>.
 2337 Makar, P.A., Gong, W., Milbrandt, J., Hogrefe, C., Zhang, Y., Curci, G., ?abkar, R., Im, U., Balzarini,
 2338 A., Baró, R., Bianconi, R., Cheung, P., Forkel, R., Gravel, S., Hirtl, M., Honzak, L., Hou, A.,
 2339 Jiménez-Guerrero, P., Langer, M., Moran, M.D., Pabla, B., Pérez, J.L., Pirovano, G., San José,
 2340 R., Tuccella, P., Werhahn, J., Zhang, J., Galmarini, S., 2015b. Feedbacks between air pollution
 2341 and weather, Part 1: Effects on weather. *Atmos. Environ.* 115, 442-469.
 2342 <https://doi.org/10.1016/j.atmosenv.2014.12.003>.
 2343 Manisalidis, I., Stavropoulou, E., Stavropoulos, A., Bezirtzoglou, E., 2020. Environmental and
 2344 health impacts of air pollution: A review. *Front. public Heal.* 8.
 2345 <https://doi.org/10.3389/fpubh.2020.00014>.
 2346 Marelle, L., Raut, J.-C., Law, K.S., Berg, L.K., Fast, J.D., Easter, R.C., Shrivastava, M., Thomas,
 2347 J.L., 2017. Improvements to the WRF-Chem 3.5.1 model for quasi-hemispheric simulations
 2348 of aerosols and ozone in the Arctic. *Geosci. Model Dev.* 10, 3661-3677.
 2349 <https://doi.org/10.5194/gmd-10-3661-2017>.
 2350 Martin, D.E., Leight, W.G., 1949. Objective temperature estimates from mean circulation patterns.
 2351 *Mon. Weather Rev.* 77, 275-283. [https://doi.org/10.1175/1520-
 2352 0493\(1949\)077<0275:OTEFMC>2.0.CO;2](https://doi.org/10.1175/1520-0493(1949)077<0275:OTEFMC>2.0.CO;2).
 2353 Martin, S.T., Schlenker, J.C., Malinowski, A., Hung, H., Rudich, Y., 2003. Crystallization of
 2354 atmospheric sulfate - nitrate - ammonium particles. *Geophys. Res. Lett.* 30.
 2355 <https://doi.org/10.1029/2003GL017930>.
 2356 Mass, C., Owens, D., 2011. Fixing WRF's high speed wind bias: A new subgrid scale drag
 2357 parameterization and the role of detailed verification, in: 24th Conference on Weather and
 2358 Forecasting and 20th Conference on Numerical Weather Prediction, Preprints, 91st American
 2359 Meteorological Society Annual Meeting.
 2360 McCormick, R.A., Ludwig, J.H., 1967. Climate modification by atmospheric aerosols. *Science*
 2361 (80-.). 156, 1358-1359. <https://doi.org/10.1126/science.156.3780.1358>.
 2362 McMurry, P.H., Friedlander, S.K., 1979. New particle formation in the presence of an aerosol. *Atmos.*
 2363 *Environ.* 13, 1635-1651. [https://doi.org/10.1016/0004-6981\(79\)90322-6](https://doi.org/10.1016/0004-6981(79)90322-6).
 2364 Miao, Y., Guo, J., Liu, S., Zhao, C., Li, X., Zhang, G., Wei, W., Ma, Y., 2018. Impacts of synoptic
 2365 condition and planetary boundary layer structure on the trans-boundary aerosol transport from
 2366 Beijing-Tianjin-Hebei region to northeast China. *Atmos. Environ.* 181, 1-11.
 2367 <https://doi.org/10.1016/j.atmosenv.2018.03.005>.
 2368 Miao, Y., Liu, S., Zheng, Y., Wang, S., 2016. Modeling the feedback between aerosol and boundary
 2369 layer processes: a case study in Beijing, China. *Environ. Sci. Pollut. Res.* 23, 3342-3357.
 2370 <https://doi.org/10.1007/s11356-015-5562-8>.
 2371 Morrison, H., van Lier - Walqui, M., Fridlind, A.M., Grabowski, W.W., Harrington, J.Y., Hoose, C.,
 2372 Korolev, A., Kumjian, M.R., Milbrandt, J.A., Pawlowska, H., 2020. Confronting the challenge
 2373 of modeling cloud and precipitation microphysics. *J. Adv. Model. earth Syst.* 12,
 2374 e2019MS001689. <https://doi.org/10.1029/2019MS001689>.
 2375 Napari, I., Noppel, M., Vehkamäki, H., Kulmala, M., 2002. Parametrization of ternary nucleation
 2376 rates for H₂SO₄-NH₃-H₂O vapors. *J. Geophys. Res. Atmos.* 107, AAC-6.
 2377 <https://doi.org/10.1029/2002JD002132>.
 2378 Nenes, A., Pandis, S.N., Pilinis, C., 1998. ISORROPIA: A new thermodynamic equilibrium model
 2379 for multiphase multicomponent inorganic aerosols. *Aquat. geochemistry* 4, 123-152.

<https://doi.org/10.1023/A:1009604003981>.
 2381 Nguyen, G.T.H., Shimadera, H., Sekiguchi, A., Matsuo, T., Kondo, A., 2019a. Investigation of
 2382 aerosol direct effects on meteorology and air quality in East Asia by using an online coupled
 2383 modeling system. Atmos. Environ. 207, 182-196.
 2384 <https://doi.org/10.1016/j.atmosenv.2019.03.017>.
 2385 Nguyen, G.T.H., Shimadera, H., Uranishi, K., Matsuo, T., Kondo, A., Thepanondh, S., 2019b.
 2386 Numerical assessment of PM_{2.5} and O₃ air quality in continental Southeast Asia: Baseline
 2387 simulation and aerosol direct effects investigation. Atmos. Environ. 219, 117054.
 2388 <https://doi.org/10.1016/j.atmosenv.2019.117054>.
 2389 North, G.R., Pyle, J.A., Zhang, F., 2014. Encyclopedia of atmospheric sciences. Elsevier.
 2390 Odum, J.R., Jungkamp, T.P.W., Griffin, R.J., Flagan, R.C., Seinfeld, J.H., 1997. The atmospheric
 2391 aerosol-forming potential of whole gasoline vapor. Science (80-.), 276, 96-99.
 2392 <https://doi.org/10.1126/science.276.5309.96>.
 2393 Park, S.-Y., Lee, H.-J., Kang, J.-E., Lee, T., Kim, C.-H., 2018. Aerosol radiative effects on mesoscale
 2394 cloud-precipitation variables over Northeast Asia during the MAPS-Seoul 2015 campaign.
 2395 Atmos. Environ. 172, 109-123. <https://doi.org/10.1016/j.atmosenv.2017.10.044>.
 2396 Penner, J.E., Dong, X., Chen, Y., 2004. Observational evidence of a change in radiative forcing due
 2397 to the indirect aerosol effect. Nature 427, 231-234. <https://doi.org/10.1038/nature02234>.
 2398 Pye, H.O.T., Murphy, B.N., Xu, L., Ng, N.L., Carlton, A.G., Guo, H., Weber, R., Vasilakos, P., Appel,
 2399 K.W., Budisulistiorini, S.H., 2017. On the implications of aerosol liquid water and phase
 2400 separation for organic aerosol mass. Atmos. Chem. Phys. 17, 343-369.
 2401 <https://doi.org/10.5194/acp-17-343-2017>.
 2402 Qiu, Y., Liao, H., Zhang, R., Hu, J., 2017. Simulated impacts of direct radiative effects of scattering
 2403 and absorbing aerosols on surface layer aerosol concentrations in China during a heavily
 2404 polluted event in february 2014. J. Geophys. Res. 122, 5955-5975.
 2405 <https://doi.org/10.1002/2016JD026309>.
 2406 Quaas, J., Boucher, O., Bellouin, N., Kinne, S., 2008. Satellite-based estimate of the direct and
 2407 indirect aerosol climate forcing. J. Geophys. Res. Atmos. 113,
 2408 <https://doi.org/10.1029/2007JD008962>.
 2409 Reid, J.S., Koppmann, R., Eck, T.F., Eleuterio, D.P., 2005. A review of biomass burning emissions
 2410 part II: intensive physical properties of biomass burning particles. Atmos. Chem. Phys. 5, 799-
 2411 825. <https://doi.org/10.5194/acp-5-799-2005>.
 2412 Rohde, R.A., Muller, R.A., 2015. Air pollution in China: mapping of concentrations and sources.
 2413 PLoS One 10, e0135749. <https://doi.org/10.1371/journal.pone.0135749>.
 2414 Rosenfeld, D., 2000. Suppression of rain and snow by urban and industrial air pollution. Science
 2415 (80-.), 287, 1793-1796. <https://doi.org/10.1126/science.287.5459.1793>.
 2416 Rosenfeld, D., Andreae, M.O., Asmi, A., Chin, M., de Leeuw, G., Donovan, D.P., Kahn, R., Kinne,
 2417 S., Kivek?s, N., Kulmala, M., 2014. Global observations of aerosol-cloud-precipitation-climate
 2418 interactions. Rev. Geophys. 52, 750-808. <https://doi.org/10.1002/2013RG000441>.
 2419 Rosenfeld, D., Lohmann, U., Raga, G.B., O'Dowd, C.D., Kulmala, M., Fuzzi, S., Reissell, A.,
 2420 Andreae, M.O., 2008. Flood or drought: How do aerosols affect precipitation? Science (80-.),
 2421 321, 1309-1313. <https://doi.org/10.1126/science.1160606>.
 2422 Rosenfeld, D., Zhu, Y., Wang, M., Zheng, Y., Goren, T., Yu, S., 2019. Aerosol-driven droplet
 2423 concentrations dominate coverage and water of oceanic low-level clouds. Science (80-.), 363,
 2424 <https://doi.org/10.1126/science.aav0566>.
 2425 Saleh, R., Robinson, E.S., Tkacik, D.S., Ahern, A.T., Liu, S., Aiken, A.C., Sullivan, R.C., Presto,
 2426 A.A., Dubey, M.K., Yokelson, R.J., 2014. Brownness of organics in aerosols from biomass
 2427 burning linked to their black carbon content. Nat. Geosci. 7, 647-650.
 2428 <https://doi.org/10.1038/ngeo2220>.
 2429 Sanchez - Romero, A., Sanchez - Lorenzo, A., Calbó, J., González, J.A., Azorin - Molina, C., 2014.
 2430 The signal of aerosol-induced changes in sunshine duration records: A review of the evidence.
 2431 J. Geophys. Res. Atmos. 119, 4657-4673. <https://doi.org/10.1002/2013JD021393>.
 2432 Sarangi, C., Tripathi, S.N., Tripathi, S., Barth, M.C., 2015. Aerosol-cloud associations over Gangetic
 2433 Basin during a typical monsoon depression event using WRF-Chem simulation. J. Geophys.
 2434 Res. Atmos. 120, 10-974. <https://doi.org/10.1002/2015JD023634>.
 2435 Satheesh, S.K., Moorthy, K.K., 2005. Radiative effects of natural aerosols: A review. Atmos.
 2436 Environ. 39, 2089-2110. <https://doi.org/10.1016/j.atmosenv.2004.12.029>.

2437 [Sato, Y., Suzuki, K., 2019. How do aerosols affect cloudiness? *Science* \(80-. \). 363, 580-581.](#)
2438 <https://doi.org/10.1126/science.aaw3720>.

2439 [Saylor, R.D., Baker, B.D., Lee, P., Tong, D., Pan, L., Hicks, B.B., 2019. The particle dry deposition](#)
2440 [component of total deposition from air quality models: right, wrong or uncertain? *Tellus B*](#)
2441 [Chem. Phys. Meteorol. 71, 1550324. <https://doi.org/10.1080/16000889.2018.1550324>.](#)

2442 [Seaman, N.L., 2000. Meteorological modeling for air-quality assessments. *Atmos. Environ.* 34,](#)
2443 [2231-2259. \[https://doi.org/10.1016/S1352-2310\\(99\\)00466-5\]\(https://doi.org/10.1016/S1352-2310\(99\)00466-5\).](#)

2444 [Seethala, C., Pandithurai, G., Fast, J.D., Polade, S.D., Reddy, M.S., Peckham, S.E., 2011. Evaluating](#)
2445 [WRF-Chem multi-scale model in simulating aerosol radiative properties over the tropics-a case](#)
2446 [study over India. *Mapan* 26, 269-284. <https://doi.org/10.1007/s12647-011-0025-2>.](#)

2447 [Seinfeld, J., Pandis, S., 1998. Atmospheric chemistry and physics: atmospheric chemistry and](#)
2448 [physics.](#)

2449 [Sekiguchi, A., Shimadera, H., Kondo, A., 2018. Impact of aerosol direct effect on wintertime PM_{2.5}](#)
2450 [simulated by an online coupled meteorology-air quality model over east asia. *Aerosol Air Qual.*](#)
2451 [Res. 18, 1068-1079. <https://doi.org/10.4209/aaqr.2016.06.0282>.](#)

2452 [Sekiguchi, M., Nakajima, T., Suzuki, K., Kawamoto, K., Higurashi, A., Rosenfeld, D., Sano, I.,](#)
2453 [Mukai, S., 2003. A study of the direct and indirect effects of aerosols using global satellite data](#)
2454 [sets of aerosol and cloud parameters. *J. Geophys. Res. Atmos.* 108,](#)
2455 [https://doi.org/10.1029/2002JD003359.](#)

2456 [Shahid, M.Z., Shahid, I., Chishtie, F., Shahzad, M.I., Bulbul, G., 2019. Analysis of a dense haze](#)
2457 [event over North-eastern Pakistan using WRF-Chem model and remote sensing. *J. Atmos.*](#)
2458 [Solar-Terrestrial Phys. 182, 229-241. <https://doi.org/10.1016/j.jastp.2018.12.007>.](#)

2459 [Shao, Y., Dong, C.H., 2006. A review on East Asian dust storm climate, modelling and monitoring.](#)
2460 [Globe. Planet. Change 52, 1-22. <https://doi.org/10.1016/j.gloplacha.2006.02.011>.](#)

2461 [Shen, H., Shi, Huawei, Shi, Huading, Ma, X., 2015. Simulation Study of Influence of Aerosol](#)
2462 [Pollution on Regional Meteorological Factors in Beijing-Tianjin-Hebei Region. *J. Anhui Agric.*](#)
2463 [Sci. 43, 207-210. <https://doi.org/10.13989/j.cnki.0517-6611.2015.25.217>.](#)

2464 [Shen, X., Jiang, X., Liu, D., Zu, F., Fan, S., 2017. Simulations of Anthropogenic Aerosols Effects](#)
2465 [on the Intensity and Precipitation of Typhoon Fitow \(1323\) Using WRF-Chem Model. *Chinese*](#)
2466 [J. Atmos. Sci. 41, 960-974. <https://doi.org/10.3878/j.issn.1006-9895.1703.16216>.](#)

2467 [Siméon, A., Waquet, F., Péré, J.-C., Ducos, F., Thieuleux, F., Peers, F., Turquety, S., Chiapello, I.,](#)
2468 [2021. Combining POLDER-3 satellite observations and WRF-Chem numerical simulations to](#)
2469 [derive biomass burning aerosol properties over the southeast Atlantic region. *Atmos. Chem.*](#)
2470 [Phys. 21, 17775–17805. <https://doi.org/10.5194/acp-21-17775-2021>.](#)

2471 [Singh, P., Sarawade, P., Adhikary, B., 2020. Carbonaceous Aerosol from Open Burning and its](#)
2472 [Impact on Regional Weather in South Asia. *Aerosol Air Qual. Res.* 20, 419-431.](#)
2473 [https://doi.org/10.4209/aaqr.2019.03.0146.](#)

2474 [Slinn, W.G.N., 1984. Precipitation scavenging, in atmospheric sciences and power production-1979.](#)
2475 [Div. Biomed. Environ. Res. US Dep. Energy, Washing. DC.](#)

2476 [Soni, P., Tripathi, S.N., Srivastava, R., 2018. Radiative effects of black carbon aerosols on Indian](#)
2477 [monsoon: a study using WRF-Chem model. *Theor. Appl. Climatol.* 132, 115-134.](#)
2478 [https://doi.org/10.1007/s00704-017-2057-1.](#)

2479 [Srinivas, R., Panicker, A.S., Parkhi, N.S., Peshin, S.K., Beig, G., 2016. Sensitivity of online coupled](#)
2480 [model to extreme pollution event over a mega city Delhi. *Atmos. Pollut. Res.* 7, 25-30.](#)
2481 [https://doi.org/10.1016/j.apr.2015.07.001.](#)

2482 [Stephens, G.L., Li, J., Wild, M., Clayson, C.A., Loeb, N., Kato, S., L'ecuyer, T., Stackhouse, P.W.,](#)
2483 [Lebsock, M., Andrews, T., 2012. An update on Earth's energy balance in light of the latest](#)
2484 [global observations. *Nat. Geosci.* 5, 691-696. <https://doi.org/10.1038/ngeo1580>.](#)

2485 [Su, L., Fung, J.C.H., 2018a. Investigating the role of dust in ice nucleation within clouds and further](#)
2486 [effects on the regional weather system over East Asia--Part 2: modification of the weather](#)
2487 [system. *Atmos. Chem. Phys.* 18. <https://doi.org/10.5194/acp-18-11529-2018>.](#)

2488 [Su, L., Fung, J.C.H., 2018b. Investigating the role of dust in ice nucleation within clouds and further](#)
2489 [effects on the regional weather system over East Asia--Part 1: model development and](#)
2490 [validation. *Atmos. Chem. Phys.* 18. <https://doi.org/10.5194/acp-18-8707-2018>.](#)

2491 [Sud, Y.C., Walker, G.K., 1990. A review of recent research on improvement of physical](#)
2492 [parameterizations in the GLA GCM.](#)

2493 [Sun, K., Liu, H., Wang, X., Peng, Z., Xiong, Z., 2017. The aerosol radiative effect on a severe haze](#)

2494 [episode in the Yangtze River Delta. J. Meteorol. Res. 31, 865-873.](#)
2495 [https://doi.org/10.1007/s13351-017-7007-4.](https://doi.org/10.1007/s13351-017-7007-4)

2496 [Takemura, T., Nakajima, T., Higurashi, A., Ohta, S., Sugimoto, N., 2003. Aerosol distributions and](#)
2497 [radiative forcing over the Asian Pacific region simulated by Spectral Radiation - Transport](#)
2498 [Model for Aerosol Species \(SPRINTARS\). J. Geophys. Res. Atmos. 108.](#)
2499 [https://doi.org/10.1029/2002JD003210.](https://doi.org/10.1029/2002JD003210)

2500 [Tang, Y., Han, Y., Ma, X., Liu, Z., 2018. Elevated heat pump effects of dust aerosol over](#)
2501 [Northwestern China during summer. Atmos. Res. 203, 95-104.](#)
2502 [https://doi.org/10.1016/j.atmosres.2017.12.004.](https://doi.org/10.1016/j.atmosres.2017.12.004)

2503 [Ten Hoeve, J.E., Jacobson, M.Z., 2012. Worldwide health effects of the Fukushima Daiichi nuclear](#)
2504 [accident. Energy Environ. Sci. 5, 8743-8757. https://doi.org/10.1039/c2ee22019a.](#)

2505 [Thompson, G., Eidhammer, T., 2014. A study of aerosol impacts on clouds and precipitation](#)
2506 [development in a large winter cyclone. J. Atmos. Sci. 71, 3636-3658.](#)
2507 [https://doi.org/10.1175/JAS-D-13-0305.1.](https://doi.org/10.1175/JAS-D-13-0305.1)

2508 [Toon, O.B., McKay, C.P., Ackerman, T.P., Santhanam, K., 1989. Rapid calculation of radiative](#)
2509 [heating rates and photodissociation rates in inhomogeneous multiple scattering atmospheres. J.](#)
2510 [Geophys. Res. Atmos. 94, 16287-16301. https://doi.org/10.1029/JD094iD13p16287.](#)

2511 [Trenback, C., Tripoli, G., Arritt, R., Cotton, W.R., Pielke, R.A., 1986. The regional atmospheric](#)
2512 [modeling system, in: Proceedings of an International Conference on Development Applications](#)
2513 [of Computer Techniques Environmental Studies. Computational Mechanics Publication,](#)
2514 [Rewood Burn Ltd, pp. 601-607.](#)

2515 [Tsay, S.-C., Hsu, N.C., Lau, W.K.-M., Li, C., Gabriel, P.M., Ji, Q., Holben, B.N., Welton, E.J.,](#)
2516 [Nguyen, A.X., Janjai, S., 2013. From BASE-ASIA toward 7-SEAS: A satellite-surface](#)
2517 [perspective of boreal spring biomass-burning aerosols and clouds in Southeast Asia. Atmos.](#)
2518 [Environ. 78, 20-34. https://doi.org/10.1016/j.atmosenv.2012.12.013.](#)

2519 [Twomey, S., 1977. The influence of pollution on the shortwave albedo of clouds. J. Atmos. Sci. 34,](#)
2520 [1149-1152. https://doi.org/10.1175/1520-0469\(1977\)034<1149:TIOPOT>2.0.CO;2.](#)

2521 [Uno, I., Wang, Z., Chiba, M., Chun, Y.S., Gong, S.L., Hara, Y., Jung, E., Lee, S., Liu, M., Mikami,](#)
2522 [M., 2006. Dust model intercomparison \(DMIP\) study over Asia: Overview. J. Geophys. Res.](#)
2523 [Atmos. 111. https://doi.org/10.1029/2005JD006575.](#)

2524 [Vehkamäki, H., Kulmala, M., Napari, I., Lehtinen, K.E.J., Timmreck, C., Noppel, M., Laaksonen,](#)
2525 [A., 2002. An improved parameterization for sulfuric acid-water nucleation rates for](#)
2526 [tropospheric and stratospheric conditions. J. Geophys. Res. Atmos. 107, AAC-3.](#)
2527 [https://doi.org/10.1029/2002JD002184.](https://doi.org/10.1029/2002JD002184)

2528 [Wang, D., Jiang, B., Lin, W., Gu, F., 2019. Effects of aerosol-radiation feedback and topography](#)
2529 [during an air pollution event over the North China Plain during December 2017. Atmos. Pollut.](#)
2530 [Res. 10, 587-596. https://doi.org/10.1016/j.apr.2018.10.006.](#)

2531 [Wang, H., Niu, T., 2013. Sensitivity studies of aerosol data assimilation and direct radiative](#)
2532 [feedbacks in modeling dust aerosols. Atmos. Environ. 64, 208-218.](#)
2533 [https://doi.org/10.1016/j.atmosenv.2012.09.066.](https://doi.org/10.1016/j.atmosenv.2012.09.066)

2534 [Wang, H., Peng, Y., Zhang, X., Liu, H., Zhang, M., Che, H., Cheng, Y., Zheng, Y., 2018.](#)
2535 [Contributions to the explosive growth of PM_{2.5} mass due to aerosol-radiation feedback and](#)
2536 [decrease in turbulent diffusion during a red alert heavy haze in Beijing-Tianjin-Hebei, China.](#)
2537 [Atmos. Chem. Phys. 18, 17717-17733. https://doi.org/10.5194/acp-18-17717-2018.](#)

2538 [Wang, H., Shi, G., Zhu, J., Chen, B., Che, H., Zhao, T., 2013. Case study of longwave contribution](#)
2539 [to dust radiative effects over East Asia. Chinese Sci. Bull. 58, 3673-3681.](#)
2540 [https://doi.org/10.1007/s11434-013-5752-z.](https://doi.org/10.1007/s11434-013-5752-z)

2541 [Wang, H., Shi, G.Y., Zhang, X.Y., Gong, S.L., Tan, S.C., Chen, B., Che, H.Z., Li, T., 2015a.](#)
2542 [Mesoscale modelling study of the interactions between aerosols and PBL meteorology during](#)
2543 [a haze episode in China Jing-Jin-Ji and its near surrounding region-Part 2: Aerosols' radiative](#)
2544 [feedback effects. Atmos. Chem. Phys. 15, 3277-3287. https://doi.org/10.5194/acp-15-3277-](#)
2545 [2015.](#)

2546 [Wang, H., Xue, M., Zhang, X.Y., Liu, H.L., Zhou, C.H., Tan, S.C., Che, H.Z., Chen, B., Li, T., 2015b.](#)
2547 [Mesoscale modeling study of the interactions between aerosols and PBL meteorology during](#)
2548 [a haze episode in Jing-Jin-Ji \(China\) and its nearby surrounding region-Part 1: Aerosol](#)
2549 [distributions and meteorological features. Atmos. Chem. Phys. 15, 3257-3275.](#)
2550 [https://doi.org/10.5194/acp-15-3257-2015.](https://doi.org/10.5194/acp-15-3257-2015)

2551 [Wang, H., Zhang, X., Gong, S., Chen, Y., Shi, G., Li, W., 2010. Radiative feedback of dust aerosols](#)
2552 [on the East Asian dust storms. J. Geophys. Res. Atmos. 115.](#)
2553 [https://doi.org/10.1029/2009JD013430.](https://doi.org/10.1029/2009JD013430)

2554 [Wang, J., Allen, D.J., Pickering, K.E., Li, Z., He, H., 2016. Impact of aerosol direct effect on East](#)
2555 [Asian air quality during the EAST-AIRE campaign. J. Geophys. Res. Atmos. 121, 6534-6554.](#)
2556 [https://doi.org/10.1002/2016JD025108.](https://doi.org/10.1002/2016JD025108)

2557 [Wang, J., Wang, S., Jiang, J., Ding, A., Zheng, M., Zhao, B., Wong, D.C., Zhou, W., Zheng, G.,](#)
2558 [Wang, L., Pleim, J.E., Hao, J., 2014. Impact of aerosol-meteorology interactions on fine](#)
2559 [particle pollution during China's severe haze episode in January 2013. Environ. Res. Lett. 9.](#)
2560 [https://doi.org/10.1088/1748-9326/9/9/094002.](https://doi.org/10.1088/1748-9326/9/9/094002)

2561 [Wang, J., Xing, J., Mathur, R., Pleim, J.E., Wang, S., Hogrefe, C., Gan, C.-M., Wong, D.C., Hao, J.,](#)
2562 [2017. Historical trends in PM_{2.5}-related premature mortality during 1990-2010 across the](#)
2563 [northern hemisphere. Environ. Health Perspect. 125, 400-408. https://doi.org/10.1289/EHP298.](#)

2564 [Wang, K., Yahya, K., Zhang, Y., Hogrefe, C., Pouliot, G., Knote, C., Hodzic, A., San Jose, R., Perez,](#)
2565 [J.L., Jiménez-Guerrero, P., 2015. A multi-model assessment for the 2006 and 2010 simulations](#)
2566 [under the Air Quality Model Evaluation International Initiative \(AQMEII\) Phase 2 over North](#)
2567 [America: Part II. Evaluation of column variable predictions using satellite data. Atmos.](#)
2568 [Environ. 115, 587-603. https://doi.org/10.1016/j.atmosenv.2014.07.044.](#)

2569 [Wang, K., Zhang, Y., Zhang, X., Fan, J., Leung, L.R., Zheng, B., Zhang, Q., He, K., 2018. Fine-](#)
2570 [scale application of WRF-CAM5 during a dust storm episode over East Asia: Sensitivity to](#)
2571 [grid resolutions and aerosol activation parameterizations. Atmos. Environ. 176, 1-20.](#)
2572 [https://doi.org/10.1016/j.atmosenv.2017.12.014.](https://doi.org/10.1016/j.atmosenv.2017.12.014)

2573 [Wang, L., Fu, J.S., Wei, W., Wei, Z., Meng, C., Ma, S., Wang, J., 2018. How aerosol direct effects](#)
2574 [influence the source contributions to PM_{2.5} concentrations over Southern Hebei, China in](#)
2575 [severe winter haze episodes. Front. Environ. Sci. Eng. 12, 13. https://doi.org/10.1007/s11783-](#)
2576 [018-1014-2.](#)

2577 [Wang, Z., Huang, X., Ding, A., 2018. Dome effect of black carbon and its key influencing factors:](#)
2578 [a one-dimensional modelling study. Atmos. Chem. Phys. 18, 2821. https://doi.org/10.5194/acp-](#)
2579 [18-2821-2018.](#)

2580 [Wang, Z., Huang, X., Ding, A., 2019. Optimization of vertical grid setting for air quality modelling](#)
2581 [in China considering the effect of aerosol-boundary layer interaction. Atmos. Environ. 210, 1-](#)
2582 [13. https://doi.org/10.1016/j.atmosenv.2019.04.042.](#)

2583 [Wang, Z., Wang, Zhe, Li, Jie, Zheng, H., Yan, P., Li, J., 2014. Development of a meteorology-](#)
2584 [chemistry two-way coupled numerical model \(WRF?NAQPMS\) and its application in a severe](#)
2585 [autumn haze simulation over the Beijing-Tianjin-Hebei area. China. Clim. Environ. Res 19,](#)
2586 [153-163. https://doi.org/10.3878/j.issn.1006-9585.2014.13231.](#)

2587 [Wang, Z.F., Li, J., Wang, Z., Yang, W., Tang, X., Ge, B., Yan, P., Zhu, L., Chen, X., Chen, H., 2014.](#)
2588 [Modeling study of regional severe hazes over mid-eastern China in January 2013 and its](#)
2589 [implications on pollution prevention and control. Sci. China Earth Sci. 57, 3-13.](#)
2590 [https://doi.org/10.1007/s11430-013-4793-0.](https://doi.org/10.1007/s11430-013-4793-0)

2591 [Wendisch, M., Keil, A., Müller, D., Wandinger, U., Wendling, P., Stifter, A., Petzold, A., Fiebig, M.,](#)
2592 [Wiegner, M., Freudenthaler, V., 2002. Aerosol-radiation interaction in the cloudless](#)
2593 [atmosphere during LACE 98 I. Measured and calculated broadband solar and spectral surface](#)
2594 [insolations. J. Geophys. Res. Atmos. 107, LAC-6. https://doi.org/10.1029/2000JD000226.](#)

2595 [Wexler, A.S., Lurmann, F.W., Seinfeld, J.H., 1994. Modelling urban and regional aerosols-I. Model](#)
2596 [development. Atmos. Environ. 28, 531-546. https://doi.org/10.1016/1352-2310\(94\)90129-5.](#)

2597 [Whitby, K.T., 1978. The physical characteristics of sulfur aerosols, in: Sulfur in the Atmosphere.](#)
2598 [Elsevier, pp. 135-159. https://doi.org/10.1016/B978-0-08-022932-4.50018-5.](#)

2599 [Wilcox, E.M., 2012. Direct and semi-direct radiative forcing of smoke aerosols over clouds. Atmos.](#)
2600 [Chem. Phys. 12, 139. https://doi.org/10.5194/acp-12-139-2012.](#)

2601 [Wong, D.C., Pleim, J., Mathur, R., Binkowski, F., Otte, T., Gilliam, R., Pouliot, G., Xiu, A., Young,](#)
2602 [J.O., Kang, D., 2012. WRF-CMAQ two-way coupled system with aerosol feedback: software](#)
2603 [development and preliminary results. Geosci. Model Dev. 5, 299. https://doi.org/10.5194/gmd-](#)
2604 [5-299-2012.](#)

2605 [Wu, J., Bei, N., Hu, B., Liu, S., Zhou, M., Wang, Q., Li, X., Lang, L., Tian, F., Liu, Z., 2019a.](#)
2606 [Aerosol-radiation feedback deteriorates the wintertime haze in the North China Plain. Atmos.](#)
2607 [Chem. Phys. 19, 8703-8719. https://doi.org/10.5194/acp-19-8703-2019.](#)

2608 [Wu, J., Bei, N., Hu, B., Liu, S., Zhou, M., Wang, O., Li, X., Liu, L., Feng, T., Liu, Z., Wang, Y., Cao,](#)
2609 [J., Tie, X., Wang, J., Molina, L.T., Li, G., 2019b. Is water vapor a key player of the wintertime](#)
2610 [haze in North China Plain? Atmos. Chem. Phys. 19, 8721-8739. \[https://doi.org/10.5194/acp-\]\(https://doi.org/10.5194/acp-19-8721-2019\)](#)
2611 [19-8721-2019](#)

2612 [Wu, L., Su, H., Jiang, J.H., 2013. Regional simulation of aerosol impacts on precipitation during the](#)
2613 [East Asian summer monsoon. J. Geophys. Res. Atmos. 118, 6454-6467.](#)
2614 [https://doi.org/10.1002/jgrd.50527.](#)

2615 [Wu, W., Zhang, Y., 2018. Effects of particulate matter \(PM_{2.5}\) and associated acidity on ecosystem](#)
2616 [functioning: response of leaf litter breakdown. Environ. Sci. Pollut. Res. 25, 30720-30727.](#)
2617 [https://doi.org/10.1007/s11356-018-2922-1.](#)

2618 [Wu, Y., Han, Y., Voulgarakis, A., Wang, T., Li, M., Wang, Y., Xie, M., Zhuang, B., Li, S., 2017. An](#)
2619 [agricultural biomass burning episode in eastern China: Transport, optical properties, and](#)
2620 [impacts on regional air quality. J. Geophys. Res. Atmos. 122, 2304-2324.](#)
2621 [https://doi.org/10.1002/2016JD025319.](#)

2622 [Xie, M., Liao, J., Wang, T., Zhu, K., Zhuang, B., Han, Y., Li, M., Li, S., 2016. Modeling of the](#)
2623 [anthropogenic heat flux and its effect on regional meteorology and air quality over the Yangtze](#)
2624 [River Delta region, China. Atmos. Chem. Phys. 16, 6071. \[https://doi.org/10.5194/acp-16-6071-\]\(https://doi.org/10.5194/acp-16-6071-2016\)](#)
2625 [2016.](#)

2626 [Xing, J., Mathur, R., Pleim, J., Hogrefe, C., Gan, C., Wong, D.C., Wei, C., Wang, J., 2015b. Air](#)
2627 [pollution and climate response to aerosol direct radiative effects: A modeling study of decadal](#)
2628 [trends across the northern hemisphere. J. Geophys. Res. Atmos. 120, 12-221.](#)
2629 [https://doi.org/10.1002/2015JD023933.](#)

2630 [Xing, J., Mathur, R., Pleim, J., Hogrefe, C., Gan, C.M., Wong, D.C., Wei, C., 2015c. Can a coupled](#)
2631 [meteorology-chemistry model reproduce the historical trend in aerosol direct radiative effects](#)
2632 [over the Northern Hemisphere? Atmos. Chem. Phys. 15, 9997-10018.](#)
2633 [https://doi.org/10.5194/acp-15-9997-2015.](#)

2634 [Xing, J., Mathur, R., Pleim, J., Hogrefe, C., Gan, C.-M., Wong, D.-C., Wei, C., Gilliam, R., Pouliot,](#)
2635 [G., 2015a. Observations and modeling of air quality trends over 1990-2010 across the Northern](#)
2636 [Hemisphere: China, the United States and Europe. Atmos. Chem. Phys. 15,](#)
2637 [https://doi.org/10.5194/acp-15-2723-2015.](#)

2638 [Xing, J., Wang, J., Mathur, R., Pleim, J., Wang, S., Hogrefe, C., Gan, C.-M., Wong, D.C., Hao, J.,](#)
2639 [2016. Unexpected benefits of reducing aerosol cooling effects. Environ. Sci. Technol. 50,](#)
2640 [7527-7534. \[https://doi.org/10.1021/acs.est.6b00767.\]\(https://doi.org/10.1021/acs.est.6b00767\)](#)

2641 [Xing, J., Wang, J., Mathur, R., Wang, S., Sarwar, G., Pleim, J., Hogrefe, C., Zhang, Y., Jiang, J.,](#)
2642 [Wong, D.C., 2017. Impacts of aerosol direct effects on tropospheric ozone through changes in](#)
2643 [atmospheric dynamics and photolysis rates. Atmos. Chem. Phys. 17, 9869.](#)
2644 [https://doi.org/10.5194/acp-17-9869-2017.](#)

2645 [Yahya, K., Wang, K., Gudoshava, M., Glotfelty, T., Zhang, Y., 2015. Application of WRF/Chem](#)
2646 [over North America under the AQMEII Phase 2: Part I. Comprehensive evaluation of 2006](#)
2647 [simulation. Atmos. Environ. 115, 733-755. \[https://doi.org/10.1016/j.atmosenv.2014.08.063.\]\(https://doi.org/10.1016/j.atmosenv.2014.08.063\)](#)

2648 [Yan, J., Wang, X., Gong, P., Wang, C., Cong, Z., 2018. Review of brown carbon aerosols: Recent](#)
2649 [progress and perspectives. Sci. Total Environ. 634, 1475-1485.](#)
2650 [https://doi.org/10.1016/j.scitotenv.2018.04.083.](#)

2651 [Yang, J., Duan, K., Kang, S., Shi, P., Ji, Z., 2017. Potential feedback between aerosols and](#)
2652 [meteorological conditions in a heavy pollution event over the Tibetan Plateau and Indo-](#)
2653 [Gangetic Plain. Clim. Dyn. 48, 2901-2917. \[https://doi.org/10.1007/s00382-016-3240-2.\]\(https://doi.org/10.1007/s00382-016-3240-2\)](#)

2654 [Yang, J., Kang, S., Ji, Z., Chen, D., 2018. Modeling the origin of anthropogenic black carbon and](#)
2655 [its climatic effect over the Tibetan Plateau and surrounding regions. J. Geophys. Res. Atmos.](#)
2656 [123, 671-692. \[https://doi.org/10.1002/2017JD027282.\]\(https://doi.org/10.1002/2017JD027282\)](#)

2657 [Yang, T., Liu, Y., 2017a. Mechanism analysis of the impacts of aerosol direct effects on a rainstorm.](#)
2658 [J. Trop. Meteorol. 33, 762-773. \[https://doi.org/10.16032/j.issn.1004-4965.2017.05.019,\]\(https://doi.org/10.16032/j.issn.1004-4965.2017.05.019\)](#)

2659 [Yang, T., Liu, Y., 2017b. Impact of anthropogenic pollution on “7.21” extreme heavy rainstorm. J.](#)
2660 [Meteorol. Sci. 742-752. \[https://doi.org/10.3969/2016jms.0074.\]\(https://doi.org/10.3969/2016jms.0074\)](#)

2661 [Yang, Y., Fan, J., Leung, L.R., Zhao, C., Li, Z., Rosenfeld, D., 2016. Mechanisms contributing to](#)
2662 [suppressed precipitation in Mt. Hua of central China. Part I: Mountain valley circulation. J.](#)
2663 [Atmos. Sci. 73, 1351-1366. \[https://doi.org/10.1175/JAS-D-15-0233.1.\]\(https://doi.org/10.1175/JAS-D-15-0233.1\)](#)

2664 [Yang, Y., Tang, J., Sun, J., Wang, L., Wang, X., Zhang, Y., Qu, Q., Zhao, W., 2015. Synoptic Effect](#)

2665 [of a Heavy Haze Episode over North China. *Clim. Environ. Res.*](#)
2666 <https://doi.org/10.3878/j.issn.1006-9585.2015.15018>.

2667 [Yang, Y., Zhao, C., Dong, X., Fan, G., Zhou, Y., Wang, Y., Zhao, L., Lv, F., Yan, F., 2019. Toward](#)
2668 [understanding the process-level impacts of aerosols on microphysical properties of shallow](#)
2669 [cumulus cloud using aircraft observations. *Atmos. Res.* 221, 27-33.](#)
2670 <https://doi.org/10.1016/j.atmosres.2019.01.027>.

2671 [Yao, H., Song, Y., Liu, M., Archer-Nicholls, S., Lowe, D., McFiggans, G., Xu, T., Du, P., Li, J., Wu,](#)
2672 [Y., 2017. Direct radiative effect of carbonaceous aerosols from crop residue burning during the](#)
2673 [summer harvest season in East China. *Atmos. Chem. Phys.* 17, 5205.](#)
2674 <https://doi.org/10.5194/acp-17-5205-2017>.

2675 [Yasunari, T.J., Yamazaki, K., 2009. Impacts of Asian dust storm associated with the stratosphere-to-](#)
2676 [troposphere transport in the spring of 2001 and 2002 on dust and tritium variations in Mount](#)
2677 [Wrangell ice core, Alaska. *Atmos. Environ.* 43, 2582-2590.](#)
2678 <https://doi.org/10.1016/j.atmosenv.2009.02.025>.

2679 [Yi?it, E., Kni?ová, P.K., Georgieva, K., Ward, W., 2016. A review of vertical coupling in the](#)
2680 [Atmosphere-Ionosphere system: Effects of waves, sudden stratospheric warmings, space](#)
2681 [weather, and of solar activity. *J. Atmos. Solar-Terrestrial Phys.* 141, 1-12.](#)
2682 <https://doi.org/10.1016/j.jastp.2016.02.011>.

2683 [Yoo, J.-W., Jeon, W., Park, S.-Y., Park, C., Jung, J., Lee, S.-H., Lee, H.W., 2019. Investigating the](#)
2684 [regional difference of aerosol feedback effects over South Korea using the WRF-CMAQ two-](#)
2685 [way coupled modeling system. *Atmos. Environ.* 218, 116968.](#)
2686 <https://doi.org/10.1016/j.atmosenv.2019.116968>.

2687 [Yoon, J., Chang, D.Y., Lelieveld, J., Pozzer, A., Kim, J., Yum, S.S., 2019. Empirical evidence of a](#)
2688 [positive climate forcing of aerosols at elevated albedo. *Atmos. Res.* 229, 269-279.](#)
2689 <https://doi.org/10.1016/j.atmosres.2019.07.001>.

2690 [Yu, F., 2006. From molecular clusters to nanoparticles: second-generation ion-mediated nucleation](#)
2691 [model. *Atmos. Chem. Phys.* 6, 5193-5211. https://doi.org/10.5194/acp-6-5193-2006.](#)

2692 [Yu, F., Luo, G., 2009. Simulation of particle size distribution with a global aerosol model:](#)
2693 [contribution of nucleation to aerosol and CCN number concentrations. *Atmos. Chem. Phys.* 9,](#)
2694 [7691-7710. https://doi.org/10.5194/acp-9-7691-2009.](#)

2695 [Yu, H., Kaufman, Y.J., Chin, M., Feingold, G., Remer, L.A., Anderson, T.L., Balkanski, Y., Bellouin,](#)
2696 [N., Boucher, O., Christopher, S., 2006. A review of measurement-based assessments of the](#)
2697 [aerosol direct radiative effect and forcing. *Atmos. Chem. Phys.* 6, 613-666.](#)
2698 <https://doi.org/10.5194/acp-6-613-2006>.

2699 [Yuan, Q., Xu, J., Liu, L., Zhang, A., Liu, Y., Zhang, J., Wan, X., Li, M., Qin, K., Cong, Z., 2020.](#)
2700 [Evidence for large amounts of brown carbonaceous tarballs in the himalayan atmosphere.](#)
2701 [Environ. Sci. Technol. Lett. 8, 16-23. https://doi.org/10.1021/acs.estlett.0c00735.](#)

2702 [Yuan, T., Chen, S., Huang, J., Wu, D., Lu, H., Zhang, G., Ma, Xiaojun, Chen, Z., Luo, Y., Ma,](#)
2703 [Xiaohui, 2019. Influence of dynamic and thermal forcing on the meridional transport of](#)
2704 [Taklimakan Desert dust in spring and summer. *J. Clim.* 32, 749-767.](#)
2705 <https://doi.org/10.1175/JCLI-D-18-0361.1>.

2706 [Zaveri, R.A., Easter, R.C., Fast, J.D., Peters, L.K., 2008. Model for simulating aerosol interactions](#)
2707 [and chemistry \(MOSAIC\). *J. Geophys. Res. Atmos.* 113.](#)
2708 <https://doi.org/10.1029/2007JD008782>.

2709 [Zhan, J., Chang, W., Li, W., Wang, Y., Chen, L., Yan, J., 2017. Impacts of meteorological conditions,](#)
2710 [aerosol radiative feedbacks, and emission reduction scenarios on the coastal haze episodes in](#)
2711 [southeastern China in December 2013. *J. Appl. Meteorol. Climatol.* 56, 1209-1229.](#)
2712 <https://doi.org/10.1175/JAMC-D-16-0229.1>.

2713 [Zhang, B., Wang, Y., Hao, J., 2015. Simulating aerosol-radiation-cloud feedbacks on meteorology](#)
2714 [and air quality over eastern China under severe haze conditions in winter. *Atmos. Chem. Phys.*](#)
2715 [15, 2387-2404. https://doi.org/10.5194/acp-15-2387-2015.](#)

2716 [Zhang, H., Cheng, S., Li, J., Yao, S., Wang, X., 2019. Investigating the aerosol mass and chemical](#)
2717 [components characteristics and feedback effects on the meteorological factors in the Beijing-](#)
2718 [Tianjin-Hebei region, China. *Environ. Pollut.* 244, 495-502.](#)
2719 <https://doi.org/10.1016/j.envpol.2018.10.087>.

2720 [Zhang, H., DeNero, S.P., Joe, D.K., Lee, H.-H., Chen, S.-H., Michalakes, J., Kleeman, M.J., 2014.](#)
2721 [Development of a source oriented version of the WRF/Chem model and its application to the](#)

2722 [California regional PM₁₀/PM_{2.5} air quality study. Atmos. Chem. Phys. 14, 485–503.](https://doi.org/10.5194/acp-14-485-2014)
 2723 [https://doi.org/10.5194/acp-14-485-2014.](https://doi.org/10.5194/acp-14-485-2014)
 2724 [Zhang, L., Gong, S., Zhao, T., Zhou, C., Wang, Y., Li, J., Ji, D., He, J., Liu, H., Gui, K., 2021.](https://doi.org/10.5194/gmd-14-703-2021)
 2725 [Development of WRF/CUACE v1.0 model and its preliminary application in simulating air](https://doi.org/10.5194/gmd-14-703-2021)
 2726 [quality in China. Geosci. Model Dev. 14, 703–718. https://doi.org/10.5194/gmd-14-703-2021.](https://doi.org/10.5194/gmd-14-703-2021)
 2727 [Zhang, L., Wang, T., Lv, M., Zhang, Q., 2015. On the severe haze in Beijing during January 2013:](https://doi.org/10.1016/j.atmosenv.2015.01.001)
 2728 [Unraveling the effects of meteorological anomalies with WRF-Chem. Atmos. Environ. 104,](https://doi.org/10.1016/j.atmosenv.2015.01.001)
 2729 [11–21. https://doi.org/10.1016/j.atmosenv.2015.01.001.](https://doi.org/10.1016/j.atmosenv.2015.01.001)
 2730 [Zhang, X.Y., Gong, S.L., Shen, Z.X., Mei, F.M., Xi, X.X., Liu, L.C., Zhou, Z.J., Wang, D., Wang,](https://doi.org/10.1029/2003GL018206)
 2731 [Y.O., Cheng, Y., 2003a. Characterization of soil dust aerosol in China and its transport and](https://doi.org/10.1029/2003GL018206)
 2732 [distribution during 2001 ACE-Asia: 1. Network observations. J. Geophys. Res. Atmos. 108,](https://doi.org/10.1029/2003GL018206)
 2733 [https://doi.org/10.1029/2003GL018206.](https://doi.org/10.1029/2003GL018206)
 2734 [Zhang, X.Y., Gong, S.L., Zhao, T.L., Arimoto, R., Wang, Y.Q., Zhou, Z.J., 2003b. Sources of Asian](https://doi.org/10.1029/2003GL018206)
 2735 [dust and role of climate change versus desertification in Asian dust emission. Geophys. Res.](https://doi.org/10.1029/2003GL018206)
 2736 [Lett. 30. https://doi.org/10.1029/2003GL018206.](https://doi.org/10.1029/2003GL018206)
 2737 [Zhang, Xin, Zhang, Q., Hong, C., Zheng, Y., Geng, G., Tong, D., Zhang, Y., Zhang, Xiaoye, 2018.](https://doi.org/10.1002/2017JD027524)
 2738 [Enhancement of PM_{2.5} Concentrations by Aerosol-Meteorology Interactions Over China. J.](https://doi.org/10.1002/2017JD027524)
 2739 [Geophys. Res. Atmos. 123, 1179-1194. https://doi.org/10.1002/2017JD027524.](https://doi.org/10.1002/2017JD027524)
 2740 [Zhang, Y., 2008. Online-coupled meteorology and chemistry models: history, current status, and](https://doi.org/10.5194/acp-8-2895-2008)
 2741 [outlook. Atmos. Chem. Phys. 8, 2895-2932. https://doi.org/10.5194/acp-8-2895-2008.](https://doi.org/10.5194/acp-8-2895-2008)
 2742 [Zhang, Y., Chen, Y., Fan, J., Leung, L.-Y.R., 2015a. Application of an online-coupled regional](https://doi.org/10.3390/cli3030753)
 2743 [climate model, WRF-CAM5, over East Asia for examination of ice nucleation schemes: part](https://doi.org/10.3390/cli3030753)
 2744 [II. Sensitivity to heterogeneous ice nucleation parameterizations and dust emissions. Climate](https://doi.org/10.3390/cli3030753)
 2745 [3, 753-774. https://doi.org/10.3390/cli3030753.](https://doi.org/10.3390/cli3030753)
 2746 [Zhang, Y., He, J., Zhu, S., Gantt, B., 2016. Sensitivity of simulated chemical concentrations and](https://doi.org/10.1002/2016JD024882)
 2747 [aerosol-meteorology interactions to aerosol treatments and biogenic organic emissions in](https://doi.org/10.1002/2016JD024882)
 2748 [WRF/Chem. J. Geophys. Res. Atmos. 121, 6014–6048. https://doi.org/10.1002/2016JD024882.](https://doi.org/10.1002/2016JD024882)
 2749 [Zhang, Y., Hu, X.M., Howell, G.W., Sills, E., Fast, J.D., Gustafson Jr, W.L., Zaveri, R.A., Grell, G.A.,](https://doi.org/10.1007/978-3-319-04379-1_10)
 2750 [Peckham, S.E., McKeen, S.A., 2005. Modeling atmospheric aerosols in WRF/CHEM, in:](https://doi.org/10.1007/978-3-319-04379-1_10)
 2751 [WRF/MM5 Users’s Workshop. National Center for Atmospheric Research.](https://doi.org/10.1007/978-3-319-04379-1_10)
 2752 [Zhang, Y., Karamchandani, P., Glotfelty, T., Streets, D.G., Grell, G., Nenes, A., Yu, F., Bennartz, R.,](https://doi.org/10.1029/2012JD017966)
 2753 [2012. Development and initial application of the global - through - urban weather research](https://doi.org/10.1029/2012JD017966)
 2754 [and forecasting model with chemistry \(GU-WRF/Chem\). J. Geophys. Res. Atmos. 117,](https://doi.org/10.1029/2012JD017966)
 2755 [https://doi.org/10.1029/2012JD017966.](https://doi.org/10.1029/2012JD017966)
 2756 [Zhang, Y., Pan, Y., Wang, K., Fast, J.D., Grell, G.A., 2010. WRF/Chem-MADRID: Incorporation](https://doi.org/10.1029/2009JD013443)
 2757 [of an aerosol module into WRF/Chem and its initial application to the TexAQS2000 episode.](https://doi.org/10.1029/2009JD013443)
 2758 [J. Geophys. Res. Atmos. 115. https://doi.org/10.1029/2009JD013443.](https://doi.org/10.1029/2009JD013443)
 2759 [Zhang, Y., Pun, B., Vijayaraghavan, K., Wu, S., Seigneur, C., Pandis, S.N., Jacobson, M.Z., Nenes,](https://doi.org/10.1029/2003JD003501)
 2760 [A., Seinfeld, J.H., 2004. Development and application of the model of aerosol dynamics,](https://doi.org/10.1029/2003JD003501)
 2761 [reaction, ionization, and dissolution \(MADRID\). J. Geophys. Res. Atmos. 109,](https://doi.org/10.1029/2003JD003501)
 2762 [https://doi.org/10.1029/2003JD003501.](https://doi.org/10.1029/2003JD003501)
 2763 [Zhang, Y., Wang, K., He, J., 2017. Multi-year application of WRF-CAM5 over East Asia-Part II:](https://doi.org/10.1016/j.atmosenv.2017.06.029)
 2764 [Interannual variability, trend analysis, and aerosol indirect effects. Atmos. Environ. 165, 222-](https://doi.org/10.1016/j.atmosenv.2017.06.029)
 2765 [239. https://doi.org/10.1016/j.atmosenv.2017.06.029.](https://doi.org/10.1016/j.atmosenv.2017.06.029)
 2766 [Zhang, Y., Zhang, X., Cai, C., Wang, K., Wang, L., 2014. Studying Aerosol-Cloud-Climate](https://doi.org/10.1007/978-3-319-04379-1_10)
 2767 [Interactions over East Asia Using WRF/Chem, in: Air Pollution Modeling and Its Application](https://doi.org/10.1007/978-3-319-04379-1_10)
 2768 [XXIII. Springer, pp. 61-66. https://doi.org/10.1007/978-3-319-04379-1_10.](https://doi.org/10.1007/978-3-319-04379-1_10)
 2769 [Zhang, Y., Zhang, X., Wang, K., He, J., Leung, L.R., Fan, J., Nenes, A., 2015b. Incorporating an](https://doi.org/10.1002/2014JD023051)
 2770 [advanced aerosol activation parameterization into WRF-CAM5: Model evaluation and](https://doi.org/10.1002/2014JD023051)
 2771 [parameterization intercomparison. J. Geophys. Res. Atmos. 120, 6952-6979.](https://doi.org/10.1002/2014JD023051)
 2772 [https://doi.org/10.1002/2014JD023051.](https://doi.org/10.1002/2014JD023051)
 2773 [Zhang, Yang, Zhang, X., Wang, K., Zhang, Q., Duan, F., He, K., 2016a. Application of WRF/Chem](https://doi.org/10.1016/j.atmosenv.2015.07.023)
 2774 [over East Asia: Part II. Model improvement and sensitivity simulations. Atmos. Environ. 124,](https://doi.org/10.1016/j.atmosenv.2015.07.023)
 2775 [301-320. https://doi.org/10.1016/j.atmosenv.2015.07.023.](https://doi.org/10.1016/j.atmosenv.2015.07.023)
 2776 [Zhang, Yang, Zhang, X., Wang, L., Zhang, Q., Duan, F., He, K., 2016b. Application of WRF/Chem](https://doi.org/10.1016/j.atmosenv.2015.07.022)
 2777 [over East Asia: Part I. Model evaluation and intercomparison with MM5/CMAQ. Atmos.](https://doi.org/10.1016/j.atmosenv.2015.07.022)
 2778 [Environ. 124, 285-300. https://doi.org/10.1016/j.atmosenv.2015.07.022.](https://doi.org/10.1016/j.atmosenv.2015.07.022)

2779 [Zhang, Yue, Fan Shuxian, Li Hao, Kang Boshi, 2016. Effects of aerosol radiative feedback during](#)
2780 [a severe smog process over eastern China. Acta Meteorol. 74.](#)
2781 [https://doi.org/10.11676/qxxb2016.028.](https://doi.org/10.11676/qxxb2016.028)
2782 [Zhao, B., Liou, K., Gu, Y., Li, Q., Jiang, J.H., Su, H., He, C., Tseng, H.-L.R., Wang, S., Liu, R.,](#)
2783 [2017. Enhanced PM_{2.5} pollution in China due to aerosol-cloud interactions. Sci. Rep. 7, 1-11.](#)
2784 [https://doi.org/10.1038/s41598-017-04096-8.](https://doi.org/10.1038/s41598-017-04096-8)
2785 [Zhao, B., Wang, Y., Gu, Y., Liou, K.-N., Jiang, J.H., Fan, J., Liu, X., Huang, L., Yung, Y.L., 2019.](#)
2786 [Ice nucleation by aerosols from anthropogenic pollution. Nat. Geosci. 12, 602-607.](#)
2787 [https://doi.org/10.1038/s41561-019-0389-4.](https://doi.org/10.1038/s41561-019-0389-4)
2788 [Zhong, M., Chen, F., Saikawa, E., 2019. Sensitivity of projected PM_{2.5}- and O₃-related health](#)
2789 [impacts to model inputs: A case study in mainland China. Environ. Int. 123, 256-264.](#)
2790 [https://doi.org/10.1016/j.envint.2018.12.002.](https://doi.org/10.1016/j.envint.2018.12.002)
2791 [Zhong, M., Saikawa, E., Liu, Y., Naik, V., Horowitz, L.W., Takigawa, M., Zhao, Y., Lin, N.-H.,](#)
2792 [Stone, E.A., 2016. Air quality modeling with WRF-Chem v3.5 in East Asia: sensitivity to](#)
2793 [emissions and evaluation of simulated air quality. Geosci. Model Dev. 9, 1201-1218.](#)
2794 [https://doi.org/10.5194/gmd-9-1201-2016.](https://doi.org/10.5194/gmd-9-1201-2016)
2795 [Zhong, S., Qian, Y., Zhao, C., Leung, R., Wang, H., Yang, B., Fan, J., Yan, H., Yang, X.-Q., Liu, D.,](#)
2796 [2017. Urbanization-induced urban heat island and aerosol effects on climate extremes in the](#)
2797 [Yangtze River Delta region of China. Atmos. Chem. Phys. 17. \[https://doi.org/10.5194/acp-17-\]\(https://doi.org/10.5194/acp-17-5439-2017\)](#)
2798 [5439-2017.](#)
2799 [Zhong, S., Qian, Y., Zhao, C., Leung, R., Yang, X., 2015. A case study of urbanization impact on](#)
2800 [summer precipitation in the Greater Beijing Metropolitan Area: Urban heat island versus](#)
2801 [aerosol effects. J. Geophys. Res. Atmos. 120, 10-903. \[https://doi.org/10.1002/2015JD023753.\]\(https://doi.org/10.1002/2015JD023753\)](#)
2802 [Zhou, C., Gong, S., Zhang, X., Liu, H., Xue, M., Cao, G., An, X., Che, H., Zhang, Y., Niu, T., 2012.](#)
2803 [Towards the improvements of simulating the chemical and optical properties of Chinese](#)
2804 [aerosols using an online coupled model-CUACE/Aero. Tellus B Chem. Phys. Meteorol. 64,](#)
2805 [18965. \[https://doi.org/10.3402/tellusb.v64i0.18965.\]\(https://doi.org/10.3402/tellusb.v64i0.18965\)](#)
2806 [Zhou, C., Gong, S.L., Zhang, X.Y., Wang, Y.Q., Niu, T., Liu, H.L., Zhao, T.L., Yang, Y.Q., Hou, Q.,](#)
2807 [2008. Development and evaluation of an operational SDS forecasting system for East Asia:](#)
2808 [CUACE/Dust. Atmos. Chem. Phys. 8, 787-798. \[https://doi.org/10.5194/acp-8-787-2008.\]\(https://doi.org/10.5194/acp-8-787-2008\)](#)
2809 [Zhou, C., Zhang, X., Gong, S., Wang, Y., Xue, M., 2016. Improving aerosol interaction with clouds](#)
2810 [and precipitation in a regional chemical weather modeling system 145-160.](#)
2811 [https://doi.org/10.5194/acp-16-145-2016.](https://doi.org/10.5194/acp-16-145-2016)
2812 [Zhou, D., Ding, K., Huang, X., Liu, L., Liu, Q., Xu, Z., Jiang, F., Fu, C., Ding, A., 2018. Transport,](#)
2813 [mixing and feedback of dust, biomass burning and anthropogenic pollutants in eastern Asia: a](#)
2814 [case study. Atmos. Chem. Phys. 18, 16345-16361. \[https://doi.org/10.5194/acp-18-16345-2018.\]\(https://doi.org/10.5194/acp-18-16345-2018\)](#)
2815 [Zhou, M., Zhang, L., Chen, D., Gu, Y., Fu, T.-M., Gao, M., Zhao, Y., Lu, X., Zhao, B., 2019. The](#)
2816 [impact of aerosol-radiation interactions on the effectiveness of emission control measures.](#)
2817 [Environ. Res. Lett. 14, 24002. \[https://doi.org/10.1088/1748-9326/aaf27d.\]\(https://doi.org/10.1088/1748-9326/aaf27d\)](#)
2818 [Zhou, Y., Gong, S., Zhou, C., Zhang, L., He, J., Wang, Y., Ji, D., Feng, J., Mo, J., Ke, H., 2021. A](#)
2819 [new parameterization of uptake coefficients for heterogeneous reactions on multi-component](#)
2820 [atmospheric aerosols. Sci. Total Environ. 781, 146372.](#)
2821 [https://doi.org/10.1016/j.scitotenv.2021.146372.](https://doi.org/10.1016/j.scitotenv.2021.146372)
2822 [Zhuang, B., Jiang, F., Wang, T., Li, S., Zhu, B., 2011. Investigation on the direct radiative effect of](#)
2823 [fossil fuel black-carbon aerosol over China. Theor. Appl. Climatol. 104, 301-312.](#)
2824 [https://doi.org/10.1007/s00704-010-0341-4.](https://doi.org/10.1007/s00704-010-0341-4)
2825